Author:
Arkwright, Michael J

Title:
An automated method for assessing spectral sensitivity in stomatopod crustaceans

An automated method for assessing spectral sensitivity in stomatopod crustaceans

Michael José-Luis Arkwright

A dissertation submitted to the University of Bristol in accordance with the requirements for award of the degree of Master of Science by Research in the Faculty of Life Sciences

January 2022

Word Count: 19,959

Abstract

Stomatopods, or mantis shrimps, are a group of crustaceans that possess an elaborate visual system which requires the eye to be compartmentalised to process different visual modalities. This study intended to investigate whether visual querying of unknown objects is processed through the chromatic midband region or the achromatic hemispheres, by producing an action spectrum that could be compared to other action spectra retrieved from the hemispheres of other stomatopod species. This spectral sensitivity curve would display absolute sensitivities as opposed to normalised ones, something lacking from the current literature. 12 *Odontodactylus scyllarus* (family: Odontodactylidae; superfamily: Gonodactyloidea) individuals were trained through operant conditioning to emerge from their burrows for a food reward upon detecting a flashing LED stimulus. Individuals were trained by a white stimulus with a simultaneously deployed food reward, before being assessed on their responses to six different wavelength stimuli (450, 500, 550, 600, 650, and 700 nm) where the reward was deployed only after a successful response. An automated system that would train and test each individual stomatopod with minimal levels of researcher labour was designed and constructed. The experimental method was continuously modified and fine-tuned throughout the research in an attempt to create an optimal automated system and procedure for future use.

Training became steadily more effective and efficient with the method modifications, however only four individuals were deemed sufficiently conditioned to attempt wavelength trials, partly due to time constraints. The most successful trial design utilised a trial ratio system, large food reward, choice window of 30s, control probability of 0.25, and neutral-density (ND) filters applied to each LED stimulus. Stomatopods could likely detect all six wavelengths but a high degree of noise in the results meant a detection threshold for each wavelength could not be extracted. Without this information, creating a spectral sensitivity curve was not possible and thus neither was revealing the ocular region responsible for it. With suggested improvements, it is most likely this automated system would successfully reveal this information. A potential spectral sensitivity curve based on physiological and ecological findings is suggested and perhaps the use of hemispheres and midband together in querying objects.

Dedication and Acknowledgements

First and foremost, a massive thank you to my supervisor Dr. Martin How, whose expertise on mantis shrimp and their visual systems was indispensable to this research. He is primarily responsible for the design and creation of the automated system, which his coding knowledge and mechanical inventiveness made possible. I am particularly grateful for his endless positivity and advice through the experiment itself and the writing of this thesis. I am also thankful to my secondary supervisor, Professor Nicholas Roberts, for his support of this research study.

In addition, I would like to thank Agus Bentlage for his help in constructing the prototype of the automated system and then teaching me how to utilise it, alongside proper aquarium maintenance. His assistance in running a large number of the trials toward the end of the research study is also greatly appreciated. I am grateful to the aquarium caretaker, Peter Gardiner, for looking after the aquarium and its aquatic inhabitants so well. His friendly demeanour made working here a pleasant experience at a time when there was little interaction with other researchers due to the COVID-19 pandemic.

A special thanks goes out to all the staff at the University of Bristol who helped make this research possible, and to any friends and family who supported me along the way. This includes my mother, Dr. Inmaculada Arkwright, who was willing to read through the entire thesis and offer her advice. Finally, I would like to express gratitude to my partner, Andrea Dixon, for her moral support and advice throughout the process all while completing her own master's degree.

Author’s Declaration

I declare that the work in this dissertation was carried out in accordance with the requirements of the University's Regulations and Code of Practice for Research Degree Programmes and that it has not been submitted for any other academic award. Except where indicated by specific reference in the text, the work is the candidate's own work. Work done in collaboration with, or with the assistance of, others, is indicated as such. Any views expressed in the dissertation are those of the author.

SIGNED: Michael Arkwright DATE: 30/12/2021

Table of Contents

List of Figures and Tables

1. Introduction

1.1. Overview of stomatopods

The order Stomatopoda, commonly known as mantis shrimps, is a fascinating group of marine crustaceans within the class Malacostraca, which was formed around 340 million years ago. All of the nearly 500 extant species belong to the suborder Unipeltata and are currently divided into seven superfamilies with distinguishing ecologies and morphologies, although the number and organisation of the superfamilies remains under debate (Ahyong & Jarman, 2009; Porter *et al.*, 2010; Van Der Wal *et al.*, 2017). They are burrow-dwelling benthic carnivores that most often inhabit the coastal waters of the tropics and subtropics, where their large numbers and predatory nature exert significant influence on the surrounding ecosystem (Caldwell & Dingle, 1975, Van Der Wal *et al.*, 2017). These crustaceans follow the standard malacostracan body plan and range in adult size between approximately 20 mm to 400 mm in length, depending on the species. They are characterised by their dorsoventrally flattened body, reduced carapace and large abdomen ending in a shield-like telson (Fig. 1) (Piper, 2007; Schram *et al.*, 2013).

One of the most striking adaptations of stomatopods is their second pair of maxillipeds which have evolved into raptorial claws that are used for hunting. The form of this appendage divides stomatopods into two functional groups: ‘spearers’ and ‘smashers’ (Van Der Wal *et al.*, 2017). Spearers generally live in burrows dug from soft substrates, and utilise their spears to capture soft-bodied prey, such as fish; whereas smashers tend to inhabit harder substrates, such as coral rubble, and use their appendages to destroy the shells of armoured prey, like crabs and snails (Caldwell & Dingle, 1975; Piper, 2007). The strike of this raptorial limb is extremely fast, and in smashers the club can reach velocities up to 14–23 m/s in *Odontodactylus scyllarus* (Fig. 1a, 23a), which creates cavitation bubbles that exert a secondary force on the prey after limb impact (deVries *et al.*, 2012; Patek *et al.*, 2004).

Although some stomatopods have dull colouration for use in camouflage (Siegenthaler *et al.*, 2018), there are many brightly coloured species (Fig. 1) that use certain markings for both interspecific and intraspecific communication; displaying aggressiveness during agonistic encounters, or signalling sex and conspecificity in male-female interactions as well as influencing mate choice (Caldwell & Dingle, 1975; Cheroske & Cronin, 2005; Chiou *et al.*, 2011; Dingle, 1964). Body postures and chemical signalling are also utilised by stomatopods, potentially in conjunction with visual markings (Cheroske & Cronin, 2005) for

highly complex signalling including deception and individual recognition (Adams & Caldwell, 1990; Caldwell, 1979, 1985; Caldwell & Dingle, 1975; Mead & Caldwell, 2010). High site fidelity, limited supply of suitable dwellings, high possibility of repeated encounters among individuals, alongside lethal weapons has led to the evolution of diverse mating systems, including monogamy - which further facilitates individual recognition (Mead & Caldwell, 2010).

A final distinguishing feature of mantis shrimps, and perhaps the most remarkable of all, is their intricate visual system which is often believed to be one of the most complex visual systems in the world (Bok *et al.*, 2014; Cronin *et al.*, 2014, 2017; Marshall *et al.*, 2007). Depending on the species, stomatopods are capable of detecting wavelengths from deep ultraviolet (UV) to far red, as well as both linear and circular polarized light (Cronin *et al.*, 2014, 2017; Marshall & Oberwinkler, 1999; Marshall *et al.*, 2007). With 12-16 spectral classes of photoreceptor, the mantis shrimp has many more photoreceptor types than any other species on Earth: 5 or 6 spectral classes have been discovered in some fish, flies and butterflies, but this is the highest found other than in stomatopods (Cronin & Marshall, 1989a, 1989b; Cronin *et al.*, 2014, 2017; Marshall & Arikawa, 2014; Thoen *et al.*, 2014). There are many proposed reasons for why this level of visual complexity and spectral diversity evolved (Cronin & Marshall, 1989a, 1989b; Cronin *et al.*, 1994c; Marshall, 1988) but these ultimately remain unproven. This review will explore the impressive visual capabilities of stomatopods, with focus on their spectral vision. This information has come from anatomical, physiological, and behavioural findings therefore this literature review will be divided into these three fields of research.

The stomatopod species elected for this research study was the peacock mantis shrimp, *O. scyllarus*. This is a shallow-living and colourful species (Fig. 1a, 23), that possesses a smasher raptorial limb (Fig. 23a), and inhabits tropical coral reefs (Caldwell & Dingle, 1975; Cronin *et al.*, 1994b; Marshall *et al.*, 2007; Patek *et al.*, 2004). It is part of the Odontodactylidae family, which sits within the large and diverse Gonodactyloidea superfamily (Marshall *et al.*, 2007; Porter *et al.*, 2010). There is a general commonality in eye morphology and physiology within a superfamily, and the highest levels of visual complexity in stomatopods have been found in the gonodactyloids, including *O. scyllarus* (Cronin *et al.*, 1994c; Harling, 2000; Marshall *et al.*, 2007; Porter *et al.*, 2010).

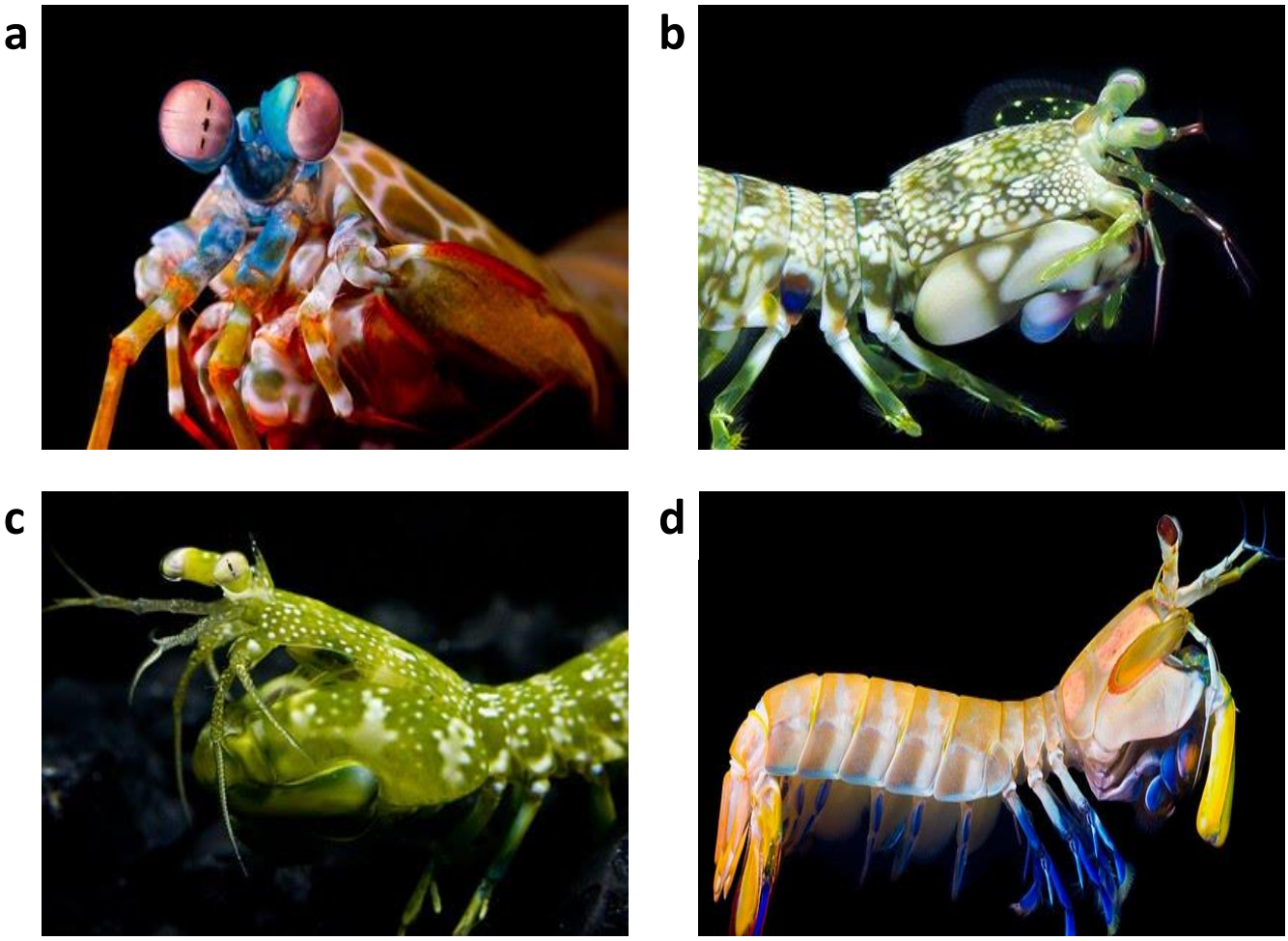

Fig. 1. Four different stomatopod species in the gonodactyloid superfamily, displaying their standard morphology and the great variation in body colouration. The eyes, raptorial appendages, and vibrant colouration are easily visible. (a) *Odontodactylus scyllarus*. (b) *Gonodactylus platysoma.* (c) *Neogonodactylus oerstedii*. (d) *Hemisquilla californiensis*. Photographs: Michael Bok.

1.2. Anatomy

The external and internal anatomy of stomatopod eyes have been detailed through observations on living specimens and preserved materials, light microscopy and both scanning and transmission electron microscopy (SEM and TEM) - revealing an incredible level of complexity and generating great scientific interest in recent decades (Harling, 2000; Manning *et al.*, 1984; Marshall *et al.*, 1991a, 1991b; Schönenberger, 1977). Stomatopods have apposition compound eyes, like many crustaceans (Cronin & Porter, 2008), that are mounted at the end of mobile stalks and can move and function independently from one another (Cronin *et al.*, 2017; Land *et al.*, 1990; Marshall, 1988; Marshall *et al.*, 1991a, 2007). Their eyes differ greatly from other crustaceans in that, with the exception of the

bathysquilloids, they are split into three parts: two hemispheres forming the dorsal and ventral halves (also known as the peripheral ommatidia), which are bisected by a midband region (Fig. 2) (Cronin *et al.*, 2014, 2017; Harling, 2000; Marshall *et al.*, 1991a, 2007). The Bathysquilloidea is the only superfamily without this tripartite eye structure, and they follow the more standard crustacean eye plan without any distinct ocular regions (Harling, 2000; Manning *et al.*, 1984). In addition, their ommatidia are not organised into regular rows, unlike the periphery and midband of other stomatopods (Harling, 2000).

Within the stomatopods there is much variation in the external morphology of the eye with at least five different cornea shapes recognised and, if present, a midband consisting of two, three, or six parallel ommatidial rows (conventionally numbered from the dorsal to ventral side) (Fig. 2). The Squilloidea have two midband rows, whereas the Gonodactyloidea and Lysiosquilloidea usually have six, but with numerous anomalies to this rule (Harling, 2000). Across the stomatopods ommatidial facets are hexagonal except for the midband facets of gonodactyloids with six midband rows, which are rectangular and considerably larger than the peripheral facets (Harling, 2000; Marshall *et al.*, 1991a). Altogether, these variations result in seven basic eye types (Harling, 2000). Although superfamilies tend to favour certain eye types, eye design alone is not consistent enough to characterise species at the superfamily or family level, as once thought possible (Manning et al., 1984), but is useful at the genus and species level (Harling, 2000). Ecological conditions and activity cycles are usually stronger indicators of external eye structure than the current (and frequently changing) superfamily taxonomy, due to evolutionary adaptations to ambient light levels. Diurnal species living in shallow, bright conditions generally have more and smaller facets (for high acuity), larger pseudopupils (for greater resolution) and six-row midbands (which are associated with colour vision); as opposed to nocturnal species or those living in deep or turbid waters which usually have fewer and larger facets, smaller pseudopuils and three-row, two-row or no midband (Abbott *et al.*, 1984; Cronin *et al.*, 1993, 1994c; Harling, 2000; Marshall *et al.*, 1991a, 2007).

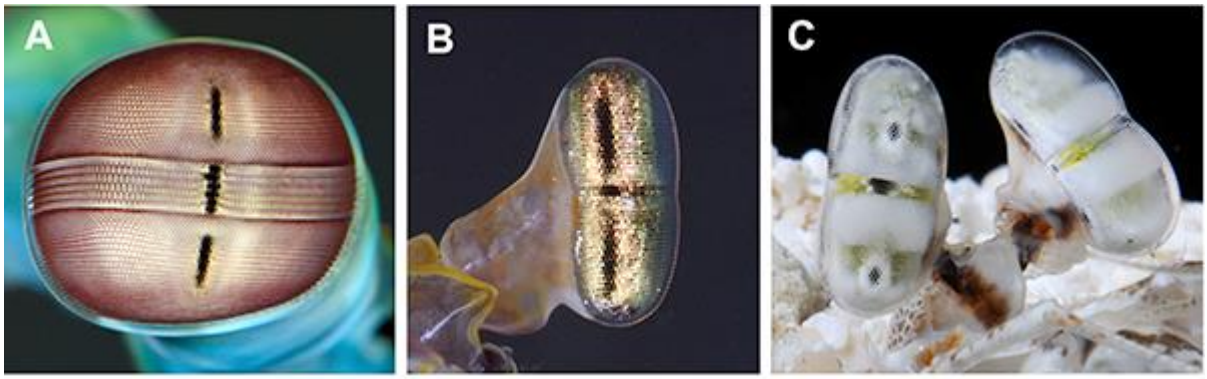

Fig. 2. Images of the compound eyes of three different stomatopod species. (a) The eye of gonodactyloid *O. scyllarus*, which has a globular shape and distinct six-row midband. All three pseudopupils are easily visible. (b) The eye of squilloid *Squilla empusa*, which has a long, bilobed structure and only two midband rows. All three pseudopupils are visible. (c) The eyes of lysiosquilloid *Lysiosquillina sulcata*, which are long and bilobed again but there are now six midband rows. Three pseudopupils can be seen in each eye. Taken from Cronin *et al.*, 2017.

The apposition structure of the eye means that each ommatidial facet is optically isolated and should view a slightly different area in space (Nilsson, 1983). Despite this, the skew of the ommatidial angles and the tripartite design allow the midband and several rows of each hemisphere to view the same area (Marshall, 1988). Over 70% of the eye views this narrow band of approximately 10°, which results in three visible pseudopupils when viewing the eye from this angle (Fig. 2) (Marshall, 1988; Marshall *et al.*, 2007). This gives each eye trinocular vision, with three overlapping visual fields and thus potentially stereoscopic single-eyed depth perception. Despite this, it is assumed that only the hemispheres are involved with depth perception; potentially acting together as rangefinders to direct the raptorial strike, while freeing up the overlapping midband to analyse other visual stimuli, such as spectral information and light polarization (Cronin *et al.*, 2017; Marshall, 1988). For this reason, stomatopod eyes are constantly moving and rotating to scan their surroundings with the midband in order to detect information on colour and polarization (Cronin *et al.*, 2017; Marshall, 1988; Marshall *et al.*, 2007).

The hemispheres provide a large visual field and are responsible for the perception of depth, contrast, shape, and motion - making these regions essential for tracking objects and directing ocular scan and fixation movements (Cronin *et al.*, 1992, 2017). The peripheral ommatidia of stomatopods have the same basic structure as the ommatidia of other apposition-eyed crustaceans, and they have a constant structure throughout the eye (Fig. 3a) (Cronin *et al.*, 2014, 2017; Marshall, 1988; Marshall *et al.*, 1991a). The major

photosensitive structure of the ommatidia, the rhabdom, is made up of interdigitating photoreceptive microvilli protruding from the eight retinular cells. The rhabdom is separated into two layers: the shorter, distal layer is constructed from the eighth retinular cell (R8), whereas the longer, proximal layer is built from the remaining seven retinular cells (R1-7) (Marshall, 1988; Marshall *et al.*, 1991a). The R8 cell usually makes up only 5-10% of the total length of the rhabdom (Marshall, 1988). The microvilli of the hemispheric R8 cells are aligned in two mutually orthogonal directions, but in the R1-7 layer (often referred to as the main rhabdom), cells R1, 4, and 5 each position their microvilli in one direction while cells R2, 3, 6, and 7 each position them perpendicular to this. These two retinular cell groups integrate their microvilli to form alternating layers of perpendicular microvilli (Fig. 3a-d) (Marshall, 1988; Marshall *et al.*, 1991a).

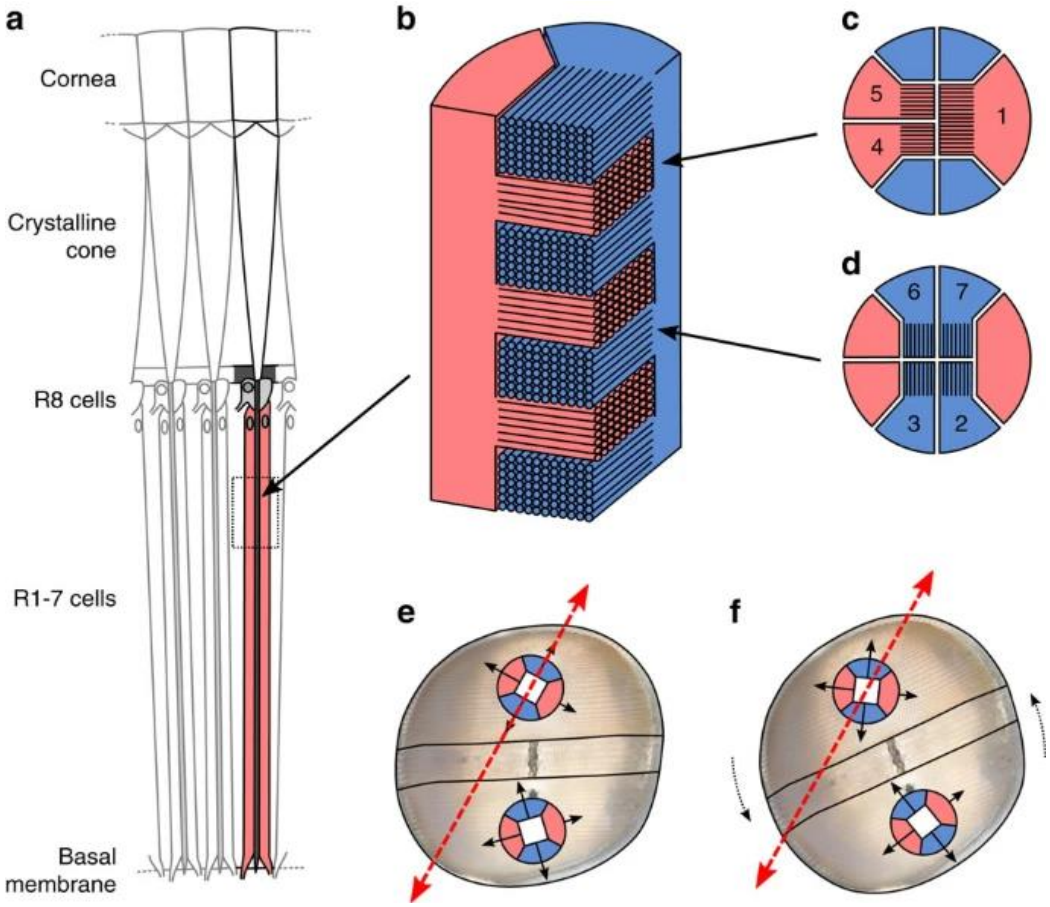

Fig. 3. (a) Diagram of a longitudinal section through a typical stomatopod eye hemisphere, displaying the structure of peripheral ommatidia. This includes the rhabdom, which is made up of the distal R8 cell and the proximal R1-7 cells. (b) Two retinular cells (coloured pink and blue) each projecting unidirectional microvilli to create alternating layers of perpendicular microvilli within the rhabdom. (c) The direction microvilli are positioned in the layers formed by R1, 4, and 5 cells (coloured pink). (d) The perpendicular direction microvilli are positioned in the layers formed by R2, 3, 6, and 7 cells

(coloured blue). (e) The bidirectional positions of microvilli in the main rhabdom of the dorsal and ventral hemispheres, whose overall microvillar orientation is rotated 45° to the other. The red dashed arrow depicts the angle of incoming polarized light, to which the dorsal microvilli are optimally aligned for maximal detection. (f) The eye has been rotated 22.5° so that both sets of dorsal and ventral microvilli are now maximally misaligned with the angle of incoming polarized light, for minimal detection. Taken from Daly *et al.*, 2016.

There is a plane of symmetry along the midband so that ommatidia on either side are mirror images of each other; in two-row midbands the line of symmetry exists between these two rows, but in six-row midbands it exists between the second and third rows. In addition to this, in species with six midband rows there is a rotational symmetry between the dorsal and ventral hemispheres, so that the microvilli in either hemisphere are rotated 45° to each other (Fig. 3e-f) (Marshall *et al.*, 1991a). Most impressively, these intricate and exact features make it possible for the R1-7 layer to detect the linear polarization of light, as the retinular cells are maximally sensitive when their microvilli are parallel to the angle of polarization of the incident light. As both retinular cell groups in this layer project microvilli in one axis, they respond most strongly to light polarized at this angle. In contrast, the R8 cell extends microvilli in two (perpendicular) axes, and is thus effectively insensitive to light polarization (Cronin *et al.*, 2017; Marshall, 1988; Marshall *et al.*, 1991a). By possessing alternating orthogonal microvilli in peripheral main rhabdoms that are then rotated 45° to the opposite hemisphere, coupled with the ability to rotate their eyes up to 70°, the stomatopod is able to perceive any angle, as well as the degree, of linear polarized light (Cronin *et al.*, 2017; Marshall *et al.*, 1991a).

The midband ommatidia of six-row stomatopods not only have significant differences from this structure but also exhibit variation between the rows (Fig. 4, 6a). The first major difference is in the increased size of the ommatidia, so that they take up a disproportionately large area of the eye. In gonodactyloids, midband ommatidia are 10% longer and twice as wide as hemispheric ommatidia, and the lysiosquilloids show some increase in width as well (Marshall, 1988; Marshall *et al.*, 1991a). The ommatidia of rows 1-4 (known as the dorsal rows) have a number of unique adaptations in the main rhabdom that allow them to analyse the spectral properties of light, providing six-row stomatopods with colour vision - one of the only known cases in marine invertebrates. The first major distinction is that the R1-7 layer of the rhabdom is split into two tiers of similar length (Fig. 4, 6a), with the microvilli of cells R1, 4 and 5 forming one tier and the microvilli of cells R2, 3, 6 and 7 forming the other (Cronin *et al.*, 2017; Marshall, 1988; Marshall *et al.*, 1991a, 1991b). It has been suggested that these cells were evolutionarily preadapted to work together due to their identical microvillar direction (Cronin *et al.*, 2017). Apart from the increase in size, the R8 cells of the dorsal rows

have a very similar structure to the peripheral R8 cells (Cronin *et al.*, 2017; Marshall, 1988; Marshall *et al.*, 1991a).

The second major adaptation is that in rows 2 and 3, strongly coloured photostable filters are found at the junctions between the R8 layer and the distal tier, and between the distal and proximal tier (Fig. 4, 6a). These are known as intrarhabdomal filters and are made up of electron-dense vesicles which contain carotenoid or carotenoprotein pigments (Cronin *et al.*, 1994a; Marshall, 1988; Marshall *et al.*, 1991a, 1991b; Porter *et al.*, 2010). Not all species possess all four filter types with some missing one or both of the proximal filters, however both distal filters are always present (Cronin *et al.*, 1994a; Marshall *et al.*, 1991a, 1991b; Porter *et al.*, 2010). The final important alteration is that the microvilli of each R1-7 cell are positioned in an orthogonal bidirectional manner, rather than the unidirectional arrangement in the hemispheric main rhabdoms. In addition, the layers of microvilli are less regular with more densely packed microvilli. These modifications, once again, make the R1-7 cells of the dorsal rows polarization insensitive (Cronin *et al.*, 2017; Marshall *et al.*, 1991a).

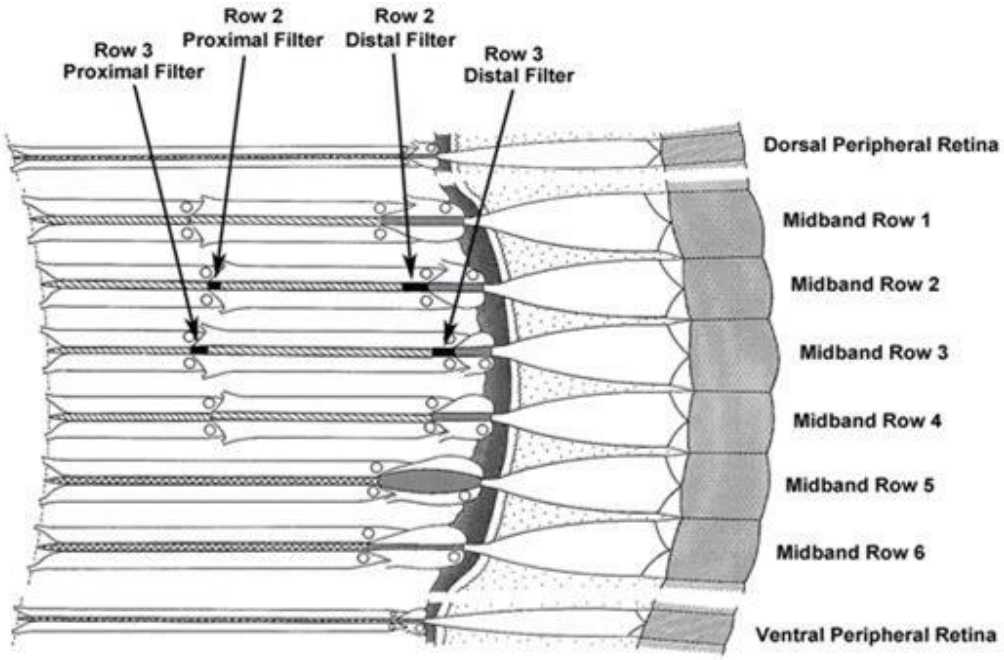

Fig. 4. Diagram of a longitudinal section through a typical stomatopod eye with a six-row midband, depicting the structure of the retina. This includes the six midband rows and peripheral ommatidia on either side of the midband. At the surface of the retina is the cornea (shaded outer layer), which is followed by the crystalline cones (white funnels). Immediately below this is the R8 layer then the R1-7 layer, together making up the rhabdom. Midband rows are numbered 1-6, from dorsal periphery to ventral periphery. Rhabdomal tiers of the R1-7 layer in midband rows 1–4 are visible, and intrarhabdomal filter positions in rows 2 and 3 are shown and labelled. Taken from Porter *et al.*, 2010.

Rows 5 and 6 (known as the ventral rows) of the midband have a more similar structure to the hemispheric ommatidia but there are still significant changes from these ommatidia and from rows 1-4. The most notable differences are in the R8 cells, which are abnormally long, taking up 20% of the entire length of the rhabdom (Fig. 4, 6a), and which project microvilli in a single direction. The R1-7 part of the rhabdom is then very similar to the peripheral rhabdoms, with the microvilli arranged ±45° (depending on the retinular cell e.g. R1, 4, 5 or R2, 3, 6, 7) to the direction of the R8 microvilli in the same row (Marshall, 1988; Marshall *et al.*, 1991a). There is another line of rotational symmetry between these two rows with row 6 microvilli rotated 90° from row 5 microvilli, so that the row 5 R8 microvilli are parallel to the midband, but the row 6 R8 microvilli are perpendicular (Marshall *et al.*, 1991a). Both the R1-7 layer and the R8 layer (with its unidirectional microvilli) in rows 5 and 6 are sensitive to linear polarization. As with the two hemispheres, the rotated microvilli of row 5 compared to row 6 ensure an extensive analysis of polarized light. This results in three spectral classes of polarization receptors: two blue-green classes (one in the R1-7 cells of the hemispheres and one in the R1-7 cells of the ventral rows) and one UV class (in the R8 cells the ventral rows) (Cronin *et al.*, 2017; Marshall, 1988; Marshall *et al.*, 1991a). It has been shown in some species that the UV sensitive R8 cell microvilli of rows 5 and 6 are birefringent filters that act as quarter-wave retarders on circular polarized light, thus converting it to linear polarized light as it passes through to the underlying R1-7 layer. The microvilli in this layer detect this light and its angle of polarization, making them functionally sensitive to circular polarized light, but mechanically to linear (Chiou *et al.*, 2008; Cronin *et al.*, 2014). This is the first documented use of a receptor for one visual modality (UV sensitivity) being used as a filter for another (circular polarization sensitivity) (Cronin *et al.*, 2014). As a testament to their visual proficiency, stomatopods are the only known animal able to detect circular polarized light (Chiou *et al.*, 2008; Cronin *et al.*, 2014, 2017; Gagnon *et al.*, 2015).

Stomatopods possessing midbands of two rows, or very rarely three rows, do not show this level of complexity, with midband ommatidia that are structurally undifferentiated from peripheral ommatidia, despite still having larger rhabdoms and facets (Cronin *et al.*, 2017; Marshall *et al.*, 1991a, 2007; Schönenberger, 1977). The dorsal hemisphere is still a mirror image of the ventral hemisphere, however no rotational symmetry is present in these stomatopods (Cronin et al., 2017; Marshall et al., 1991a). In some squilloid species, the rhabdomal structure of all ommatidia has even become simplified, with the R8 cell essentially becoming degenerate (Marshall *et al.*, 1991a; Schönenberger, 1977). Other species, however, apparently have a fully-formed R8 cell so this trend is not constant across two-row stomatopods (Cronin, 1985). This undifferentiated midband does not appear to

expand the visual capabilities of the hemispheres in any capacity (Cronin *et al.*, 1994c, 2017), leading toward theories that the remaining midband rows are vestigial, ancestral traits (Harling, 2000). Phylogenetic analyses based on morphological, physiological, and genetic data indicate that the ancestor to Stomatopoda already had a six-row midband and four intrarhabdomal filters. This suggests that some stomatopods lost visual complexity, perhaps when moving to darker habitats or becoming nocturnal (Cronin *et al.*, 2014, 2017; Harling, 2000; Porter *et al.*, 2010). Focus will now be placed on the physiological functions and spectral capabilities of six-row midbands, with no further discussion of less complex midbands.

1.3. Physiology

It was hypothesised as soon as the ommatidial ultrastructure of gonodactyloids was first described using light microscopy and TEM, that rows 1-4 of the midband (with their tiered rhabdoms) function to provide some form of spectral sensitivity, if not true colour vision (Marshall, 1988). Microspectrophotometry (MSP) and electrophysiological intracellular recordings on six-row stomatopods have since revealed the presence of up to 16 distinct photoreceptor classes, with 12 being present just in the first four midband rows (Fig. 6) (Bok *et al.*, 2014; Cronin & Marshall 1989a, 1989b; Marshall & Oberwinkler, 1999; Thoen *et al.*, 2014, 2017a). Within the visible spectrum (400-700 nm), the distal and proximal tiers of rows 1-4 each contain their own photoreceptor type (totalling eight), while the main rhabdom of rows 5 and 6 possess another, and the peripheral main rhabdoms have one more - for a total of 10 spectral classes, each with their own visual pigment peak absorbance (λ_{max}) within the range 400-550 nm. Within the tiered rhabdoms, the distal tier photopigment consistently absorbs at slightly shorter wavelengths than the corresponding proximal tier photopigment, with peak absorbance generally around 25 nm lower (Cronin & Marshall 1989a, 1989b; Cronin *et al.*, 2014, 2017; Marshall *et al.*, 1991b).

The sensitivity spectra of the two photoreceptor classes in the main rhabdoms of the ventral rows and the periphery both have broad and flat-topped functions, generally peaking in the blue-green part of the spectrum (Fig. 5, 7c) (Cronin & Marshall 1989a, 1989b; Cronin *et al.*, 2014, 2017). The remaining six photoreceptor classes are all sensitive to the UV spectrum of light, each with unique sensitivity functions within 300-400 nm (Fig. 6). They are present only in the R8 cells of the rhabdoms, with one type found in the peripheral ommatidia, another in the two ventral rows, while each row of the four dorsal rows contains a unique UV photoreceptor type (Bok *et al.*, 2014; Cronin *et al.*, 1994d, 2014, 2017; Marshall & Oberwinkler, 1999; Thoen *et al.*, 2017a). The hemispheres and ventral rows do not appear

to process chromatic information and are not involved in the analysis of spectral properties (Cronin *et al.*, 2017; Marshall *et al.*, 2007). In comparison, two-row stomatopods only appear to have one photoreceptor class and although filter-mediated contrast detection, or even colour discrimination, is possible with a single photopigment, they are likely monochromatic (Cronin, 1985; Lunau, 2014; Marshall, 1988).

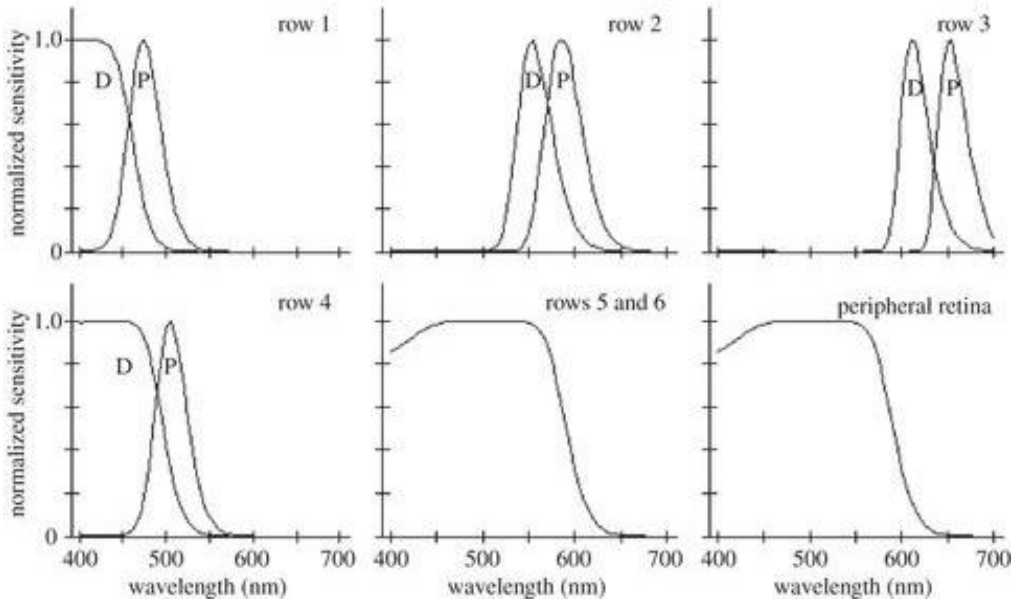

Fig. 5. Normalised sensitivity functions of the 10 photoreceptor classes within the main rhabdoms of gonodactyloid *O. scyllarus*. These functions were calculated using MSP measurements of visual pigment absorbance spectra, physical length of each receptor class, and a visual pigment density of 0.008 density units per micrometre. For midband rows 2 and 3, MSP measurements of total intrarhabdomal filter absorbance were also factored in. Within the tiered rows (rows 1-4) there are two narrowed sensitivity functions, with the distal tier (D) uniformly positioned at shorter wavelengths than the proximal tier (P). The absorbance spectra of R8 cells were not available for these calculations, but they may well narrow the broader functions of row 1 and 4 distal tiers. The broad and flat-topped sensitivity functions in the untiered rhabdoms (rows 5 and 6, periphery) are due to self-screening by the photopigments in these long main rhabdoms. Taken from Cronin *et al.*, 2014.

Surprisingly, molecular genetic research on retinular cells has shown that the number of opsin transcripts in the eye massively exceeds the number of spectral classes. In both *Pseudosquilla ciliata* and *Neogonodactylus oerstedii* (which both have up to 16 spectral classes) 33 expressed transcripts were sequenced (Porter *et al.*, 2013, 2020), and even in the squilloid *Squilla empusa* which only has one photoreceptor class, at least six transcripts were identified (Cronin *et al.*, 2010; Porter *et al.*, 2009). Within the visible part of the spectrum, there were many more opsin transcripts (31 in *P. ciliata*, 30 in *N. oerstedii*) than

spectral classes (10), thus there must be coexpression of several middle-wavelength sensitive (MWS) and/or long-wavelength sensitive (LWS) opsins in the same photoreceptor class retinular cells. In the UV spectrum, however, only two opsin transcripts (a third was identified as a potential pseudogene in *N. oerstedii*) for short-wave/ultraviolet sensitive (SWS/UVS) opsins were identified, despite the presence of up to six UV spectral classes (Bok *et al.*, 2014; Porter *et al.*, 2013, 2020). This number of spectral classes is achieved by differential filtering of these two photopigments, by filters found in the crystalline cones and constructed from numerous mycosporine-like amino acid (MAA) pigments (Bok *et al.*, 2014). These filters act as long-pass, short-pass (the only recorded example of a short-pass optical filter in nature), and even notch filters on incoming light to create the six photoreceptor types in the underlying R8 cells, with different absorbance maxima within the range 310-380 nm (Bok *et al.*, 2014; Cronin *et al.*, 2014; Marshall & Oberwinkler, 1999; Thoen *et al.*, 2017a).

As has been documented before among arthropods, it is believed that rampant duplication and subsequent diversification of opsin genes has led to this vast amount of different opsins in the same photoreceptor class (Cronin *et al.*, 2010; Porter *et al.*, 2009, 2020). Possible theories as to how stomatopods are able to maintain narrow absorption spectra in photoreceptors with multiple visual pigments include: that some opsin transcripts remain untranslated or the opsin protein is non-functional; one of the expressed opsins dominates the photopigments in a photoreceptor type; and that some of the expressed opsins have non-visual functions, among other hypotheses (Porter *et al.*, 2020). The evolutionary advantage of such a varied complement of opsins remains unproven, but some speculate that frequent duplication of opsin genes may have enabled such extreme photoreceptor diversity to evolve (Cronin *et al.*, 2010).

The structure of the four dorsal ommatidia is extremely important in the spectral vision of stomatopods. When light enters the rhabdom it must pass through three successive photoreceptive regions (R8 layer, distal tier, proximal tier) that absorb progressively longer wavelengths of light (Cronin & Marshall 1989a, 1989b; Cronin *et al.*, 2014, 2017; Marshall *et al.*, 1991b). The absorbance ranges of corresponding distal and proximal tier photopigments (Fig. 5, 7b), which both lie within violet to green wavelengths of the visible spectrum, often overlap. As a result, when the distal tier absorbs these shorter wavelengths, they are effectively removed from the spectrum making this tier a long-pass filter. Thus, the proximal tier can only absorb the longer wavelengths within its absorption range in its falling limb, effectively shifting its sensitivity to longer wavelengths. This is known as serial filtering (Cronin & Marshall 1989a; Cronin *et al.*, 1994b, 2014; Marshall *et al.*, 1991b). The R8 layer may also act as a long-pass filter on the row 1 (which has a relatively long R8 cell to

potentially enhance this function) distal tier, which absorbs at short wavelengths (Fig. 6). Furthermore, the crystalline cone UV filter may perform the same function for the row 4 distal tier, while working as a short-pass filter for the R8 cell (Bok *et al.*, 2014; Cronin *et al.*, 1993, 2014; Marshall *et al.*, 1991b).

The intrarhabdomal filters are present to further enhance this function in rows 2 and 3, as these spectral filters remove all shorter wavelengths of light, so that the underlying photopigments can only absorb with their long-wavelength tail. This pushes the green-sensitive photopigments in these tiers to absorb much longer wavelengths, especially the proximal tier as the proximal filter usually absorbs longer wavelengths than the distal filter (Cronin *et al.*, 1994a, 2014; Marshall *et al.*, 1991b, 2007). This results in a 40-75nm difference between sensitivity peaks of the tiers as opposed to 25 nm for the isolated visual pigments of the tiers (Fig. 5, 7) (Cronin & Marshall 1989a, 1989b; Cronin *et al.*, 1994b; Marshall *et al.*, 1991b). This is not possible with serial filtering alone, but intrarhabdomal filters enable stomatopods to sample wavelengths from 300 nm all the way up to 720 nm, in extreme cases (Cronin *et al.*, 2014; Marshall *et al.*, 2007; Thoen *et al.*, 2014). The exact spectral range of each photoreceptor class in the four dorsal rows depends on the species and phylogenetic group, but in general from distal to proximal tier: row 1 covers violet and blue, row 2 yellow and orange, row 3 orange and red, and row 4 blue and cyan (Fig. 6) (Cronin & Marshall 1989a, 1989b; Cronin *et al.*, 2017).

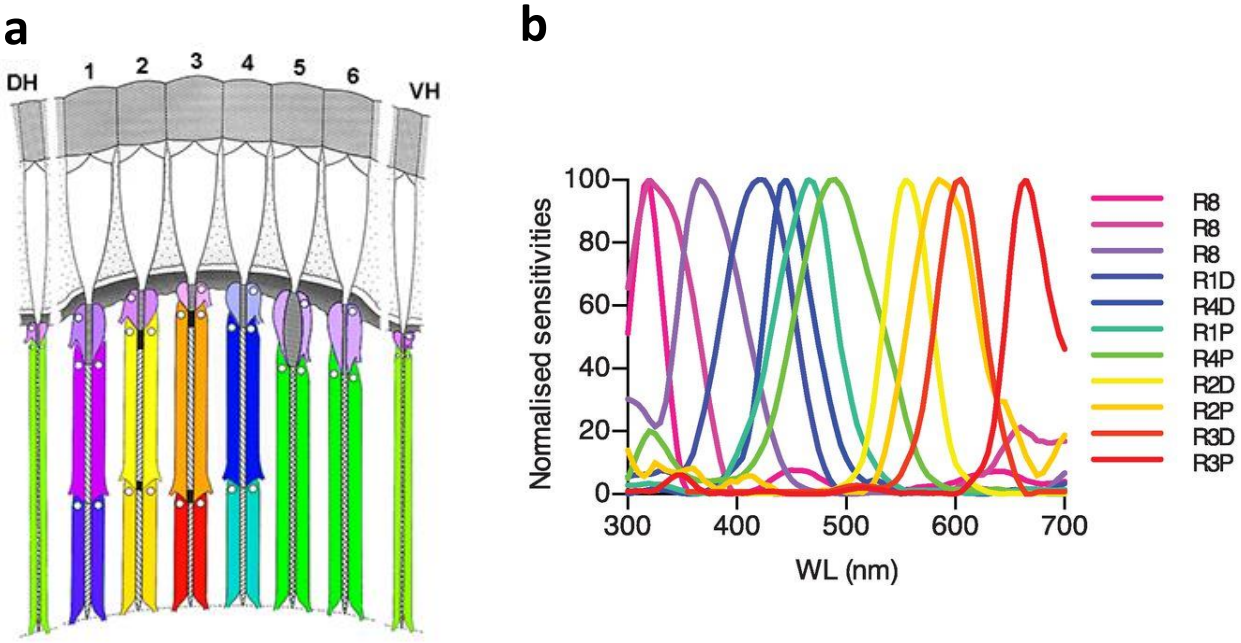

Fig. 6. (a) Diagram of a longitudinal section of the gonodactyloid *N. oerstedii* stomatopod eye, depicting the structure of the six midband rows and peripheral ommatidia on either side of the midband. At the surface of the retina is the cornea (shaded outer layer), which is followed by the

crystalline cones (white funnels). Immediately below this is the R8 layer then the R1-7 layer, together making up the rhabdom. Midband rows are numbered 1-6, from dorsal hemisphere (DH) to ventral hemisphere (VH). Tiering of the main rhabdom in rows 1–4 is shown, and intrarhabdomal filter positions in rows 2 and 3 are visible as black rectangles. Each photoreceptor class is coloured to match the wavelength it is maximally sensitive to, apart from the UV sensitive R8 cells where differing shades of violet are used. Taken from Cronin *et al.*, 2017. (b) Normalised spectral sensitivities of gonodactyloid *Haptosquilla trispinosa* photoreceptor classes, acquired from intracellular electrophysiological recordings. Once again, the colour of each sensitivity function indicates the spectral appearance of the peak absorbance wavelength, apart from the R8 cell functions which are coloured varying shades of pink and violet. Taken from Thoen *et al.*, 2014.

Serial and intrarhabdomal filtering are also vital in narrowing the absorbance ranges of the underlying photoreceptor class, by efficiently removing shorter wavelengths from the equation; otherwise the sensitivity functions would all overlap, reducing the ability for hue discrimination (Cronin & Marshall 1989a, 1989b; Cronin *et al.*, 1994a, 1994c, 2014; Marshall *et al.*, 1991b). Retinoid-based visual pigments have broad absorbance spectra, and so only 3-4 photoreceptor classes can cover the visible light spectrum (400-700nm) without sacrificing spectral discrimination (Barlow, 1982; Bowmaker, 1983), yet stomatopods have 16 classes to contend with. In fact, the long untiered rhabdoms actually have broader sensitivity functions than the visual pigments alone due to self-screening, potentially exacerbating the issue (Cronin *et al.*, 2014; Marshall *et al.*, 1991b). By narrowing and sharpening these spectra, stomatopods have created a viable visual system with up to 16 separate, narrow peaks across 300-700 nm, spaced fairly evenly apart (Fig. 6b) - suggesting fine spectral discrimination (Cronin & Marshall 1989a, 1989b; Cronin *et al.*, 2014; Thoen *et al.*, 2014, 2017b). Alongside this, as the photoreceptors are already sorted into strict spectral classes within the retina, less processing is needed in the brain as a result, so spectral analysis should be rapid (Cronin *et al.*, 2014; Thoen *et al.*, 2014).

The drawback of this filtering, due to the intrarhabdomal filters especially, is a reduction in the amount of photons reaching the underlying visual pigment, which severely reduces sensitivity (Cronin *et al.*, 1994a, 1994c, 2014; Marshall *et al.*, 1991b). This is particularly prominent in the row 3 proximal tier red photoreceptor, as longer wavelengths rapidly attenuate with ocean depth. Detection of longer wavelengths must be ecologically important as many gonodactyloids inhabiting shallow ranges, where light intensity and spectrum width are essentially the same as that above-water, have kept these long-wavelength filters despite the cost. The reduction in sensitivity is clearly too high in deeper-living species, which have lost this filter, where there is little long-wavelength light to detect anyway (Cronin *et al.*, 1994a, 1994c, 2014).

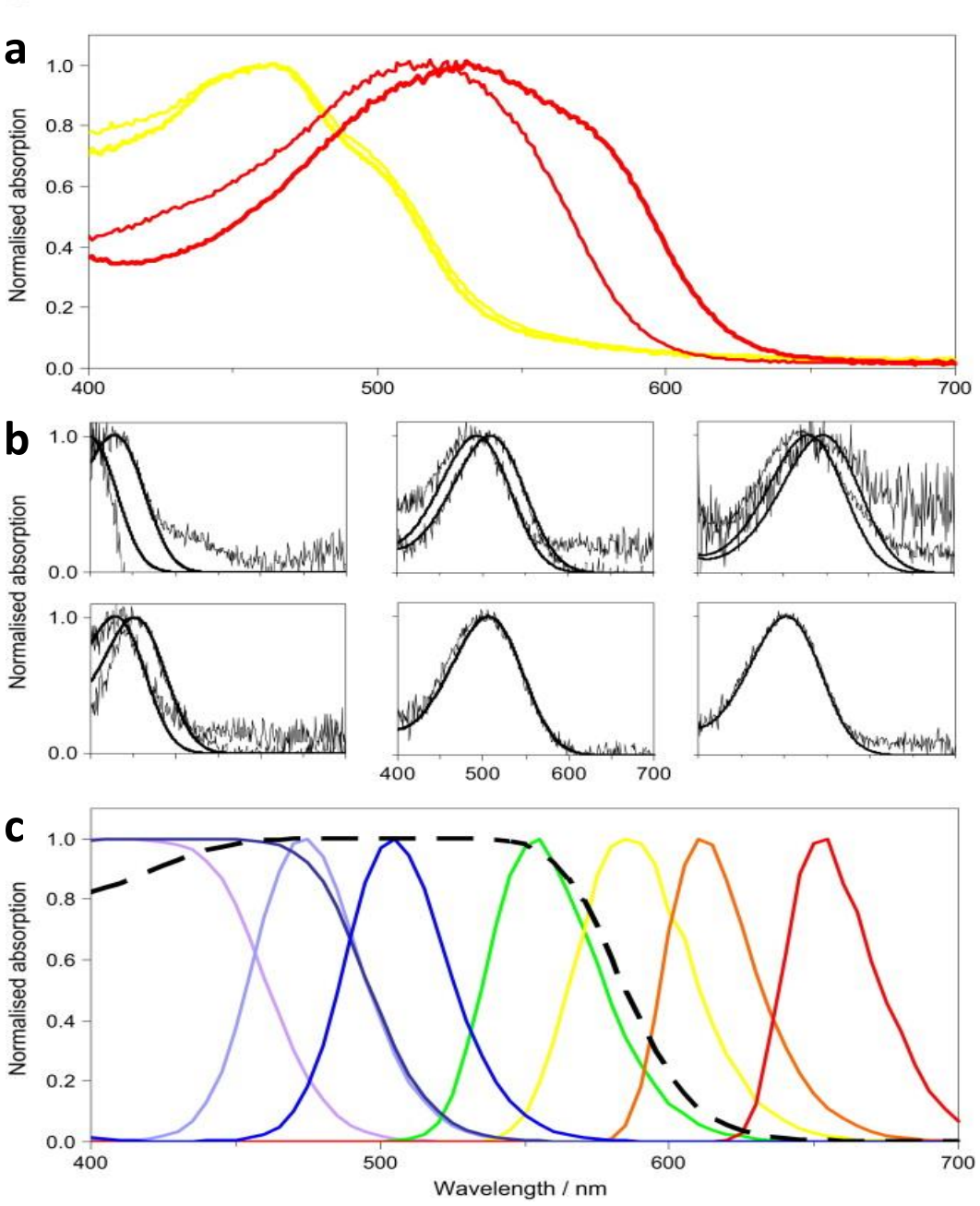

Fig. 7. (a) Normalised absorbance spectra of *O. scyllarus* intrarhabdomal filters taken from MSP measurements. From left to right the functions represent: row 2 distal filter, row 2 proximal filter (very similar to the distal), row 3 distal filter, row 3 proximal filter. The colour of the functions approximately matches the colour of the filters themselves i.e. the row 2 filters are both yellow and the row 3 filters are both red. (b) Normalised absorbance spectra of *O. scyllarus* visual pigments taken from MSP measurements. In the top row, from left to right the panels represent the photopigments in row 1 of the midband, row 2, and row 3. In the bottom row, from left to right the panels represent photopigments in row 4, rows 5 and 6, and the hemispheres. In rows 1-4 there are a pair of functions, where the function at shorter wavelengths represents the distal tier pigment and the function at longer wavelengths represents the proximal tier pigment. (c) The spectral sensitivities of the *O. scyllarus* photoreceptor classes within the visible spectrum, calculated from the results of (a) and (b). The

dashed line function represents rows 5 and 6, which is close to the hemisphere values. From left to right the coloured functions represent: row 1 distal tier, row 4 distal tier, row 1 proximal tier, row 4 proximal tier, row 2 distal tier, row 2 proximal tier, row 3 distal tier, row 3 proximal tier. The colour of the coloured functions approximately matches the spectral appearance of the peak absorbance wavelength. Taken from Marshall *et al.*, 2007.

Just as different species of stomatopods will possess different sets of photopigments depending on their ecology and phylogeny (Cronin & Marshall 1989a, 1989b; Cronin *et al.*, 1994b, 1994c; Marshall *et al.*, 2007), they will also contain different sets of intrarhabdomal filters (Fig. 8). The first difference is in the number of filter classes which varies from two to four, depending on if both, one, or neither proximal filter in rows 2 and 3 are absent. As a general rule, shallow-living gonodactyloids possess all four filter types, whereas lysiosquilloids and deep-living gonodactyloids are often missing one or both proximal types. As mentioned, the intrarhabdomal filters induce a severe cost to sensitivity, which is exacerbated with depth as ambient light levels are reduced and long wavelengths are rapidly attenuated. Thus, proximal filters are removed with depth of the species to gain sensitivity at the expense of spectral coverage, and the same often happens in species living in less colourful environments (like the lysiosquilloids), murky or turbid water, and nocturnal species (Cronin *et al.*, 1994c, 2014; Porter *et al.*, 2010). In fact, the trend continues onto the even deeper-living two-row squilloids and midband-less bathysquilloids (Harling, 2000) which have abandoned all filters and rhabdom tiering, becoming essentially monochromatic but with much greater sensitivity to light (Cronin *et al.*, 1994c; Van Der Wal *et al.*, 2017).

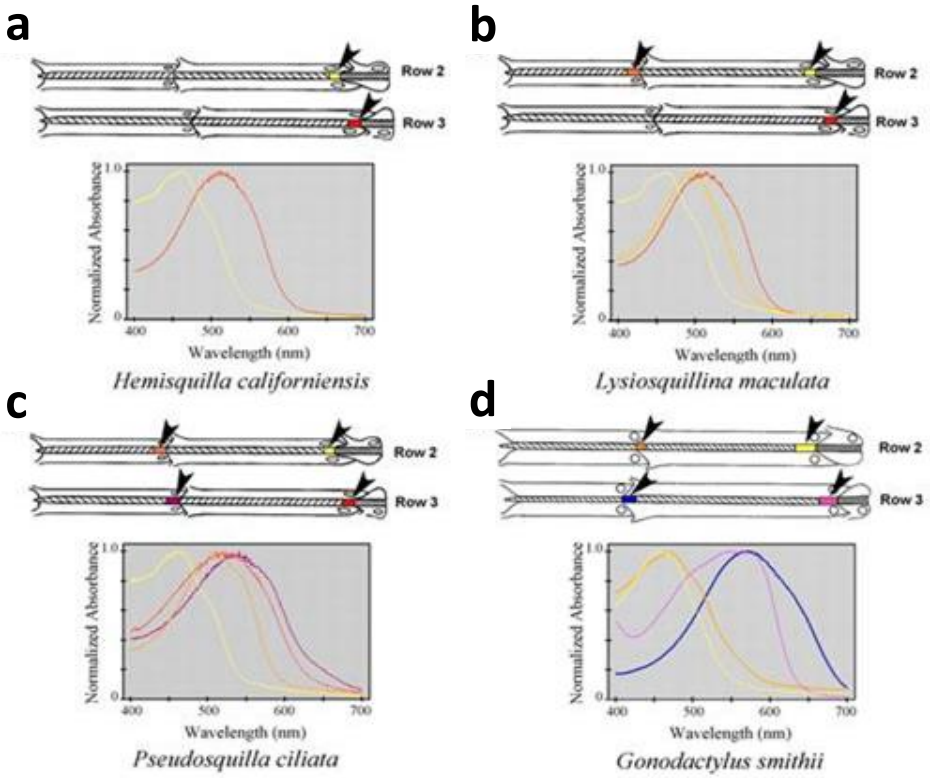

Fig. 8. Diagrams of intrarhabdomal filter arrangement in midband rows 2 and 3, and the normalised absorbance spectra of each filter for four stomatopod species. Filters are represented on the diagrams by coloured rectangles and black arrows indicate their position. The colour of the filters matches their corresponding absorbance function, and this colour itself indicates the spectral appearance of the real-life filters. (a) *H. californiensis*, which only possesses both distal filter classes. (b) *Lysiosquillina maculata*, which possesses two distal filter classes and the row 2 proximal filter class. (c) *Pseudosquilla ciliata*, which possesses all four filter classes. (d) *Gonodactylus smithii*, which possesses all four filter classes. Taken from Porter *et al.*, 2010.

If the proximal intrarhabdomal filter is absent, the distal filter of that row is extremely densely packed with screening pigment - this is likely to push the sensitivities of the underlying photoreceptors to even longer wavelengths as there is no second filter to enhance the process. The lack of proximal filter means that the distal and proximal tiers have closer sensitivity functions than in species with two (different) filters, which weakens the potential for spectral discrimination (Marshall *et al.*, 1991b). Taxonomic-wide studies utilising MSP on these intrarhabdomal filters have revealed the number of filter classes in each filter position: the row 2 distal position has only two classes but the proximal position has seven, whereas both positions in row 3 have three spectral classes, according to most recent data (Cronin *et al.*, 1994a; Porter *et al.*, 2010). As expected, shallow-living families within the Gonodactyloidea present the greatest diversity of filter pigments, especially in longer wavelengths (Cronin *et al.*, 1994a, 1994c, 2014; Porter *et al.*, 2010). If filters in the same row

have similar absorbance spectra, the distal filter is generally shorter and less densely packed with screening pigment than the proximal filter, as this will allow a broader spectrum of light to pass through before being pushed to longer wavelengths by the proximal filter (Marshall *et al.*, 1991b).

When MSP was performed on the intrarhabdomal filters of shallow and deep populations of three stomatopod species, it revealed two things in the deep populations: filters in all positions were shorter and less densely packed with pigment and row 3 filters had blue-shifted absorption spectra as well. These filter modifications allowed more light and a broader spectrum to pass through to underlying photoreceptors (Cronin & Caldwell, 2002). A visual system that can be tuned during development is highly beneficial as planktonic larvae could settle anywhere with variable photic environments before growing into adults (Cronin & Caldwell, 2002; Cronin *et al.*, 2002). Tuning was apparently achieved solely through filters as visual pigments remained constant across populations (Cronin *et al.*, 2002). Postlarval and adult stomatopods are capable of actively shifting the absorption spectra of row 3 filters to shorter wavelengths (and adults can also alter the length of the proximal filter) if they are moved to different photic environments, however row 2 filters cannot be tuned in this way (Cheroske *et al.*, 2006; Cronin *et al.*, 2001). This ability is clearly most useful in species with a large depth range, which have been shown to have more plasticity than shallow-living species. Interestingly, closely related species that now live in shallow intertidal or subtidal habitats retain some plasticity (Cheroske *et al.*, 2006). It has been suggested that the row 2 proximal filter position displays such a high level of spectral class diversity to adapt the underlying photoreceptor to the photic environment of that particular species, as the row 2 filters cannot be actively tuned (Porter *et al.*, 2010). Filters are never removed if an individual moves to a darker habitat, instead, the whole photoreceptor degenerates when absorbing insufficient light. This perhaps indicates it is fairly simple for species to evolutionarily lose midband rows when moving to low-light environments (Cronin *et al.*, 2014; Porter *et al.*, 2010).

1.4. Behaviour

The intricate visual system of six-row stomatopods suggests a visual capacity beyond any other animal in the realms of spectral range, colour discrimination, and polarization sensitivity. However, without behavioural research this is simply conjecture. The basic requirements for colour vision include at least two photoreceptor classes sensitive to different wavelengths of the spectrum and a neural pathway to compare the outputs of these receptors (Kelber *et al.*, 2003; Lunau, 2014). For this reason, neural wiring can give strong evidence towards colour vision (Kelber *et al.*, 2003; Lunau, 2014), however mantis shrimp

neural circuitry is not overly well understood (Cronin *et al.*, 2017; Marshall *et al.*, 2007; Thoen *et al.*, 2017b, 2018).

Investigation of the afferent neurons from the stomatopod eye has not revealed where spectral information is processed in the optic lobe of the brain. Nor has it disproven either of the two major colour-processing system hypotheses: the serial dichromatic theory and the 12-channel binned theory (Thoen *et al.*, 2017b). Many studies posit that mantis shrimps process colour information in a multiple two-channel colour-opponent system, comparing the distal to the proximal tier in each of the four dorsal rows. With the tiers in a corresponding row being placed spectrally adjacent to each other (Fig. 5, 6, 7b) and as there are four of these 'pairs' of sensitivities, the serial dichromatic processing system would give a fine discrimination threshold of 1-5 nm (Fig. 9) (Cronin *et al.*, 2017; Marshall *et al.*, 1991b, 2007; Thoen *et al.*, 2014). Whereas in the 12-channel binned processing system, wavelengths would be detected by the corresponding photoreceptor out of the 12 photoreceptor classes in rows 1-4 (4 R8 cells, 4 distal tiers, 4 proximal tiers). This would result in 12 independent colour channels (or 'bins') without cross-channel comparison, thus producing a form of 'colour recognition' rather than discrimination (Cronin *et al.*, 2017; Thoen *et al.*, 2014, 2017b). This would result in quick and reliable identification of colours without any need for processing delay in the brain, as colour information is essentially pre-processed in the retina, and perhaps the removal of illuminance as a problem in colour constancy (Thoen *et al.*, 2014). Further research using electrophysiology and electron microscopy on the lamina neurons is suggested to obtain more evidence supporting either theory (Thoen *et al.*, 2017b). This leaves behavioural testing to prove the existence of colour vision, of which there is relatively little on mantis shrimps.

Evidence from past behavioural tests has displayed colour vision in many diverse species and is vital to definitively prove if animals can detect and respond to spectral stimuli (Kelber *et al.*, 2003). A version of the grey card experiment (Von Frisch, 1914) was performed on *O. scyllarus*, where individuals were taught to select a coloured cube alongside two grey cubes for a food reward (Marshall *et al.*, 1996). The grey cubes were of various shades so that some would inevitably have the same brightness as the colour cube, to prevent the stomatopod using achromatic cues to make the correct choice. These stomatopods learned to discriminate red, yellow and green cubes from grey, yet surprisingly were unable to do so with blue, for the first evidence of true colour vision in a crustacean (Kelber *et al.*, 2003; Marshall *et al.*, 1996).

Another common colour vision test is to perform choice trials using monochromatic stimuli at two (or more) different wavelengths (Kelber *et al.*, 2003). Individuals of *Haptosquilla*

trispinosa underwent a two-way choice trial between a colour they had been trained to using food rewards and a test colour at varying wavelength intervals within 400-650 nm (Thoen *et al.*, 2014). The stomatopods could reliably discriminate the trained wavelength at intervals of 50-100 nm from the test wavelength, and thus must possess some form of hue discrimination. The ability to discriminate was lost at smaller intervals of 12-25nm displaying a surprisingly coarse discrimination threshold (much worse than that of humans (Koshitaka *et al.*, 2008)) (Fig. 9), especially for a species with up to 10 spectral classes within the visible spectrum (Cronin & Marshall, 1989a, 1989b). Interestingly, this roughly matches the difference in peak absorbance between corresponding distal and proximal tier photopigments (Cronin & Marshall, 1989a, 1989b). This discrimination threshold is far above the 1-5 nm value projected for the serial dichromatic processing system (Thoen *et al.*, 2014), and so Thoen *et al.* (2014) hypothesises that stomatopods may utilise the 12-channel binned processing system. This would explain the poor discrimination ability exhibited in the study of Thoen *et al.* (2014) and perhaps the previous finding from Marshall *et al.* (1996), where individuals could not differentiate blue and grey.

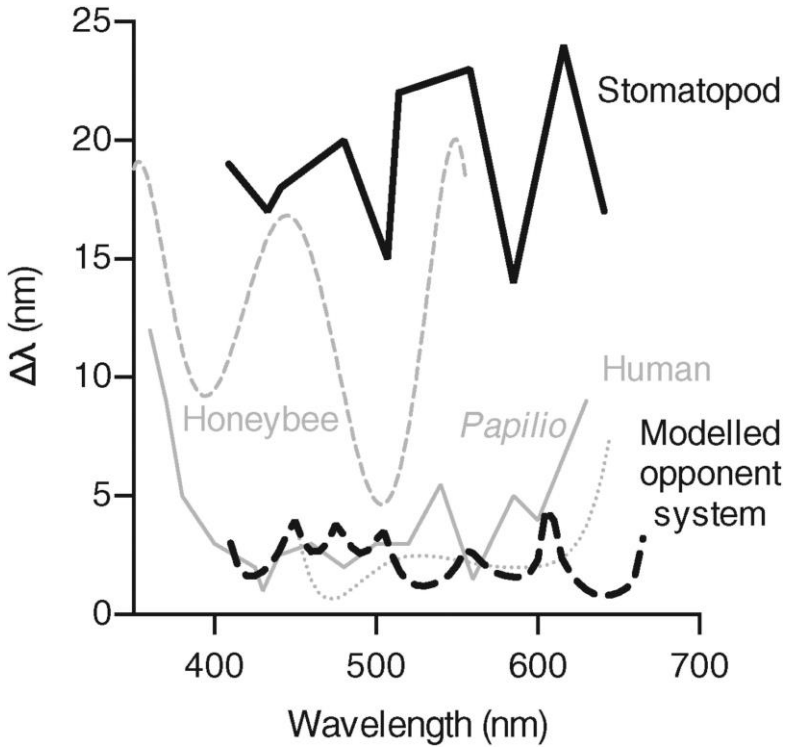

Fig. 9. Spectral discrimination curves of humans (grey dotted line), honeybees (grey dashed line), and *Papilio xuthus* butterflies (grey solid line). For the stomatopod *H. trispinosa*, two spectral discrimination curves are shown: one retrieved from trained choice tests (black solid line), and one modelled on the multiple dichromatic opponency processing system (black dashed line). Taken from Thoen *et al.*, 2014 - figure originally modified from Koshitaka *et al.*, 2008.

A similar procedure was carried out on *H. trispinosa* in another study, however this time using exclusively UV signals - with LEDs emitting narrow-band signals peaking at 314 nm, 351 nm, and 378 nm (Bok *et al.*, 2018). Brightness was controlled for by randomising the intensity of the signals between different settings. Individuals were able to discriminate between 314 nm and 378 nm, and between 351 nm and 378 nm, indicating that mantis shrimps not only detect UV light but have the first known case of polychromatic 'colour' vision in the UV spectrum; meaning they have more than one photoreceptor class within the UV spectrum (Bok *et al.*, 2014, 2018). The 27 nm difference between 351 nm and 378 nm suggests the discrimination capabilities in the UV spectrum may be similar to the discrimination threshold of ~25 nm in certain parts of the visible spectrum for the same species, as shown by the previous experiment (Bok *et al.*, 2018; Thoen *et al.*, 2014). How UV information is processed is not explained by the serial dichromatic hypothesis, but such coarse discrimination in the UV is perhaps further support of a 12-channel binned processing system in stomatopods.

1.5. Aims of the research

As evident thus far, stomatopods with six midband rows have a fantastically complex visual system with many unique adaptations for spectral and polarization vision seen nowhere else in nature. It seems that mantis shrimps have such complex eyes that they must compartmentalise channels of sensitivity for different visual tasks. For example, gaze stabilisation is likely to be driven by motion sensors in the hemispheres (Daly *et al.*, 2016; Gonzales, 2020), and polarization information is processed in the hemispheres and rows 5 and 6 (Cronin *et al.*, 2014, 2017; Marshall *et al.*, 1991a, 2007). This would imply that gaze stabilisation and polarization sensitivity are most likely achromatic as the hemispheres and rows 5 and 6 do not process chromatic information (Cronin *et al.*, 2017; Marshall *et al.*, 2007). This compartmentalisation could go as far as certain spectral (and polarization) channels being associated with certain cues or signals and then perhaps a behavioural response (Chiou *et al.*, 2011; Franklin *et al.*, 2016). For example, *N. oerstedii* (Gonodactyloidea) individuals opposing conspecifics that had had the agonistic UV signal from their meral spot experimentally eliminated, engaged in a higher rate of offensive behaviours (Franklin *et al.*, 2016). In addition to this, female *H. trispinosa* (Gonodactyloidea) individuals were more aggressive to and reluctant to mate with male conspecifics that had had a bright blue, polarized light reflecting signal experimentally removed from their first maxillipeds (Chiou *et al.*, 2011).

In fact, a 12-channel binned processing system may have evolved to enable rapid recognition of certain ecological cues, similar to responses observed in the butterfly *Pieris rapae* to different spectral cues (Daly *et al.*, 2017; Marshall & Arikawa, 2014). In contrast to gaze stabilisation and polarization sensitivity, querying and analysing unknown objects is likely to use the full spectral sensitivity of the chromatic midband. Despite the vast amount of study on the stomatopod visual system, there has been minimal research on the spectral sensitivity of these creatures - even the three behavioural studies mentioned investigated colour discrimination rather than sensitivity (Bok *et al.*, 2018; Marshall *et al.*, 1996; Thoen *et al.*, 2014). Colour discrimination refers to the ability to differentiate between two or more wavelengths based solely on their spectral properties, whereas spectral sensitivity denotes the light intensity required to detect single wavelengths across the spectrum. It is essential that behavioural spectral sensitivity is also well understood, as it will reveal the sensitivity of different stomatopod species to wavelengths across the spectrum, perhaps pointing to evolutionary and ecological significance behind their unique results.

This leads into the purpose of the research presented here: investigating which parts of the eye are used for detecting and identifying a flashing LED stimulus by measuring the spectral sensitivity of this behaviour, and thus whether chromatic (midband) or achromatic (hemispheres) channels are being used to detect this kind of stimulus. The intention was to create an action spectrum for the stomatopod *O. scyllarus* from the blue to red ends of the visible spectrum based on behavioural experiments, similar to those produced for humans, domestic ducks, turkeys and hummingbird hawkmoths (Fig. 10) (Barber *et al.*, 2006; Telles *et al.*, 2014). For quite a number of stomatopod species, photoreceptor sensitivity functions have been measured using MSP or intracellular recordings (Fig. 6b), however the maximum sensitivities of the receptor classes were always normalised (Cronin & Marshall, 1989a, 1989b; Cronin *et al.*, 1994b; Thoen *et al.*, 2014, 2017a). These normalised receptor spectral sensitivities do not reveal the absolute spectral sensitivity that an action spectrum, which are generally measured from behavioural responses, would. Absolute behavioural sensitivities reveal the real-world spectral sensitivities of the whole organism, as opposed to an isolated photoreceptor. With this action spectrum, it would be possible to determine if one or multiple spectral classes were responsible for the sensitivity function produced and whether it originated from the hemispheres or the midband respectively. The test species, *O. scyllarus*, is a gonodactyloid possessing six midband rows (Fig. 2a) with four intrarhabdomal filters (Fig. 7a) (Cronin *et al.*, 1994b, 2014; Marshall *et al.*, 2007). As such, it is very likely that *O. scyllarus* is able to detect wavelengths from the UV to red ends of the spectrum (Cronin *et al.*, 1994b, 2014; Marshall *et al.*, 2007), and engages in complex communication based on spectral body signals like other gonodactyloids, such as *N. oerstedii* (Franklin *et al.*, 2016)

and *H. trispinosa* (Chiou *et al.*, 2011) – something to consider when analysing the spectral sensitivity of this species.

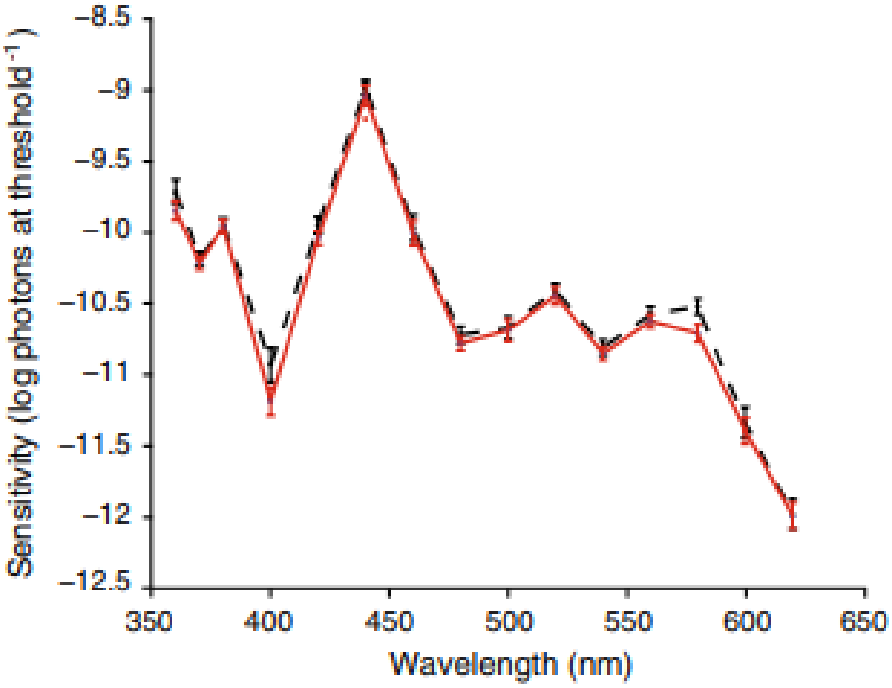

Fig. 10. Spectral sensitivity of the hummingbird hawkmoth *Macroglossum stellatarum* across the UV and visible light spectrum. Sensitivity thresholds determined through trained choice tests. Results presented in two ways: including behaviour where no choice was made (solid red line), and excluding behaviour where no choice was made (dashed black line). Taken from Telles *et al.*, 2014.

Another fundamental aim of this research was to create, trial, and refine an automated system that would be able to train the stomatopods to approach a light stimulus with a food reward. Their sensitivity to different wavelengths would then be tested by determining the threshold light intensity required to initiate the trained response. Although the use of conditioning has been widely used across many animal taxa, including stomatopods, when testing visual capabilities like colour vision (Barber *et al.*, 2006; Bok *et al.*, 2018; Kelber *et al.*, 2003; Marshall *et al.*, 1996; Lind, 2016; Olsson *et al.*, 2020; Telles *et al.*, 2014; Thoen *et al.*, 2014), the use of automated systems for testing any sensory modality is fairly rare. There has been some use of automated systems in testing visual capabilities (Keller *et al.*, 2000; Hemmi, 1999; Vagell *et al.*, 2019), however the potential of these systems has not been fully exploited. This research will hopefully display the efficacy and practicality of automated systems in behavioural studies, and encourage their further use.

2. Methods and materials

2.1. Animal collection and maintenance

In total, 12 individual peacock mantis shrimps (*Odontodactylus scyllarus*) were purchased from an aquarium supplier (Tropical Marine Centre, Bristol) over a period of 10 months. The animals were kept at the University of Bristol in 45 L tropical saltwater aquaria, constructed from 5 mm thick glass and with dimensions 20 x 35.5 x 70 cm. Each tank contained an artificial burrow of diameter 7 cm, constructed from a PVC plastic pipe and wedged into a substrate of sand and small rocks. Larger rocks and artificial seaweed were placed in the aquaria for environmental enrichment (Fig. 11). Saltwater was mixed from dechlorinated tap water and powdered aquarium salt (Premium Reef Salt, Tropical Marine Centre, Bristol), and delivered to each aquarium via a recirculation and filtration system. Each aquarium was supplied with air bubbles delivered through a submerged air-stone. Water temperature was maintained at 25-27 °C, salinity at ~35 ppt, pH level at 7-9, and O_2 density at 6-8 mg/L, while the amounts of nitrite, nitrate, and ammonia were kept at healthy low levels (nitrite: ~0 ppm, nitrate: 0-40 ppm, ammonia: ~0 ppm). To keep these conditions stable, maintenance and water quality checks were performed daily, the aquaria were constantly filtered and aerated, and water changes were carried out when water chemistry left the parameters outlined above.

Fig. 11. Photograph of an *O. scyllarus* test subject in the tank and experimental arena. The burrow pipe is behind the individual. Numerous metal M3-sized dome nuts that served as the food reward receptacles are visible in front of the individual.

Ceiling lights were placed on a timer, switched on from 07:00 to 19:00, to give the stomatopods a semblance of the natural day-night cycle. Additional illumination was provided by a white LED strip light positioned directly above the tanks, which followed a timer from 8:00 to 18:00. Outside of trials, card covers were placed on top of the tanks to shield the mantis shrimp from direct illumination. These measures were followed in order to reduce the occurrence of ‘shell rot’, a condition that is linked to abnormally high light levels in the aquaria. Before the commencement of trials, animals were fed cockles twice a week. Once trials had begun, animals were fed one cockle a week outside of trials, but this was later dropped so that the animals were only given food during trials.

2.2. General concept and system design

To investigate spectral sensitivity in mantis shrimps, it was opted to train individuals through operant conditioning to respond to a spectrally filtered light stimulus to obtain a food reward - in a manner similar to many other behavioural experiments (Barber *et al.*, 2006; Bok *et al.*, 2018; Marshall *et al.*, 1996; Lind, 2016; Olsson *et al.*, 2020; Telles *et al.*, 2014; Thoen *et al.*,

2014). As shown by these experiments, this is typically a very labour intensive process, but well suited to automation. To this end, an automated system was designed by Martin How and Agus Bentlage that could run the necessary trials on the stomatopods and would create a new approach to research spectral sensitivity. A dominant factor of this research was the continual fine-tuning of this automated system, so that an optimal system and corresponding method could be achieved. Due to this, modifications to the system and experimental design were enacted throughout the research, which are documented and explained later, rather than having a set experimental design prior to beginning trials.

The automated system was controlled using a Raspberry Pi single board computer (Raspberry Pi 4B - 4GB, Raspberry Pi Foundation) coupled to a 16-channel servo controller HAT (16-Channel PWM/Servo HAT, Adafruit Industries). These controlled an LED white light stimulus whose intensity could be modified accurately through high frequency (200 Hz) pulse-width-modulation (PWM), and a servo motor (MG996R Digital Servo, TowerPro) that rotated a carousel delivering food rewards. In addition, the Raspberry Pi collected information about mantis shrimp behaviour from a camera with a fish-eye lens (ZeroCam Fisheye NightVision, Raspberry Pi Foundation) mounted above the aquarium, providing a top-down view of the experimental arena. An engineering diagram illustrating this experimental apparatus is shown in Fig. 12. The overall aim was to design an inexpensive modular system that would allow for multiple animals to be trained and tested in parallel with minimal levels of researcher labour. Not only this, but the automated system would also avoid any possible pitfalls of conscious or unconscious bias from human researchers performing manual training, an issue that has been identified on multiple occasions in other studies (Romano *et al.*, 2021; Rosenthal & Lawson, 1964). The intention was that future researchers would be able to utilise this system, with minor alterations, on other test species and for experiments on other visual traits besides spectral sensitivity.

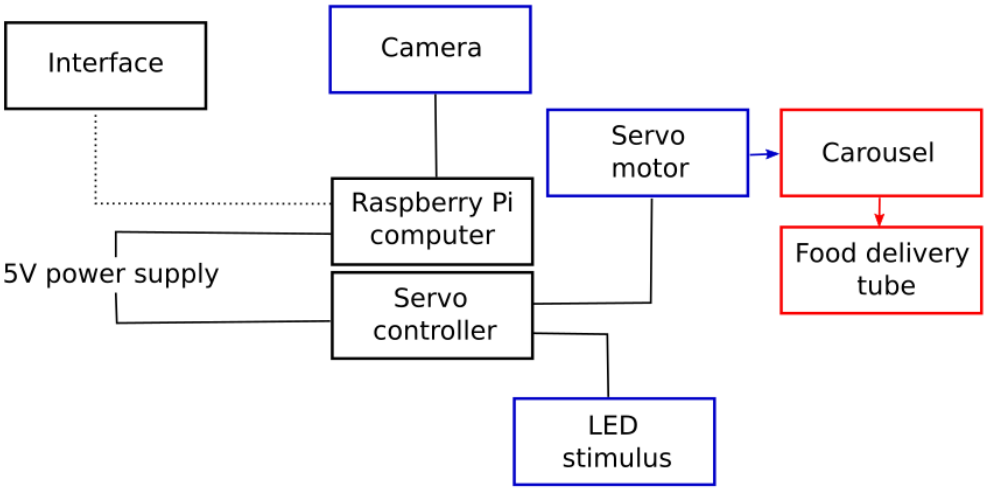

Fig. 12. Engineering diagram of the automated system final design, displaying the connections between the important component parts. Black boxes denote computer components, blue boxes denote computer-connected hardware, and red boxes denote peripheral components. Solid lines represent a physical connection between parts, whereas dotted lines represent an online connection. Arrows indicate a physical effect on the following component rather than just a physical connection.

2.3. Prototype design

The first designs for the structure of the automated system were created on the open-source graphics editor program Inkscape (Fig. 13d), and then individual pieces were cut out of perspex by laser cutting technology. These were then assembled and other necessary components added, to create the finished prototype (Fig. 13a-c). This prototype was tested by running numerous conditioning trials (from now referred to as 'priming trials') on one stomatopod over a number of months, making note of any issues. This functioned as a preliminary study, to determine, not only how well the system operated, but also how well the mantis shrimp responded to the trials and if conditioning was even possible. This solitary stomatopod was housed in a slightly smaller tank than those previously described, before being moved to those larger tanks where the automated system final design was utilised. The prototype was designed to be easily placed onto (and removed from) the front glass wall of the tank, with the food delivery tube protruding into the water (Fig. 13c), to run the trials. The system was always removed from the tank after the session of trials had finished. During trials, the arena was illuminated by two infrared (IR) LEDs that were connected to the servo controller (Fig. 13a) and attached to both sides of the tank with masking tape. To provide power to the system, two external cables were plugged into a mains socket and connected to the Raspberry Pi computer and servo controller.

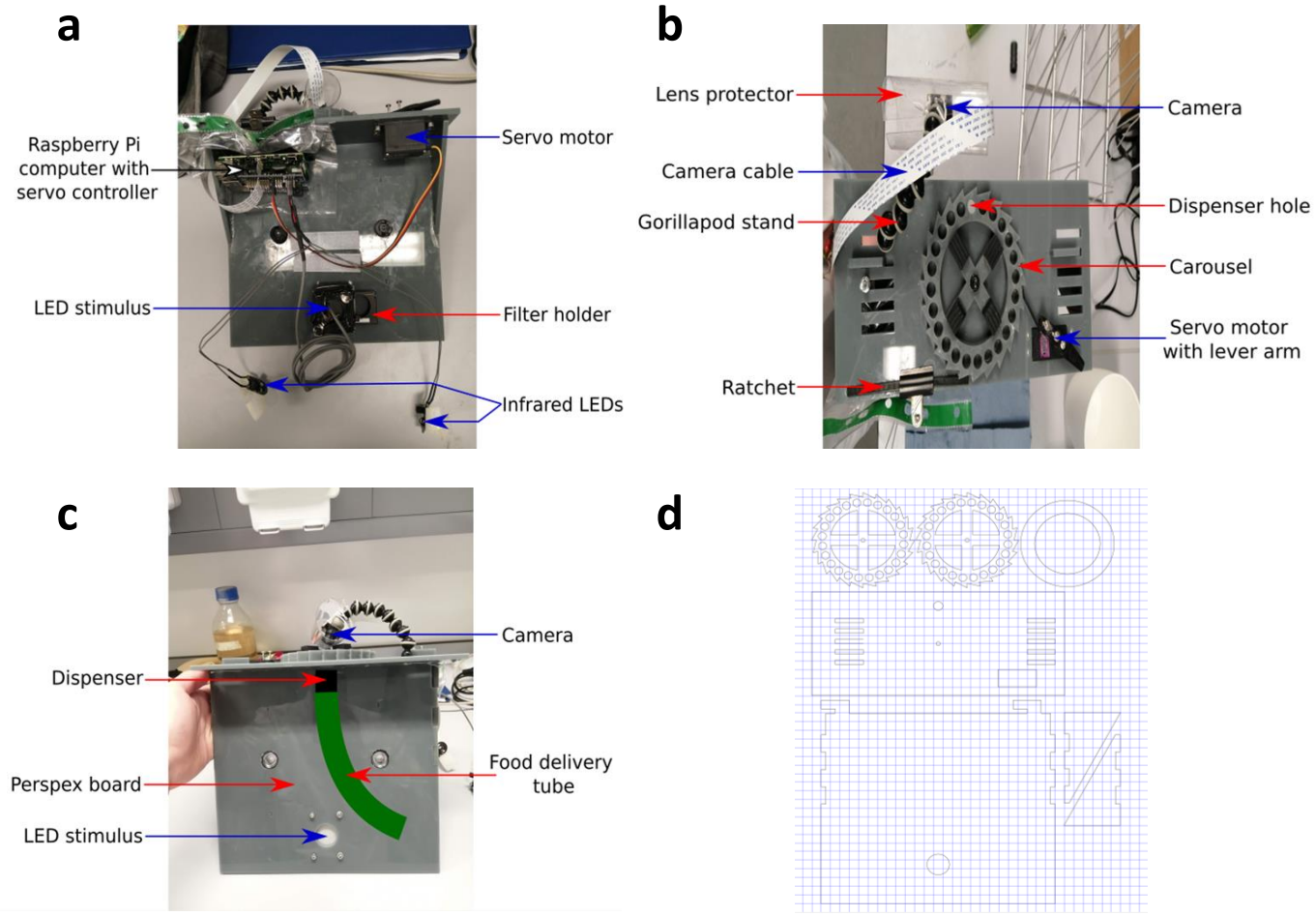

Fig. 13. Photographs and blueprints of the structure of the prototype of the automated system. Black arrows with white arrowheads indicate computer components, blue arrows indicate computer-connected hardware, and red arrows indicate peripheral components. (a) Rear view. (b) Top-down view. (c) Front view, with graphically inserted dispenser and food delivery tube (as there were no available photographs of these component parts). (d) Blueprint designs of the system prototype in Inkscape.

The preliminary experiments that were performed using this prototype revealed a number of design flaws that required attention. Firstly, the overall structure of the prototype was quite unstable and fragile, while the Raspberry Pi computer was weakly attached to the main frame with a metal clip, and the wires were disorganised (Fig. 13a-c). Furthermore, the IR LEDs (Fig. 13a) did not provide sufficient light for the camera to track the stomatopod consistently, resulting in numerous tracking errors. In the prototype design, the food delivery tube curved to drop the reward in the corner of the tank so as not to block the LED stimulus positioned at the centre (Fig. 13c). This resulted in the reward and stimulus residing in different parts of the tank, which could potentially inhibit the stomatopod's ability to associate the two. A number of difficulties concerning the camera also came to light, the first being the

unattached plastic lens protector that was rather flimsy and awkwardly shaped (Fig. 13b). In addition to this, the camera cable connecting the camera to the Raspberry Pi computer often became tangled (Fig. 13b), pulling the camera out of place so that it required frequent readjusting. Finally, the connection of the camera stand to the perspex board was again quite flimsy and loose (Fig. 13b), resulting in the camera breaking off from the perspex board on several occasions.

2.4. Final design

Blueprints of an improved final design were drawn up on Inkscape once again (Fig. 14d). The first change to the system was to enlarge the structure to fit the taller aquarium tanks that the stomatopods had been moved to (dimensions previously stated in section 2.1). To make the system more robust, orderly, and splash-resistant, a box constructed from perspex sheets was built onto the back of the design, giving more support to the structure than the simple prototype T-shape design. This box contained the Raspberry Pi computer and servo controller, both screwed onto the main perspex board, and all the necessary wiring, keeping them organised and out the way (Fig. 14a). The Raspberry Pi computer and servo controller now connected to one mains cable that extended outside the box to be connected to the mains power (Fig. 14a), rather than having to connect two separate cables to a mains socket for every session of trials. The ineffective IR LEDs were removed from the design and an overhead white LED strip light was used to illuminate the aquaria instead.

To improve association between stimulus and reward, the carousel was moved from the centre to the right-hand side of the structure and the delivery tube was lengthened so that it could reach the bottom of the tank (Fig. 14b-c). With these alterations, the delivery tube could be positioned to drop the reward directly underneath the light stimulus. The unattached, flimsy plastic lens protector was replaced by one fixed onto the camera which had a more compact shape around the camera, and an opening was made in the top perspex board so the camera cable could lead directly to the Raspberry Pi computer without getting twisted out of shape (Fig. 14a-b). Finally, the connection of the camera to the perspex board was screwed on more securely for the final design to prevent it loosening or breaking off (Fig. 14b). When the final design was complete, seven models were constructed, before being used to run priming and testing trials on the mantis shrimps. Each individual model of the automated system will now be referred to as a ‘training unit’ or a ‘podtrainer’ as they were named and numbered during research e.g. podtrainer 1, podtrainer 2 etc (Table 3).

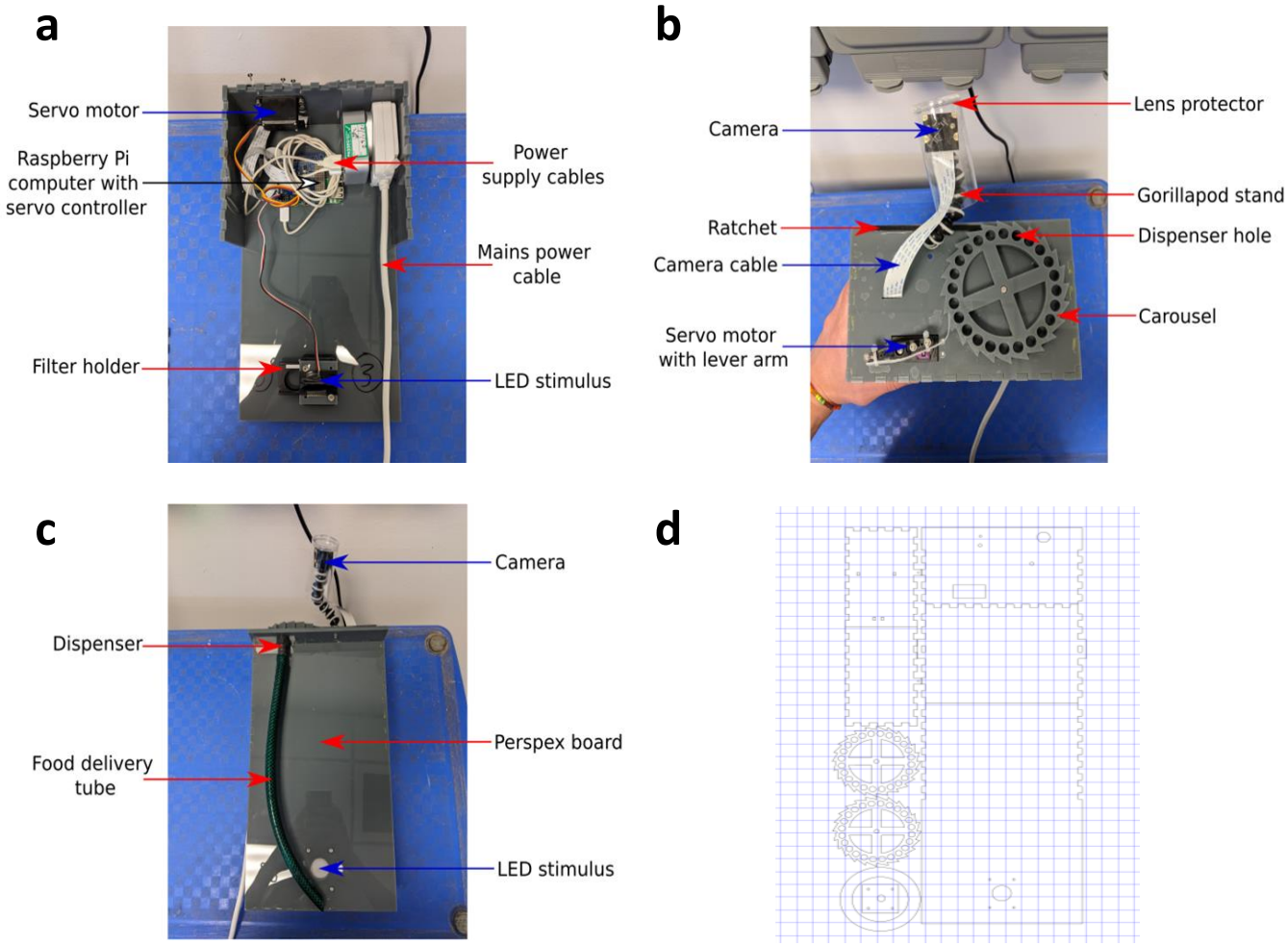

Fig. 14. Photographs and blueprints of the structure of the final design of the automated system. Black arrows with white arrowheads indicate computer components, blue arrows indicate computer-connected hardware, and red arrows indicate peripheral components. (a) Rear view, with the back perspex board removed to show wiring. (b) Top-down view. (c) Front view. (d) Blueprint designs of the system final design in Inkscape.

2.5. Code

Each training unit was controlled by a single Python script running on the Raspberry Pi computer. This code invoked a number of libraries to control the camera, servo HAT, LED stimulus, and servo motor. Mantis shrimp movements were tracked using the OpenCV library and the animal's frame-by-frame location was used to determine whether the animal was ready to undertake a trial (i.e. was located in the manually determined burrow zone), should receive a food reward (i.e. was located within the reward zone), or was elsewhere in the aquarium (Fig. 15b). The tracking system worked by subtracting the current video frame from a background template, and then finding the biggest area of difference. The background template was constantly updated with a small proportion of the current frame

e.g. new template = (old template *0.99) + (current frame *0.01). In this example, 99% of the background template was kept but 1% of the current frame was added, slowly updating to incorporate gradual changes in light environment and eradicate any moving objects. The Python code used information specified in a parameter file unique to each training unit, in which the user could adjust various settings according to experimental procedure (Fig. 15a). To save matching data in one file for later extraction, individuals were consistently paired with the same podtrainer (with one exception that changed podtrainer once), given a certain 'podname' (Table 3), and the 'wavelength' of the trial specified. Data from the trials was automatically saved to the folder on the Raspberry Pi computer.

2.6. Basic procedure

Here the basic method will be outlined, which was essentially the same when utilising the prototype and the final design, and the periodic alterations to the procedure will be detailed in section 2.7. For the food rewards, organic material (consisting of either frozen cockles, prawns, or mussels) was finely chopped and stuffed into marine grade (resistant to corrosion by seawater) M3-sized stainless steel nuts, before being refrozen prior to trials. The training systems were placed onto the front of the aquaria and 10 frozen food rewards placed in successive slots for each food carousel. Air bubble flow into the aquaria was stopped during trials to prevent the tracker being confused by surface ripples. Using VNC Viewer as the computer interface, appropriate settings were confirmed in the parameter file (Fig. 15a). Either 'priming' trials, to condition the mantis shrimp to associate the light stimulus with food reward, or 'testing' trials, to collect data on responses to the light stimulus prior to food reward, could be run through the parameter file. Under the 'trainingtype' parameter, either 'priming' or 'testing' was inserted to enact the corresponding trial. This was later replaced with a priming to testing ratio (Table 2), which was controlled under the 'trainingratio' parameter. Once the trial type was confirmed and the parameter file saved, the tracking zone, burrow zone, and reward zone were manually determined. The tracking zone contained the whole floor of the arena; the burrow zone the area around the burrow entrance where the stomatopod's protruding head could be seen; and the reward zone the area around the food delivery point at the front of the tank (Fig. 15b). The training system was then initiated to run for 10 trials, this constituting one session.

In both priming and testing, each trial was preceded by a pre-trial pause of random length between 150-450 s (Fig. 15a). At the end of this pause, the system would scan for the tracked position of the stomatopod in the arena, and if it was located in the burrow zone or was currently untracked the trial would begin. In the event that the mantis shrimp was

tracked outside the burrow zone, the system would continue to periodically scan at 1 minute intervals until the mantis shrimp returned to the burrow or the tracker disappeared. This would activate the white LED stimulus, which would then begin to flash at a rate of 3 seconds on, 1 second off. At this point, the two trial types would differ. In priming trials, the light intensity of the LED stimulus was set to full intensity (PWM = 1, section 2.2) between trials. The initiation of the LED stimulus simultaneously activated a 'wait time' and a 'choice window'. The 'wait time' was the amount of time between the initiation of the LED stimulus and the delivery of a food reward, achieved through the activation of the servo motor to turn the carousel and thus drop one food reward down the delivery tube. The 'choice window' was the amount of time given from the initiation of the LED stimulus for the tracked stomatopod to enter the reward zone to retrieve the food reward and the trial be counted a success. If the stomatopod had not entered the reward zone by the termination of this choice window, the trial was counted as a failure. Any apparent response to the stimulus without entering the reward zone or retrieval of the reward after the choice window had ended was ignored. The flashing stimulus ceased and the trial terminated when the reward zone was entered or the choice window expired. The time taken for the stomatopod to successfully enter the reward zone from the initiation of the LED stimulus and within the choice window was assigned as the 'retrieval time'.

Testing trials had the ultimate aim of determining the threshold intensity required at each wavelength to elicit the trained response. In such trials, the intensity of the LED stimulus was randomised (PWM between 0-1) for every testing trial. There was no wait time and no food reward would be delivered unless the mantis shrimp performed the trained task of entering the reward zone within the choice window. This was to prevent any olfactory (from the food), motion (from the reward being delivered), or auditory (from the motor and carousel turning or the metal nut landing in the tank) cues alerting the stomatopods to the presence of the reward, rather than visual cues (the LED). The choice window and retrieval time functioned in the same manner to priming trials. For both trial types, the end of the trial would initiate the pre-trial pause for the subsequent trial, giving time for the mantis shrimp to return to its burrow and consume its food reward ready for the next trial. As a reward was delivered for every priming trial, this resulted in the same amount of trials as food rewards i.e. 10. However, for testing trials a reward was only delivered when the stomatopod entered the reward zone within the choice window. If the stomatopod failed a trial, the system would append a new trial to the sequence until all 10 food rewards had been delivered or the session was prematurely ended by the researcher.

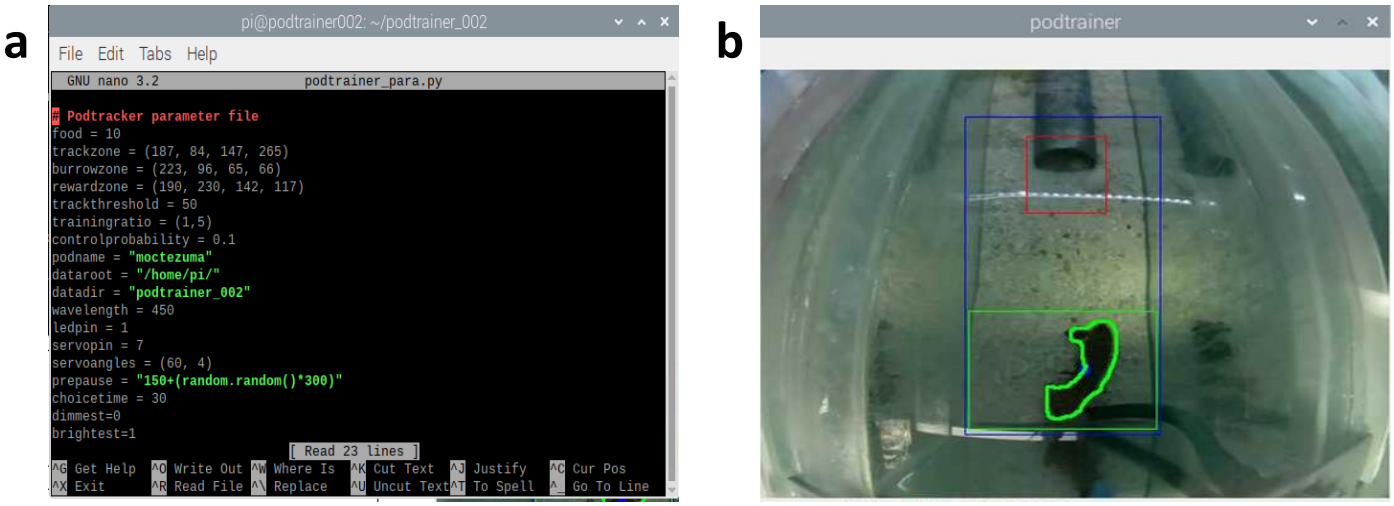

Fig. 15. (a) The parameter file for podtrainer 2, showing all the adjustable settings. (b) Screenshot of the podtrainer 4 camera showing the top-down view of the arena, including the stomatopod itself, the burrow pipe at the back, and the food delivery tube at the front. The blue rectangle delineates the track zone, the red rectangle the burrow zone and the green rectangle the reward zone. The green outline and central blue dot on the stomatopod's body represents the output of the tracking system. This screenshot depicts the moment the stomatopod successfully entered the reward zone from the burrow zone during a testing trial, to receive a food reward.

The priming trials exposed the stomatopods to a white LED stimulus at the front of the tank, while simultaneously dropping a food reward below this stimulus. The intention was for the stomatopods to leave their burrows to investigate the front of the tank (due to the flashing light or the olfactory signals from the food), discover the food reward, and form an association between the flashing LED and the reward. After this, it was up to researcher discretion to decide when the mantis shrimp was sufficiently conditioned to attempt testing trials - generally around when they were consistently passing at least 8 of these 10 trials. Then, a series of initial testing trials were performed to prove that the mantis shrimps were associating the flashing white LED with the food reward, rather than using the olfactory, auditory, or motion cues present in priming trials to know when to enter the reward zone. These testing trials were also essential to show if the stomatopods had been successfully trained to enter the reward zone when detecting the LED stimulus, and if so would provide evidence of learning. It was necessary to prove through testing trials that the stomatopods were fully conditioned, as priming would not prove this and test subjects may then have performed poorly on spectrally filtered tests. A broadband white light was utilised at these training stages rather than narrowband spectral colour light to ensure the stomatopods were not trained to associate certain wavelengths with the reward, as this could bias their responses to later tests. As such the trials in this training period are referred to as the 'white light trials'.

When it was deemed that an individual was passing enough testing trials with the bare LED to be considered fully conditioned, which was up to researcher discretion again, the testing of different spectral colour lights on that individual would begin. Six different wavelength filters were utilised to create six narrowband signals each spaced 50 nm apart, at 450, 500, 550, 600, 650, and 700 nm. The filter for the primed individual would be randomly selected through the use of a random number generator. The filter would then be screwed into the filter holder (Fig. 14a), directly in front of the LED of the corresponding podtrainer. After 1-3 sessions of 10 rewards, another filter would be randomly selected out of the remaining five and so on until all six filters had been tested. When an individual had been tested with all six filters in this way, the whole process would be repeated. This constituted the major assessment period of the research and these trials are referred to as the 'spectral light trials'.

2.7. Method progression

Due to the progressive and fine-tuning nature of this research, a number of alterations were made to the experimental procedure, alongside the improvement of the automated system from the prototype to the final design. This experimental research ran from October 2020 until July 2021. During the first months (October - December), the pre-constructed prototype was utilised to run an effective preliminary study on one mantis shrimp. The aim was to run four sessions of 10 priming trials a week until the mantis shrimp was sufficiently conditioned to replace these with testing trials. Unfortunately, this particular individual did not respond well to the priming trials, and thus testing trials were not attempted in this time period. The data from these priming trials are not presented as this preliminary experiment is not relevant beyond improvements made to the prototype and method. The method remained fairly constant throughout, with a wait time of 5 s and a choice window of 120 s. Food rewards were stuffed into marine grade stainless steel M3-sized dome nuts of diameter 3 mm, however the nuts were not stuffed to full capacity to keep the amount of food small and the stomatopods motivated. The small reward zone was drawn around the area immediately surrounding the delivery point at the bottom of the food delivery tube.

Through January and February, the final design for the automated system was drafted and constructed. From January, more stomatopods were acquired, slowly increasing the number of test subjects. By the beginning of March, the final design was ready for use and priming trials began with the same parameters as before. The first week of trials was used to test out the new system, after which data from trials were recorded for the next 5 months. Numerous modifications to the experimental method were made throughout this period in an effort to improve the conditioning of the subjects, the ability to extract detection thresholds from the

data, and the accuracy of the results. A catalogue of the alterations and advancements (the initiation of testing and spectral light trials) made to the method outlined above is presented in Table 2.

Three things here require further detail. First, in perhaps the most radical of all the method modifications, a trial ratio was created to train and test the mantis shrimps (Table 2 (M4)), rather than the basic procedure outlined in section 2.6. This priming:testing trial ratio was written into the Python script and adjusted through the 'trainingratio' setting in the parameter file (Fig. 15a). After consistently poor results in testing trials, this ratio was created in an attempt to improve the conditioning and eventually the testing responses of the stomatopods. The process was to start with a high priming:testing ratio and slowly decrease it to a low ratio as the individual improved over time. The standard procedure was that training began at a 5:1 ratio, then as the individual improved the priming number would gradually be decreased until 1:1, and then with continually improving performance the testing number would be increased up to 1:5. The hope was that starting each session with priming trials would strengthen the association between stimulus and reward again, so the stomatopods could pass the immediately following testing trials. Moreover, by having these testing trials interspersed with priming trials, this association strength and thus performance levels would be kept high. Highly successful stomatopods would require fewer priming trials to keep responding to the stimulus in testing trials. If an individual was able to consistently pass most testing trials on the 1:5 ratio, they would begin spectral light trials still using the 1:5 ratio. If the individual performed poorly the testing number was slightly lowered, but if this persisted the stomatopod would be reverted to white light trials. These trials were run at a 1:5 ratio to obtain mostly testing data per session, and the low number of priming trials also gave the stomatopods as few non-visual cues as possible.

Second, in another major method alteration later on in the study, randomly-occurring control trials were added where the LED stimulus would not flash and no reward would be deployed. Again, these control trials were written into the Python code. The probability of a control trial randomly occurring after the end of the previous trial was manipulated by the 'control probability' setting in the parameter file (Fig. 15a). Control trials were required as further proof that the stomatopods were responding to the visual signal of the light stimulus, rather than other sensory cues or false positive errors (Table 1). Each random control trial added a trial to the length of the session, thus a control occurrence probability of 0.1 was deemed to be frequent enough to collect sufficient data without making the sessions overly long.

Third, many of the alterations were carried out in an attempt to reduce the occurrence of false positives and negatives, and thus increase the accuracy of the results. Several different causes of false positives and negatives came to light over the course of the research and are outlined in Table 1. These different types of errors will be discussed in detail and as such have been given labels in Table 1 that will be referred to from now on.

Table 1.

The different causes of false positive and negative results throughout the research, each described in detail and given a label for future reference.

Type of erroneous result	Label	Description
False positive	FP1	A stomatopod simply swimming around the tank entered the reward zone during the choice window without responding directly to the flashing LED stimulus.
False positive	FP2	A stomatopod utilised additional sensory cues to enter the reward zone during the choice window. This error was only possible during priming trials as the additional cues were not present in testing trials.
False positive	FP3	Occasionally, after a stomatopod had returned to its burrow from the reward zone, the tracker would glitch and become stuck on the ghost image of the individual within the reward zone. The tracker would falter on this ghost image, disappearing just long enough for the next trial to be initiated. The tracker would then quickly glitch back onto the ghost image in the reward zone, and the system would record a successful result with a very rapid retrieval time.
False positive	FP4	Stomatopods began periodically checking the reward zone for rewards irrespective of the state of the LED stimulus. If this occurred during the choice window of a trial it would create a false positive result.
False positive	FP5	Some stomatopods began staying in the reward zone instead of returning to their burrow after each trial. By remaining motionless, the tracker would eventually lose track (as they became incorporated into the background tracking template) enabling the next trial to begin. Small movements within the choice window would then be recorded as a positive response, irrespective of the LED stimulus.
False negative	FN1	When stomatopods left their burrows to retrieve a reward, the

		tracker would sometimes follow the lower abdomen or even just the telson of the individual, rather than the whole body. As the front of the body was not tracked this could result in the tracker not entering the reward zone when the individual had successfully retrieved a reward.
False negative	FN2	As the burrows were constructed out of open-ended pipes, some individuals faced the back of the tank rather than the front towards the LED. As the LED was not in their field of vision, they could not respond to it.
False negative	FN3	A stomatopod did not respond to the LED stimulus due to a lack of motivation, not through inability to detect it. This could be caused by overfeeding, or by the rewards containing insufficient food to motivate their retrieval.

Table 2.

Alterations and advancements made to the experimental method, with the date the change was first implemented and the reason behind this change. On dates where more than one modification was made, these are numbered matching the reason for the modification in the final column. A label has been given to each time the method was modified (e.g. M1), which is recorded below the date and correspond to labels on the graphs produced from the results (sections 3.1, 3.2, supplementary). The 'priming wait time' denotes the amount of time between the initiation of the LED stimulus and the deployment of the food reward. The 'choice window' signifies the amount of time given from the initiation of the LED stimulus for the individual to enter the reward zone and the trial be counted a success, otherwise the trial was marked as a failure.

Date and label	Method modification(s)	Reason for modification
12/3/2021 M1	1) Priming wait time increased from 5 s to 7 s 2) Choice window increased from 120 s to 300 s for priming trials	1) Gives the stomatopod more time to definitively detect the light stimulus before the food reward has been deployed, to improve association between the two during priming trials. 2) Increases the amount of time the stomatopod has to retrieve the reward while the stimulus is still flashing, to improve association during priming trials.
7/4/2021 M2	Initiation of testing trials for all stomatopods. Performed ~10 testing trials with a 300 s choice window per session, but would move	The stomatopods were passing enough priming trials to begin testing.

	to priming trials for any remaining food rewards from the session immediately after this	
19/4/2021 M3	1) Wait time removed (0 s) 2) Choice window decreased from 300 s to 30 s for testing trials, kept at 300 s for priming trials 3) Application of LEE neutral-density (ND) filter to overhead strip light, reducing light intensity directly above tanks from 81.30 to 23.42 μW cm^{-2} (Fig. 17)	1) Poor performance on testing trials but good performance on priming trials suggested a weak association between the LED stimulus and reward, and the reliance on other sensory cues available only during priming trials. The wait time was removed so that the reward would be deployed at the same time as the onset of the stimulus in an attempt to strengthen the association. 2) Retrieval times slower than 30 s were deemed too slow with too high a chance of false positives (such as FP1 errors) to be used as evidence of LED detection. Choice window kept high for priming trials to encourage association between stimulus and reward, as before. 3) To reduce the intensity of the strip light and thus create greater contrast between the aquarium ambient light levels and the LED stimulus, to make the stimulus more visible to the stomatopods.
28/4/2021 M4	1) Creation and use of the trial ratio 2) Choice window changed to 120 s for priming and testing trials 3) Reward zone enlarged to contain approximately the bottom ⅓ of tracking zone 4) Back end of artificial burrow blocked with rocks 5) Stomatopods tested 5 times a week and supplementary feed dropped	1) Continued poor performance in testing trials and declining performance in priming trials called for a reboot of the whole process. The theory behind the decline was that the high number of failed testing trials was habituating the stomatopods to the stimulus so they would no longer respond quickly, even in priming trials. For this reason, the trial ratio was created and implemented (section 2.7). 2) The use of the priming:testing ratio meant only one choice window could be specified, as the parameter file could no longer be opened between testing and priming trials to change the choice window. Therefore 120 s was decided to be sufficient time for effective conditioning during priming trials, but not too long to lose reliability during testing trials. 3) To prevent the occurrence of FN1 errors, by ensuring the entire body of the stomatopod (and thus the tracker) entered the reward zone when retrieving rewards. 4) To prevent the occurrence of FN2 errors, by forcing

		stomatopods to face the front of the tank toward the LED stimulus. 5) Stomatopods were tested 5 times a week rather than 4 to strengthen the association between stimulus and reward through more frequent sessions and fewer gaps between them, and to increase the amount of data collected. The supplementary feeding was dropped alongside this to keep the stomatopods' motivation for food rewards high.
7/5/2021 M5	Increase of food reward size by stuffing more organic material into the same M3-sized nut	To further motivate the stomatopods to leave their burrows when the stimulus flashed - the previous reward seemed too small to motivate them, thereby reducing the chance of FN3 errors.
17/5/2021 M6	Initiation of spectral light trials for sufficiently conditioned individuals	Some individuals were performing well enough in testing trials to move onto testing their responses to different wavelengths.
2/6/2021 M7	Choice window decreased from 120 s to 60 s	The choice window of 120 s was decided to be too long with too high a chance of false positives (FP1, FP2, and FP4) to be used as reliable evidence of stimulus detection and response. By now some individuals had begun periodically checking the reward zone, so the choice window was lowered to reduce the chance of these FP4 errors in particular. Furthermore, stomatopods were passing priming trials below 60 s and didn't appear to need more time than this to associate the stimulus and reward.
3/6/2021 M8	Control trials added with a probability of occurrence of 0.1	Control trials were needed for stronger evidence that the stomatopods were responding to the LED stimulus, instead of additional cues or FP4 and FP5 errors (section 2.7).
4/6/2021 M9	Larger marine grade stainless steel M4-sized cap nuts (4 mm diameter) now utilised as food receptacle to further increase reward size	After the success of increasing the reward size to motivate the stomatopods to leave their burrows when the stimulus flashed before, the reward size was increased again to even further motivate them.
8/6/2021 M10	Choice window decreased from 60 s to 30 s	The choice window of 60 s was decided to be too long with too high a chance of false positives (FP1, FP2, and FP4) to be used as reliable evidence of stimulus detection and response. Furthermore, stomatopods were passing priming trials below 30 s and didn't appear to need more time than this to associate the

		stimulus and reward.
7/7/2021 M11	1) Addition of LEE ND filter to LED stimulus (one layer of 0.6ND - blocks 60% of light) to reduce light intensity 2) Control probability increased from 0.1 to 0.5	1) The stomatopods were performing extremely well at all PWM values for each of the 6 wavelength filters. This meant the LED intensity needed to be reduced to be able to locate the detection threshold for each wavelength (i.e. the light intensity at which the stomatopods were passing 50% of testing trials). ND filter was also added for individuals on white light trials so they became accustomed to this much dimmer light, before moving to spectral light trials. 2) The low random control probability of 0.1 was resulting in very few control trials, and the fairly high rate of these control trials coming back positive suggested the stomatopods were checking the reward zone at certain intervals. By greatly increasing the number of random control trials, this would severely affect the amount of time between priming/testing trials, making it even more random and unpredictable than before. This would hopefully make it harder for the stomatopods to estimate time between trials, leaving the stimulus as the only cue of a reward.
8/7/2021 M12	Control probability decreased from 0.5 to 0.25	The control probability of 0.5 resulted in excessive control trials which greatly extended the length of the sessions, and many successive control trials potentially had a negative impact on the following priming/testing trials for some individuals. The probability was reduced to 0.25 rather than 0.1, so that control trials were still fairly frequent for the reasons explained directly above.

At the beginning of the data collection period there were only two *O. scyllarus* test subjects, but over time more individuals were brought in at certain varying times. Due to this, each stomatopod experienced certain methods and not others depending on when they were present in the lab, the number of available podtrainers, and the recent performance of the stomatopods (some individuals were ignored after constant failure). Each individual produced unique data depending on the methods they experienced and if/which wavelength filters were tested on them.

Table 3.

The names of the individual stomatopods in the chronological order that these individuals first underwent trials and the podtrainer unit they were paired with. The number in the stomatopod name matches the podtrainer unit number, and the letter differentiates individuals that were paired with the same podtrainer (at different times). The first individual was the only stomatopod to change podtrainer, and this changeover occurred at line M3-4 (Fig. S3a).

Stomatopod name	Podtrainer unit number
Pod 21a	2 & 1
Pod 1a	1
Pod 3a	3
Pod 2a	2
Pod 4a	4
Pod 5a	5
Pod 1b	1
Pod 1c	1
Pod 3b	3
Pod 6a	6
Pod 7a	7
Pod 7b	7

2.8. Data analyses

All of the data automatically saved to the Raspberry Pi computer was downloaded and moved to an Excel spreadsheet. Here the data was organised, and the retrieval times and dates of the trials calculated. The retrieval time was calculated by subtracting the time of reward retrieval by the time the stimulus went on, both in Unix time. The date was converted from Unix time by performing this formula: '(X / 86400) + DATE(1970, 1, 1) = ', with the X value being the Unix experiment start time. Retrieval times above 30 s were marked as failures because they were now considered unreliable responses with too high a possibility of FP1, FP2, and FP4 errors (Table 2). All failures (both these and the original failures) were

given a retrieval time of 30 s, as this enabled all the data to be plotted on a single graph where any evidence of improvement would be easily visualised. Results below 2 s were rejected as physically improbable (if not impossible) and were likely caused by FP3 or FP5 errors. To create rolling averages for the three separate trial types (priming, testing, and control), averages of 5 successive results were calculated across the total number of trials for that individual. If there were fewer than 20 trials of one trial type within 100 total trials, the rolling average was rather calculated from 3 successive trials. If there were fewer than 3 trials of a certain type on one graph, then no rolling average was calculated.

Spectrophotometry measurements were recorded of the training unit LED irradiance values, the wavelength filter transmission values, the light irradiance values directly above the aquaria, and the aquarium glass transmission values (these were not utilised in calculations but should have affected all LED intensity values equally, being therefore inconsequential). This was performed using a USB2000 Spectrometer (Ocean Insight, Largo, USA). The irradiance curve of each podtrainer's bare LED was plotted using these spectrophotometry measurements (Fig. 16, S2). The maximum light intensity of the bare LED for each training unit was determined using the Riemann sum method to calculate the area under the irradiance curve between 400-750 nm (Table 4). As the PWM value varied for testing trials, the light intensity of the LED for each individual (unfiltered) white light trial was calculated by multiplying the total light intensity (of that training unit) by the PWM value for that trial. The spectral filter irradiance curves were plotted by multiplying the total irradiance values by the filter transmission values (Fig. 16, S2). The maximum light intensity of each spectral filter and the subsequent light intensity of each spectrally filtered trial was calculated in the same way as before (Table 4). To work out the light intensity of the bare LEDs after the addition of 0.6 ND filter (Table 2 (M11)), the total light intensity of each LED had to be multiplied by 0.4 (as 60% of light was blocked by the ND filter). Total light intensity of the spectral filters was also multiplied by 0.4 after the addition of ND filter. These values were multiplied by the PWM values of appropriate (LED with ND) testing trials to calculate individual testing trial light intensity values once again. The level of light irradiance above the aquaria from the overhead strip light (and to a lesser extent the ceiling lights) was measured before and after ND filter had been applied to the strip light (Fig. 17). Total overhead light intensity was extracted by calculating the area beneath the irradiance curve as before; finding it was 81.30 $\mu W\ cm^{-2}$ before applying ND filter and 23.42 $\mu W\ cm^{-2}$ afterwards (Table 2).

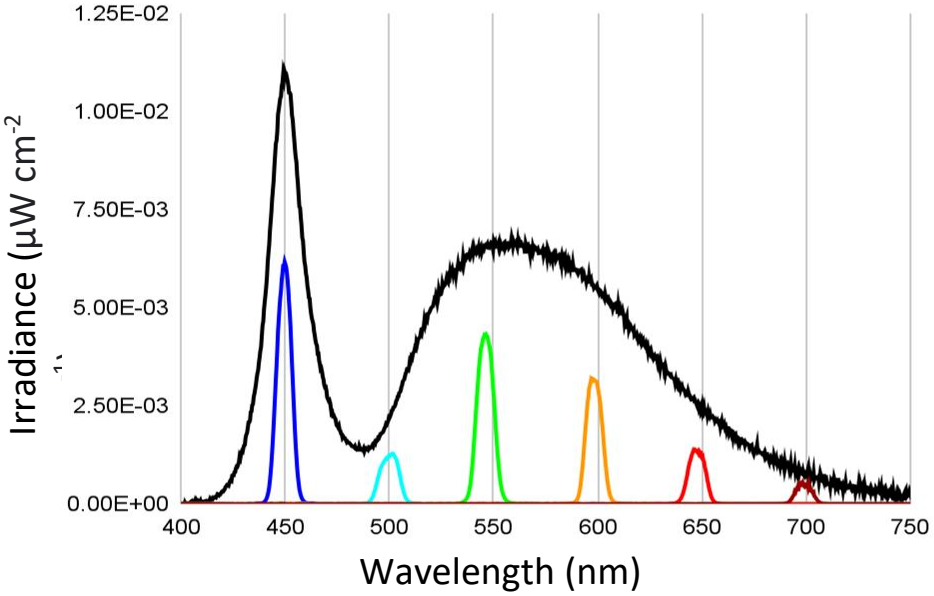

Fig. 16. Podtrainer 1 LED spectral irradiance curves. The black line depicts the bare white LED irradiance values, whereas the coloured lines depict the six spectrally filtered irradiance curves: blue - 450 nm, cyan - 500 nm, green - 550 nm, orange - 600 nm, red - 650 nm, dark red - 700 nm. The colour of the spectrally filtered irradiance curves approximately matches the spectral appearance of that wavelength. The graphs for the remaining six podtrainers are recorded in the supplementary section.

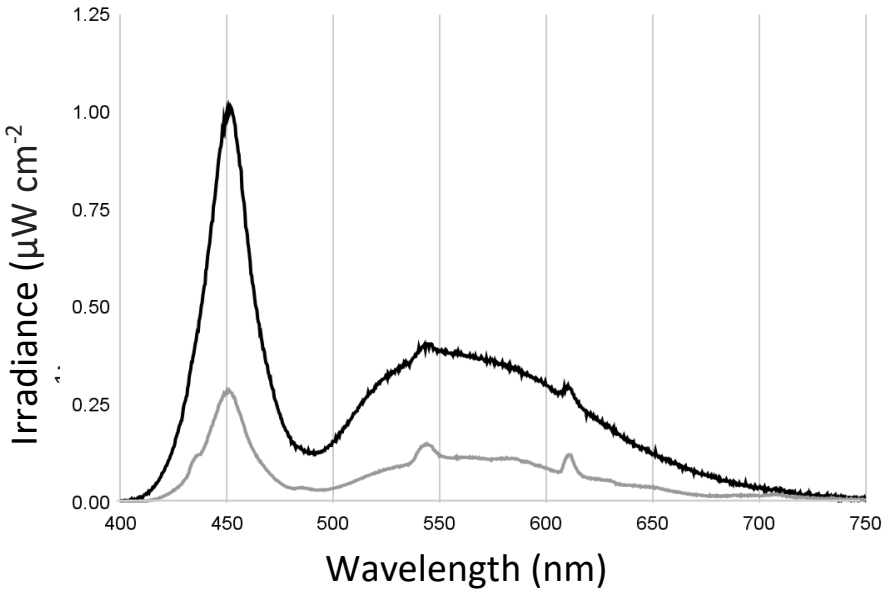

Fig. 17. Total light irradiance values measured from directly above the aquaria before (black) and after (grey) the application of ND filter to the overhead strip light (Table 2 (M3)).

Graphs of the total overhead tank irradiance (Fig. 17), as well as each podtrainer LED irradiance and spectral filter irradiances (Fig. 16, S2) were created on Microsoft Excel. Graphs displaying the results from the white light (Fig. 18, S3, S4) and spectral light trials (Fig. 19, 20, S5) of each individual were produced using SPSS. MATLAB was utilised to plot a sigmoidal curve on the retrieval times against the light intensity for each of the spectrally filtered trials (Fig. 21, S6, S7, S8, S9).

Table 4.

Total light intensity values of the bare and spectrally filtered LED for each of the seven podtrainer units. The total intensity after the addition of ND filter to the LED (Table 2 (M11)) is also stated in bold. Values are given in the units μW cm^{-2}.

	Podtrainer 1	Podtrainer 2	Podtrainer 3	Podtrainer 4	Podtrainer 5	Podtrainer 6	Podtrainer 7
Bare LED	1.16 **0.46**	1.54 **0.61**	0.83 **0.33**	0.087 **0.035**	1.29 **0.51**	2.20 **0.88**	1.35 **0.54**
450 nm	0.052 **0.020**	0.064 **0.025**	0.035 **0.014**	0.0042 **0.0017**	0.063 **0.025**	0.064 **0.026**	0.031 **0.012**
500 nm	0.014 **0.0056**	0.019 **0.0076**	0.011 **0.0043**	0.0010 **0.00042**	0.015 **0.0059**	0.036 **0.014**	0.015 **0.0060**
550 nm	0.042 **0.017**	0.056 **0.022**	0.030 **0.012**	0.0031 **0.0012**	0.046 **0.018**	0.068 **0.027**	0.034 **0.014**
600 nm	0.030 **0.012**	0.041 **0.016**	0.021 **0.0085**	0.0021 **0.00084**	0.033 **0.013**	0.056 **0.022**	0.028 **0.011**
650 nm	0.014 **0.0054**	0.018 **0.0073**	0.0095 **0.0038**	0.00098 **0.00039**	0.015 **0.0059**	0.037 **0.015**	0.019 **0.0077**
700 nm	0.0049 **0.0020**	0.0065 **0.0026**	0.0035 **0.0014**	0.00039 **0.00016**	0.0053 **0.0021**	0.015 **0.0060**	0.013 **0.0052**

3. Results

To logically analyse the vast amount of data produced from this long-term research study, the information was converted into graphs to make trends easily visible. Ultimately, data was collected from 12 individual stomatopods but only 4 individuals performed well enough to be tested with the spectral filters. Data from all of the individual stomatopods are shown separately on the graphs to show the progression, or lack thereof, and performance of each individual over the course of the trials. The use of an average between all of the test subjects would not have been suitable due to the widely different methods utilised for each individual, the use of different podtrainers with highly variable LED intensities for separate individuals (Table 4), and the vast range in number of trials across the individuals. Due to individuals beginning trials at different times, and moving to spectral light trials when trained, each individual has a different amount of data and controls are only present for individuals that were undergoing trials after we had implemented this measure (M8). As such, a large number of graphs were produced in this study and many of these will be displayed in the supplementary section. Due to the aforementioned reasons concerning all the intricacies of the data, quantitative analysis was deemed overly complicated and unsuitable, and so all data were qualitatively evaluated and graphs visually analysed. For this reason, conclusions can only be drawn on what the data suggest rather than what they demonstrate. When assessing the performance of individuals, the rolling average line will be used to evaluate their success; if the rolling average reaches a consistently low retrieval time, this will be considered a strong performance. Consistent failure or high average retrieval time will be considered a weak performance. The latency to reach this consistently low average (if achieved) will also be assessed. For individual graphs where control results are present, these will also be taken into account when evaluating performance.

The many methodological modifications were taken into consideration when analysing the results and have been clearly marked on the graphs by vertical dashed lines. Each line has a label at the top which corresponds to a method change in Table 2 (e.g. M1), and the line's position on the graph indicates when the method change was implemented. The first line simply shows the method being used on the individual at the initiation of their trials but may not match the date that method was first implemented (Table 2). The method change M6 is missing on white light graphs as this indicates the initiation of spectral light trials for the successful individuals at the time. On some occasions there were substantial gaps in carrying out trials on certain individuals (not shown on the graphs) so when trials resumed for this test subject, multiple different modifications may have been applied which is indicated on the graph (e.g. M3-5). Reasons for these gaps in experimental trials include that

the individual was performing consistently poorly so trials were temporarily halted; the individual moulted; the individual progressed to spectral light trials but performed poorly after a while so was returned to white light trials; and changing between wavelength filters on spectral light trials.

3.1. Training period - white light trials

The white light trials consisted of the trials where no filter was added to the LED and trials were performed on the mantis shrimps using broadband white light. These graphs essentially display the training period of each stomatopod and whether they were successfully conditioned to associate the LED stimulus with the food reward and enter the reward zone within the choice window. It was hoped that these graphs would provide evidence of the test subjects learning how to successfully perform the task, through steady improvement in priming and then testing trials. This would be the ultimate proof of the automated system's success in training and conditioning the stomatopods. As explained, the method alterations experienced by each individual differ substantially creating very different sets of data. The vertical dashed lines on the graphs enable a much deeper understanding of trends in the data and the potential reasons behind them. The data from four individuals are shown below (Fig. 18), with the graphs for the remaining 8 individuals displayed in the supplementary section (Fig. S3, S4). The responses of the individuals were extremely varied as one can see from Fig. 18: Pod 5a performed well however with a long latency period of mostly failed trials (Fig. 18a); Pod 1c performed well with short latency but went through a period of failing all trials in the middle and had some dubious control results (Fig. 18b); Pod 1a performed fairly well in priming trials but failed almost all testing (Fig. 18c); and Pod 7a failed all trials (Fig. 18d). Individual results are highly varied in Fig. S3 and S4 as well.

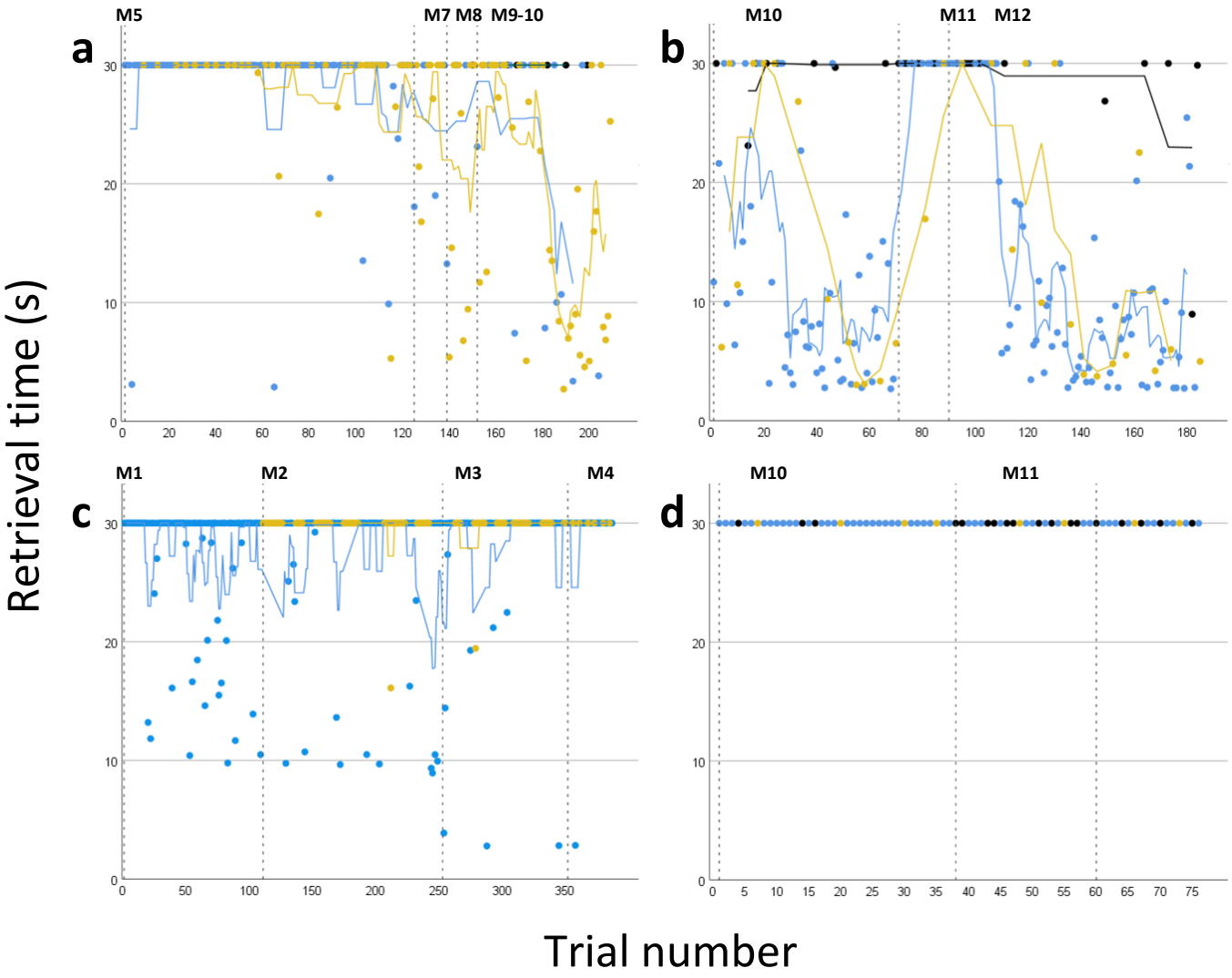

Fig. 18. Results of the white light trials for four separate individuals. Blue markers indicate priming trial results, orange markers testing trial results, and black markers control trial results. A rolling average line is shown for each trial type, with the colour matching that of the markers. vertical dashed lines topped with labels corresponding to Table 2 indicate a particular method change at that point in time. (a) Pod 5a. (b) Pod 1c. (c) Pod 1a. (d) Pod 7a.

3.2. Assessment period - spectral light trials

The spectral light trials involved the use of the six wavelength filters after the stomatopods had been fully trained. Although these graphs do not give an indication of spectral sensitivity, they display how the individuals responded to each spectral filter and how this response changed over repeated trials - demonstrating if the individuals were able to detect and respond to the different wavelengths. Only two individuals were tested with all six filters, Pod 2a and Pod 5a, whose results are shown below (Fig. 19, 20). Both individuals performed consistently well with low testing average retrieval times (orange line) at all six wavelengths,

with generally no or short latency periods apart from a few graphs (Fig. 19c, 19e, 20e, 20f) This presents evidence that they could detect these wavelengths and had associated the light stimulus with the food reward. Each individual had vastly different amounts of trials with different spectral filters due to random selections of the filter used and time constraints. Two other individuals, Pod 3a and Pod 4a, were tested with some of the filters and their results are recorded in the supplementary section (Fig. S5). Pod 3a died prematurely before completing all of the filters, while Pod 4a performed poorly with the wavelength filters and so was brought back to training on white light.

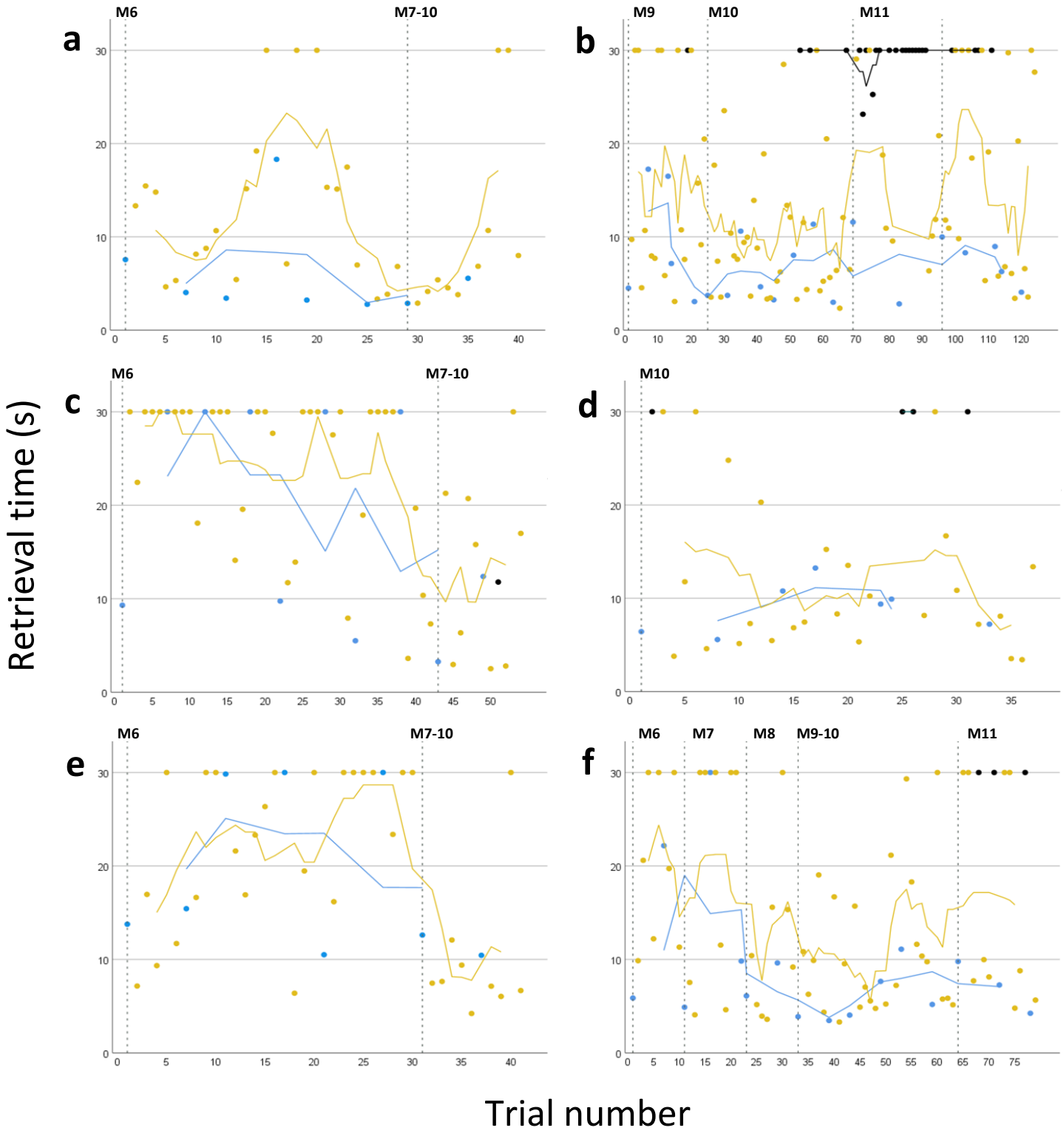

Fig. 19. Results of the spectral light trials for Pod 2a. Blue markers indicate priming trial results, orange markers testing trial results, and black markers control trial results. A rolling average line is shown for each trial type, with the colour matching that of the markers. vertical dashed lines topped with labels corresponding to Table 2 indicate a particular method change at that point in time. Each graph represents trials under a different spectral filter. (a) 450 nm. (b) 500 nm. (c) 550 nm. (d) 600 nm. (e) 650 nm. (f) 700 nm.

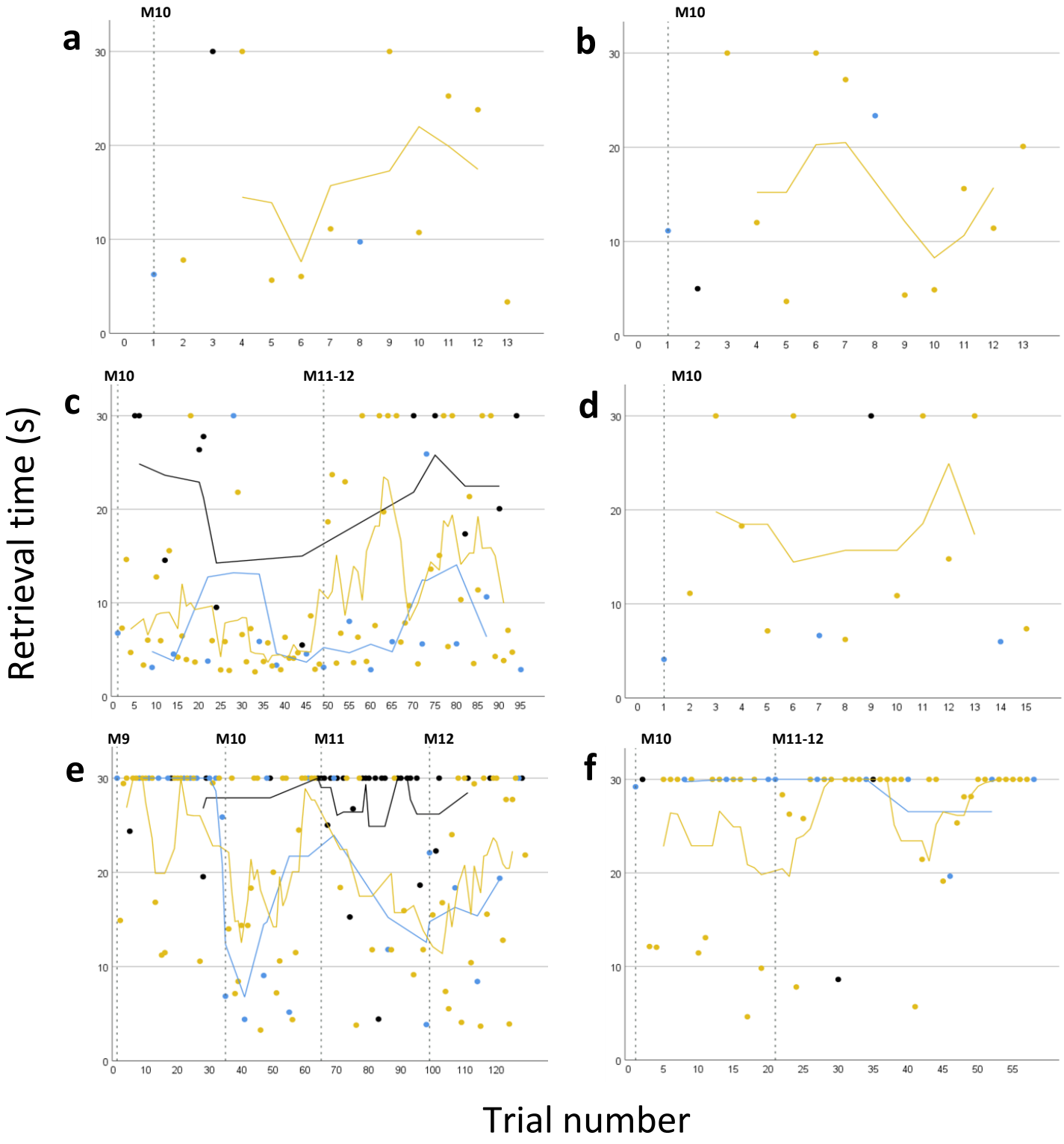

Fig. 20. Results of the spectral light trials for Pod 5a. Blue markers indicate priming trial results, orange markers testing trial results, and black markers control trial results. A rolling average line is shown for each trial type, with the colour matching that of the markers. vertical dashed lines topped with labels corresponding to Table 2 indicate a particular method change at that point in time. Each graph represents trials under a different spectral filter. (a) 450 nm. (b) 500 nm. (c) 550 nm. (d) 600 nm. (e) 650 nm. (f) 700 nm.

3.3. Detection threshold graphs

Using data from the spectral light trials, attempts were made to create graphs with retrieval time against the calculated light intensity (section 2.8) and fit a sigmoid curve to the data. The intention was to extract a detection threshold value, where the stomatopod was passing approximately 50% of trials at that intensity, for each of the different wavelengths tested. The X50 values were determined by taking the intensity value where average retrieval time was 17.5 s, as an indirect approximation of this value. The X50 value was taken as the midpoint between 5 s and 30 s, rather than 0 s and 30 s, because even well-trained individuals did not generally reach a lower average retrieval time than 5 s and to be so consistently rapid would have been physically difficult. For this value to be accurate, a sigmoid curve must be extracted from the data with the vertical-most part of the curve meeting the X50 value.

For the wavelengths that were for some time tested beneath ND filter (Fig. 19b, 19f, 20c, 20e-f), two detection threshold graphs have been produced: one consisting solely of data after the addition of ND filter (post-ND data) (M11), and the other consisting of combined data from before and after the addition of ND filter (combined data) (Fig. 21a-b, S6a-b, S6e, S8c, S9a-d). This was made possible due to the conversion of the PWM values of all trials to intensity values, and utilising this as the x-axis. This was essential for comparison between different wavelengths, as the intensity values varied widely between training units (Table 4). The remaining graphs were produced from data before the addition of ND filter (pre-ND data). Unfortunately, it was not possible to fit such a curve to most of the graphs due to the shape of the data. Four of these graphs are shown below, displaying two successful and two unsuccessful sigmoid fits (Fig. 21). The rest are recorded in the supplementary section (Fig. S6, S7, S8, S9). Only four graphs are considered to have successfully fitted a sigmoid curve, some more definitively than others (Fig. 21a-b, S8c, S9b).

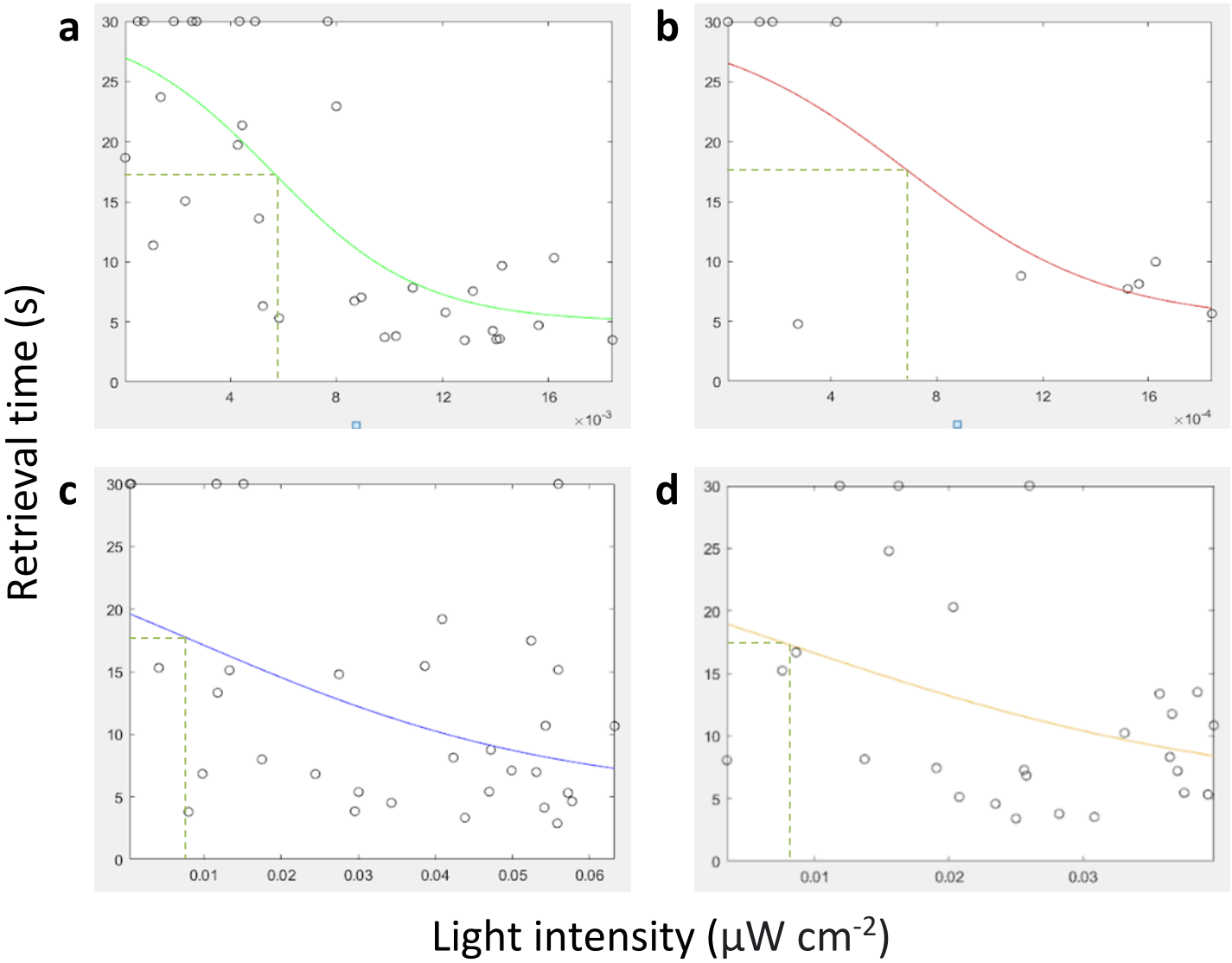

Fig. 21. Detection threshold graphs created from the data recorded from certain individuals at certain wavelengths. Markers indicate individual testing trial results and the solid-coloured line represents the successful or unsuccessful attempt to fit a sigmoid curve to the data. The colour of the line approximately matches the spectral appearance of the wavelength. Some graphs consist of data recorded solely before the addition of ND filter to the LED stimulus (Table 2 (M11)) - labelled pre-ND data; others consist of data recorded solely afterwards - labelled post-ND data; and others consist of combined data from before and after - labelled combined data. The dashed lines represent the point at 17.5 s where the X50 light intensity value was calculated, to 3 decimal places. Note the x-axis scale varies between panels. (a) Pod 5a at 550 nm, post-ND data, X50 = 0.006 µW cm-2. (b) Pod 2a at 700 nm, post-ND data, X50 = 0.001 µW cm-2. (c) Pod 2a at 450 nm, pre-ND data, X50 = 0.008 µW cm-2. (d) Pod 2a at 600 nm, pre-ND data, X50 = 0.008 µW cm-2.

4. Discussion

There were two main objectives to this study: first to prove the capacity of the automated system to train and test animal subjects, and second to extract the spectral sensitivity of *O. scyllarus* and the ocular region responsible for detecting flashing LED stimuli of different spectral properties. For this reason, the discussion will be split into two halves, debating these two objectives respectively. The first will assess the successes (and shortcomings) of method and system modifications, and potential further improvements, alongside the performances of the mantis shrimps; whereas the second will analyse how an action spectrum would have been extracted from the data had the plotting of sigmoid curves been successful (section 3.3), in addition to hypotheses on what part of the eye this spectral sensitivity curve represents.

4a. Automated system and method

4a.1. System and method modifications

The improvements made to the prototype to create the final design were highly effective: the structure was much sturdier and more organised; the delivery tube was perfectly positioned to drop rewards below the stimulus; and the white strip light provided much more light than the weak IR LEDs, making the tracker much more accurate. Despite these vast improvements, a few new issues presented themselves. There were a number of occurrences when the servo motor did not push the carousel far enough for the ratchet to catch on the next slot and no food reward would be dropped. This could lead to the carousel jamming and no subsequent rewards would be delivered either. Whenever this situation arose it was quickly rectified by fine-tuning the turn positions of the servo motor controlling the food carousel (Fig. 15a). Another serious defect was the tendency of the tracking system to cause FP3 errors (when the tracker glitched onto the ghost image of the stomatopod in the reward zone - Table 1). To mitigate this, various tweaks were made to the tracking algorithm, modifying the rate at which the background template was updated with the current video frame, until a compromise was identified between robustly identifying the mantis shrimp and integrating other changes (e.g. changes in light level or movement of other objects in the aquarium) into the tracking template.

In the pursuit of an optimal method, many modifications were made to the experimental procedure, as have been thoroughly detailed (Table 2). There were several goals in mind when enacting these alterations including increasing the ability to extract detection

thresholds from the data, and the accuracy and reliability of the results, but first and foremost was to improve the training and performance of the mantis shrimps. When analysing the results and the impact of the various method changes it is essential to remember that all retrieval times above 30 s were marked as 30 s, along with any failures. As the choice window for priming and testing trials was well above 30 s for most of the research, the graphs are not indicative of how the individuals were performing at the time of the trials until line M10 (when the choice window was reduced to 30 s). As explained (Table 2; section 2.8), it was decided that results above 30 s were too likely to be false positives to be accepted as successes and were rejected when plotting the graphs. This was not so important for priming trials as the main intention was to train the individuals, so a decrease in any retrieval time could convey this; but was essential for testing trials where proof of association between the LED stimulus and reward was key. For this reason, the results will be discussed as the graphs display them - as if all results above 30 s were indeed failures.

4a.1.1. Improving training and performance

Most of the earlier method changes had the sole intention of enhancing the conditioning of the mantis shrimps, thus improving their performance in priming and especially testing trials. From the start of the study the stomatopods performed fairly well in priming trials but with little consistent improvement, and universally poorly in testing trials (Fig. 18c, S3a-d). As results were only recorded from the first method change, it is not possible to deduce how increasing the wait time and choice window (M1) affected the following priming trials. After initiating testing trials (M2), the next alteration was to remove the wait time completely and reduce aquaria ambient light levels (M3). These efforts appeared to have no significant impact, if anything performance slightly deteriorated in Pod 1a and Pod 3a (Fig. 18c and S3b). Although the trial ratio (M4) didn't appear to improve priming results much at first, there was a distinct improvement in priming trials for Pod 2a and a small improvement for Pod 3a (Fig. S3c and S3b). However, even these two individuals displayed essentially no success in testing trials along with all the other individuals observed at this time (Fig. 18c, S3a-d), indicating that still no stomatopod had been properly trained and had perhaps been making use of additional cues in priming trials.

The first significant improvement in testing trials came after considerably increasing the food size reward (M5), which seemed to motivate the stomatopods far more to retrieve rewards. It appeared the small rewards did not keep the mantis shrimps motivated but instead were not sufficient reward to elicit a reliably quick response. Other cases of operant conditioning recorded that animal subject responses were slowed or otherwise reduced if the reward were small or less palatable, but this was only after a change from a larger or more palatable

reward (Ninomiya *et al.*, 2007; Salinas *et al.*, 1993; Wise *et al.*, 1978). The larger rewards boosted performance in priming trials in all individuals undergoing trials at this time (Fig. S3a-d) and also in testing trials for all of these again bar one (Fig. S3a). Most impressively, the two individuals that began training immediately after this reward size increase, Pod 1b and Pod 5a (Fig. S4a and 18a), showed progress in priming and testing much quicker than the individuals trained before them, although only Pod 5a consistently progressed. A second reward size increase was carried out later (M9) in the hope of further enhancing this effect, which came to fruition for Pod 4a and Pod 5a (Fig. S3d and 18a). Furthermore, two of the five individuals trained after this change progressed extraordinarily quickly with very short latencies in both priming and testing trials (Fig. 18b and S4c), further highlighting the influence of this reward increase. It was expected that with such large, repeated rewards, individuals would become satiated and slow or stop responding over a single session (as in Wise *et al.* (1978)), however no strong evidence of this was found.

It is difficult to ascertain which changes were the most effective in reducing retrieval times and latencies as the methods were built on each other and could well have worked in conjunction to lead to the marked improvement seen after M5. It appears large food rewards are vital in conditioning mantis shrimps and they didn't seem to reduce motivation through satiation, although eventually this would occur with increasing reward size (Wise *et al.*, 1978). The trial ratio procedure functioned as a sleeker and much less time-consuming procedure than the one utilised previously where around 10 testing trials were implemented, before reverting to priming trials to deliver any remaining rewards from failed tests. The individuals often failed most or all of the ~10 testing trials, meaning up to 10 priming trials would need to be executed immediately after, doubling the length of sessions from before the inception of testing trials (M2). By creating a simple, graded system where the amount of testing trials could be increased incrementally as the individual's performance improved, the ratio substantially reduced the length of sessions. However, the ratio did not rapidly lead to a significant improvement in retrieval times (M4), this response came after enlarging the food reward (M5) and was enhanced after enlarging it again (M9). Despite this, it is likely that the two alterations worked in conjunction, as the reward was first enlarged only 9 days (constituting 6 sessions) after the implementation of the ratio. Whatever the case, through these two improvements a much more effective and efficient training system had been created that thoroughly conditioned subjects much more rapidly and that proved it was possible to condition the individuals with a 30 s choice window from the beginning (Fig. 18b, S4b-c), dispensing with the need for longer, unreliable choice windows.

4a.1.2. Improving accuracy - false positives

Alongside more effective conditioning, many of the modifications were enacted to improve the accuracy of the results and thus the reliability of the data. Throughout the research, the choice window of the trials was reduced several times for both priming and testing from the initial 300 s to eventually 30 s (Table 2). This was done to reduce the occurrence of false positives, which became a significant issue over time. There were a number of ways a false positive could occur, that are all described in Table 1, and measures were taken to reduce their occurrence during trials and their presence in the data post-trials.

Although the FP5 cheating occurred very rarely and was only ever documented in two individuals (Pod 2a and Pod 4a), the FP4 checking became fairly widespread amongst the cohort and happened frequently (as shown by control trials). These two behaviours may have arisen from the FP3 errors, when food rewards would be delivered due to tracker glitches, rewarding stomatopods that emerged from their burrows even when there was no light stimulus. Reducing the choice window down to 30 s should have been extremely effective in reducing FP1, FP2 (for olfactory but not instant auditory and motion cues), and some FP4 errors. The rejection of any results below 2 s prior to graph formation would hopefully remove most false positives resulting from FP3 and FP5 errors. With more reliable data, the need for manual overseeing of the system to ensure results were not misrecorded became less and the independence of the system grew. Improving the function of the tracker so that it did not freeze on ghost images or lose track of immobile individuals would be very advantageous and perhaps designing a mechanism to disturb cheating individuals back to their burrow.

After the realisation that individuals were potentially periodically checking the reward zone rather than responding to the stimulus, it was imperative that control trials were created to monitor this (M8). Of course, it was possible that these individuals were utilising a combination of detecting the LED for genuine trials but checking the reward zone outside of these. However, without a significant difference between the control trials and the priming/testing trials, detection of the white or spectral lights could not be proven. The controls generally failed at first, but occasional successes indicated some individuals had begun checking the reward zone for rewards regardless of the stimulus (Fig. 18b, 19b, 20c, 20e, S4b-c). After the increase of control probability from 0.1 to 0.5 (M11) there were more control successes, in part logistically due to the increase in controls but the long intervals between rewards (from the many controls) may also have encouraged the mantis shrimps to check more frequently. Reducing the control probability down to 0.25 (M12) produced a

good balance: the length of the now excessively long sessions was drastically cut down, but this probability was still high enough to result in a sufficient number of controls and, as a consequence, highly random interval lengths between priming/testing trials. To further reduce control success, the potential length of random intervals could be increased to make estimation of when the next trial begins more difficult. To further illuminate the difference between controls and priming/testing the difference in retrieval time could be calculated, as responses to the stimulus should be much quicker on average than checking of the reward zone. Investigating whether the stomatopods were checking at certain time intervals, rather than randomly, could produce fascinating research on the time-keeping abilities of stomatopods of which there is none.

4a.1.3. Improving accuracy - false negatives

Two more minor alterations of enlarging the reward zone and blocking the back of the burrow pipe were executed at the same time (Table 2), both with the intention of elevating the accuracy of the results. However, this time these measures were put in place to reduce the occurrence of false negatives not false positives (Table 1). The enlarged reward zone ensured that whatever body part was being tracked would enter the reward zone when the individual retrieved the reward. Obstructing the back end with large rocks forced all individuals to view the front of the tank and the stimulus - this didn't guarantee the individual would respond but it ensured the result would be fair. These simple but important modifications instantly reduced the occurrence of FN1 and FN2 errors respectively. As discussed, the enlarged food rewards greatly enhanced the motivation of the stomatopods, which will have led to a decrease in FN3 errors as well.

4a.1.4. Improving the ability to extract detection thresholds

The final major aim of continuously fine-tuning the method was to augment the ability to extract light detection thresholds from the data. During the study it became quite obvious that the individuals undergoing spectral light trials were performing extremely well across a wide range of intensities (Fig. 19, 20, S5). Although this provided some evidence that *O. scyllarus* was able to detect light at these wavelengths, the specific detection thresholds could not be extracted as the light intensity range (of testing trials) was never low enough that the subjects could not consistently detect the stimulus (Fig. 21c-d, S6c-e, S7a-e, S8a-b, S8d). The consistently successful trials could also be explained through the association of another cue to the light stimulus which alerted stomatopods to the initiation of a trial, or the frequent level of checking. Assuming the light intensity range was too high, this had to be

lowered in order to straddle the detection threshold where individuals were passing 50% of trials. Attempting this, one layer of 0.6 ND filter was applied to each podtrainer LED (M11), with the aim of shifting this intensity range down so the dimmest light intensity was below the threshold and the brightest above it. Concerning white light trials, this seemed to cause a huge temporary drop in performance for Pod 1c and Pod 3b (Fig. 18b, S4c) that both perhaps had difficulty responding to this considerably dimmer stimulus at first (Table 4). This drop could actually have been caused by the higher number of controls implemented at the same time (M11), causing these individuals to stop responding after long stretches with no reward and fruitless attempts whenever checking for rewards. This hypothesis seems less likely, however, as retrieval times instantly deteriorated after M11 rather than after several controls and performance did not improve immediately after reducing control probability (M12) but later on.

As mentioned, only two stomatopods successfully underwent trials with all six wavelength filters and unfortunately only four of these filters were utilised after the addition of ND filter to the LED: 500, 550, 650, and 700 nm. Only the 700 nm filter was tested on both individuals after adding ND filter. The ND filter resulted in a slightly worse average retrieval time for most graphs (Fig. 19b, 19f, 20c, 20f), but not all (Fig. 20e). The slower average is likely due to greater difficulty detecting the dimmer trials of this new intensity range. This clear difference in retrieval time between dimmer and brighter trials is the key to producing a successful sigmoid curve. Detection threshold graphs display that the ND filter functioned fairly well in creating a sigmoid curve, either using solely post-ND data or combined data, especially in these graphs: Fig. 21a-b, S8c, S9b. Despite this, the ND filter did not function as well as expected because no sigmoid curve was extracted from the post-ND data of Pod 2a at 500 nm (Fig. S6b) or Pod 5a at 700 nm (Fig. S9d), and the most distinctive sigmoid curve was produced from the combined data of Pod 5a at 550 nm (Fig. S8c). Potential further improvements are discussed in the second half of the discussion (section 4b). Adding the ND filter did succeed in making the data more useful (no pre-ND graphs managed to produce a sigmoid curve) as some preliminary data on particular wavelength sensitivities has been extracted, but more work is needed before spectral sensitivity can be reliably determined through use of this automated system.

4a.1.5. Further improvements

The majority of the podtrainers were constructed from monochromatic grey perspex, until materials ran out and monochromatic white perspex was utilised. Any further studies should construct all training units from the same monochromatic material, as differences to the

background colour of the stimulus could influence the detection of certain wavelengths (Fleishman & Persons, 2001; Lind, 2016; Olsson *et al.*, 2020). Implementing a definitive point when individuals are considered fully trained and suitable for spectral light trials (e.g. passing at least 80% of trials for 5 consecutive sessions) would perhaps make the experiment more streamlined and uniform between individuals. Alongside this, the method should be kept constant throughout the research. In a natural but complicated crustacean process that was fatal to numerous test subjects, the individuals would periodically moult every couple of months. If successful, the new exoskeleton is soft and vulnerable for a number of days so stomatopods reduce feeding levels and do not leave their burrows unless forced (Reaka, 1975). For this reason, for a few days before, during, and after moulting, these individuals would fail all trials. Removal of this data and any other anomalous drops would aid in removing false negative results. This could be done by halting trials for a moulting individual for a week, or perhaps reviewing video recordings of all suspicious trials and removing inaccurate data - which could also be utilised to eliminate false positives.

4a.2. Training period results

All individuals passed at least one priming and testing trial each, except Pod 7a that did not pass a single trial (Fig. 18d). Most individuals performed fairly well on priming trials, with some inconsistently passing trials with an unimproving average retrieval time (Fig. 18c, S3b, S4a, S4d) and others displaying the desired downward trend in retrieval time with varied latencies (Fig. 18a-b, S3c-d, S4b-c), but some responded poorly with little improvement (Fig. 18d, S3a). Those with the downward trend indicate successful training in the priming stage, and although those with an unimproving trend had clearly learnt the stimulus response there appeared to be some obstacle to continuous improvement. Fewer individuals responded well to testing trials, with six performing very poorly (Fig. 18c-d, S3a, S3c, S4a, S4d) and six showing some downward trend in retrieval time, again with varied latencies (Fig. 18a-b, S3b, S3d before M10, S4b-c), although only two of these being consistent and distinctive over a considerable number of trials (Fig. 18a-b). Although these last six graphs are fairly strong evidence of individuals having learnt the stimulus response, only those two graphs form the best evidence of individuals being effectively conditioned. Five individuals did not respond overly well to this experiment, especially in the testing capacity (Fig. 18c-d, S3a, S4a, S4d).

As discussed in 4a.1, the different method modifications had a huge impact on the results, but responses of individuals undergoing trials in the exact same time frame under the same experimental method exhibited vastly different responses. There are a number of potential reasons behind this, but an immediately obvious one was the tremendous variation in bare

LED light intensity between training units (Table 4). For example, Pod 2a and Pod 4a were acquired at the same time and yet Pod 2a responded well to trials much sooner than Pod 4a (especially in priming) and thus progressed onto spectral trials much earlier (Fig. S3c and S3d). Podtrainer 2 possessed one of the brightest LEDs of all the podtrainers whereas podtrainer 4 had an abnormally dim one that was far dimmer than all the other LEDs (Table 3, 4). In fact, the podtrainer 4 LED was almost 18 (17.7) times dimmer than podtrainer 2 and approximately 25 times dimmer than the brightest podtrainer (podtrainer 6). With such an extreme difference it is likely that Pod 4a had much more difficulty detecting the LED, which could have had a large impact on the individual's response to trials and its ability to be conditioned. In contrast, there were more cases where LED brightness did not seem an overly important factor in how well contemporarily trained individuals performed, however the differences in brightness were much less extreme. Pod 3a (Fig. S3b) performed much better than Pod 1a and Pod21a (Fig. 18c and S3a) despite having the dimmest LED of the three; and Pod 1c and Pod 3b (Fig. 18b and S4c) performed much better than Pod 7a (Fig. 18d) and were consistently passing trials with low retrieval times much sooner than Pod 6a (Fig. S4b), despite once again both having dimmer LEDs.

Other factors must be at play, and the most obvious one is that the innate character of the individuals strongly influences how soon they start responding (latency) and how well they respond (average retrieval time). It is well documented in behavioural research that some individuals are naturally more inquisitive or dominant and so respond more readily and learn better (Davis *et al.*, 2009; Lozano-Montes *et al.*, 2019; Pongrácz *et al.*, 2012). The sex of an individual may also affect their response to a stimulus or their participation rates, for example *H. trispinosa* males participated significantly less than females in trained choice tests where a UVB signal was present (Bok *et al.*, 2018). Unfortunately, the sex of the test subjects was not determined in this experiment due to the difficulty and danger in having to remove the individuals from their tanks for a genital examination. An influence from character or sex appears very likely in cases where individuals with dimmer or similar LEDs to other individuals started responding much sooner with much quicker retrieval times, as in the cases above and with Pod 5a compared to Pod 1b (Fig. 18a and S4a). In fact, despite the exceptionally dim LED, Pod 4a managed to substantially reduce its priming and testing retrieval times to the point where it progressed to spectral light trials (Fig S3d, line M7-8). Unfortunately, Pod 4a did not respond well to spectral trials so was moved back to white trials soon after, where it continued to perform well on priming but essentially ceased responding on testing trials. The podtrainer 4 stimulus was most likely far too dim on spectral light trials for consistent detection (Table 4), but this individual might showcase the

importance of character in responding even to dim LEDs. Additionally, it is possible that sudden drops in performance were due to moulting.

In general, individuals performed worse in testing than priming trials, shown by the priming rolling average generally beginning to decrease sooner and reaching lower retrieval times than the testing average. This is attributed to two factors: the constant full brightness of the LED stimulus for priming, and the additional instant auditory and motion cues of the motor turning the carousel and the reward landing in the tank (olfactory signals from the reward likely diffuse too slowly to elicit such a quick response (Smith & McClean, 1989)). Most individuals exhibited rapidly fluctuating trends, especially early on in research - this could be attributed to the initial longer choice windows that was allotted to the mantis shrimps; or perhaps just the general erratic behaviour of animal subjects. In terms of the control results, most of the controls failed but there were more than expected (mostly due to FP3 and FP4 errors, with the occasional FP5), reaching concerningly low averages for some graphs (Fig. 18b, S4b-c). These results do reduce the significance of successful trials but ultimately do not disprove stimulus detection, as control results were usually above priming/testing results (apart from in Fig. S4b) and the fact that checking and genuine detection are not mutually exclusive. From all this evidence it is probable the automated system can successfully train stomatopods and demonstrate stimulus detection, however previously stated further steps need to be taken to remove errors and illuminate a greater separation between control and testing results.

4a.3. Assessment period results

Now placing major focus on testing results rather than priming, the four individuals that underwent spectral light trials responded fairly well to all of the six wavelengths tested. Pod 4a, the individual who performed worst (Fig. S5d-e), was tested with two wavelength filters before regressing to white light trials. As discussed above, the LED of podtrainer 4 was particularly dim so the fairly weak performance was credited to this. Interestingly, Pod 4a rarely responded at 500 nm but much more frequently at 600 nm, which is likely due to this wavelength being twice as bright for podtrainer 4 (Table 4). Although 10 times brighter than podtrainer 4, podtrainer 3 was fairly dim compared to the remaining training units and possibly contributed to the fairly lacklustre performance of Pod 3a (Fig. S5a-c). Surprisingly, Pod 3a responded better at 500 nm than 600 nm despite this wavelength being twice as dim once again (Table 4). The stimulus was dimmest at 700 nm being approximately three times dimmer than at 500 nm and understandably, despite a good start, Pod 3a responses quickly deteriorated and most trials failed. Additionally, Pod 3a only completed one session at 700

nm before moulting and dying that night. As the individual had been preparing for or beginning the moulting process, this may be the major cause behind the reluctance to respond (Reaka, 1975).

Pod 2a and Pod 5a were tested with relatively bright podtrainer LEDs of a similar intensity (Table 4), generally performing very well across the six wavelengths (Fig. 19 and 20). Both individuals seemingly did not respond well on their first wavelength (displaying some longer latency), 550 nm for Pod 2a and 650 nm for Pod 5a, although separate explanations are theorised. Under the contemporary choice window of 120 s Pod 2a was performing very well, uniformly passing testing trials with most retrieval times above 30 s - the same occurred toward the end of its white light trials which is why it progressed onto spectral light trials (Fig. S3c). A conspicuous downward trend perhaps suggests that Pod 2a was adjusting to a narrowband spectral stimulus from the broadband white stimulus, before continued strong performance on the next wavelength - 450 nm. On the other hand, Pod 5a did not respond overly well at the time and regressed to training for 3 sessions (Fig. 18a, line M9-10) to ensure it had been properly conditioned, before returning to actively respond at 450 nm. Pod 5a did perform poorly on 700 nm as well, which is again likely due to the very low intensity of the stimulus at this wavelength, and yet it was a similar intensity for Pod 2a who performed extremely well here.

Due to frequent method modifications, variable amounts of trials between wavelengths, and differing LED intensity values, any differences in sensitivity between wavelengths are difficult to elucidate at this point. There is possibly some reduced sensitivity at the 700 nm wavelength, as both Pod 3a and Pod 5a failed most trials here, which is concordant with the penalty to sensitivity incurred by the intrarhabdomal filtering required for stomatopods to detect long wavelengths, especially at this far red end (Cronin *et al.*, 1994a, 1994c, 2014; Marshall *et al.*, 1991b; Porter *et al.*, 2010). This is confounded by the impressively rapid average retrieval time of Pod 2a at this wavelength (Fig. 19e). No innate preference or aversion for any particular wavelength is clearly visible, despite findings that *O. scyllarus* displayed increased preference for yellow objects and reduced preference for red objects, compared to green objects (Daly *et al.*, 2017). This requires further investigation as any innate preference or aversion could seriously impede the ability of the automated system to extract accurate detection thresholds.

For Pod 2a, Pod 5a, and Pod 3a at 500 nm, the priming average was generally slightly below the testing average. This is attributed to the same two reasons as before (section 4a.2), of the high and constant priming stimulus intensity and the additional auditory and

motion cues. Unfortunately, the controls present quite a problem in much of the spectral light data, with there being clear evidence of checking of the reward zone once again. The amount of control trials varies widely between graphs due to changing control protocols (Table 2), for example Pod 3a and Pod 4a have no controls. However, of the graphs possessing controls there is often at least one control success (Fig. 19b-c, 20b-c, 20e-f). In the three cases where there was a large number of controls (Fig. 19b, 20c, 20e), two of them had control averages that were at points very similar or below the testing average (Fig. 20c, 20e). Both of these belonged to Pod 5a, suggesting that out of stomatopods that had displayed checking behaviour, some showed a greater tendency to check than others. In these two cases, there was not a particularly significant difference between controls and tests so evidence of stimulus detection at that wavelength is weakened. Despite this, the data overall seems to support that *O. scyllarus* can detect all these six wavelengths in agreement with calculated sensitivity functions (Fig. 5, 7) (Cronin *et al.*, 1994b, 2014; Marshall *et al.*, 2007). Although the greater removal of false positive errors, especially FP4, to emphasise a significant difference between controls and tests is, again, fundamental to further research; the automated system did succeed in testing several individuals at different wavelengths and displaying evidence of detection for each.

4b. Spectral sensitivity and chromaticity

4b.1. Creating the spectral sensitivity curve and extracting chromaticity

The ultimate intention of this research was to utilise the automated system to create an initial spectral sensitivity graph for *O. scyllarus* within the visible spectrum, that would be utilised to determine the part of the eye responsible for querying stimuli of different wavelengths. Unfortunately, the vast majority of detection threshold graphs did not produce a distinct sigmoid curve, which is necessary to extract accurate X50 detection threshold values. The success of some graphs after adding ND filter to the LED (Fig. 21a, 21b, S8c, S9b) may indicate that with continued further improvements it would be possible to create such a spectral sensitivity graph with this automated system. Noise from false positives and negatives would have to be removed in ways previously detailed and perhaps further enhanced by reviewing video recordings and removing inaccurate results. Ensuring each wavelength tested has a similar total intensity appears essential, as the X50 values we extracted from the 'successful' graphs were lowest for 700 nm (0.001 μW cm^{-2}, Fig. 21b), then 650 nm (0.003 μW cm^{-2}, Fig. S9b), then 550 nm (0.006 μW cm^{-2} for post-ND data, Fig. 21a; 0.005 μW cm^{-2} for combined data, Fig. S8c). This is the opposite of what was expected from physiological evidence that stomatopods require evermore extreme and sensitivity-

reducing intrarhabdomal filtering to detect longer wavelengths (Cronin *et al.*, 1994a, 1994c, 2014; Marshall *et al.*, 1991b; Porter *et al.*, 2010). It is therefore deduced that these curious results are not accurate detection thresholds. In addition, very few trials were executed on Pod 2a at 700 nm (Fig. 21b) so this graph may not be overly accurate. As explained, the LED intensity range must straddle the detection threshold and one potential way to ensure this could be (for each wavelength tested) to start with a very dim LED and incrementally increase the brightness when the individual consistently fails. The LED intensity would be increased up until the sensory threshold at X50 and slightly beyond to produce the definitive sigmoid curve. To keep the subjects conditioned, these 'testing' trials would be alternated with bright 'priming' trials through the use of the trial ratio (Table 2 - M4). Keeping the method constant throughout this time could also be helpful, and testing more individuals for many more sessions on each wavelength would produce more sigmoid curves for each wavelength, that could then be averaged out to achieve a more accurate X50 value.

To produce the desired action spectrum, successful X50 values for different individuals would have been averaged out at each wavelength tested, and plotted on a single graph across the visible spectrum. As the spectral filters all lay 50 nm apart, all values between these wavelengths would have to be interpolated - resulting in a rudimentary spectral sensitivity curve. To demonstrate that a simple spectral sensitivity curve could be produced through use of the automated system was the main intention here, but the use of smaller wavelength intervals (e.g. 10 nm) is recommended in future. If a spectral sensitivity curve had been produced for *O. scyllarus*, the region of the stomatopod tripartite eye responsible for detecting the spectrally variable flashing LED stimuli could have been investigated. Extensive research on the stomatopod visual system has revealed that the hemispheres possess one photoreceptor class in the visible spectrum and thus process achromatic information, whereas the dorsal rows of the midband possess up to eight photoreceptor classes in the visible spectrum and thus process chromatic information (Cronin *et al.*, 2017; Marshall *et al.*, 2007). Spectral sensitivity functions of the hemispheres of other gonodactyloid species have been determined electrophysiologically (Cronin & Marshall, 1989a, 1989b; Kleinlogel & Marshall, 2006), and could be compared to the hypothetically produced action spectrum to reveal the responsible ocular region.

If the functions matched, then the hemispheres are most likely responsible and *O. scyllarus* detects the stimuli through achromatic channels. If they did not match, then the dorsal rows are most likely responsible and chromatic channels are utilised instead to detect the stimuli. Gonzales (2020) created an action spectrum based on the optokinetic responses of *Gonodactylus chiragra* and *Pseudosquilla ciliata* (Fig. 22), that strongly suggested motion detection and gaze stabilisation were processed in the hemispheres and were therefore achromatic. This conclusion was reached, in turn, by comparing the action spectrum produced to previous research on the peripheral spectral sensitivities of *G. chiragra* and *P. ciliata* (Cronin & Marshall, 1989b; Kleinlogel & Marshall, 2006). If a spectral sensitivity curve for *O. scyllarus* had been successfully produced by this study, it would have been compared to the function produced by Gonzales (2020).

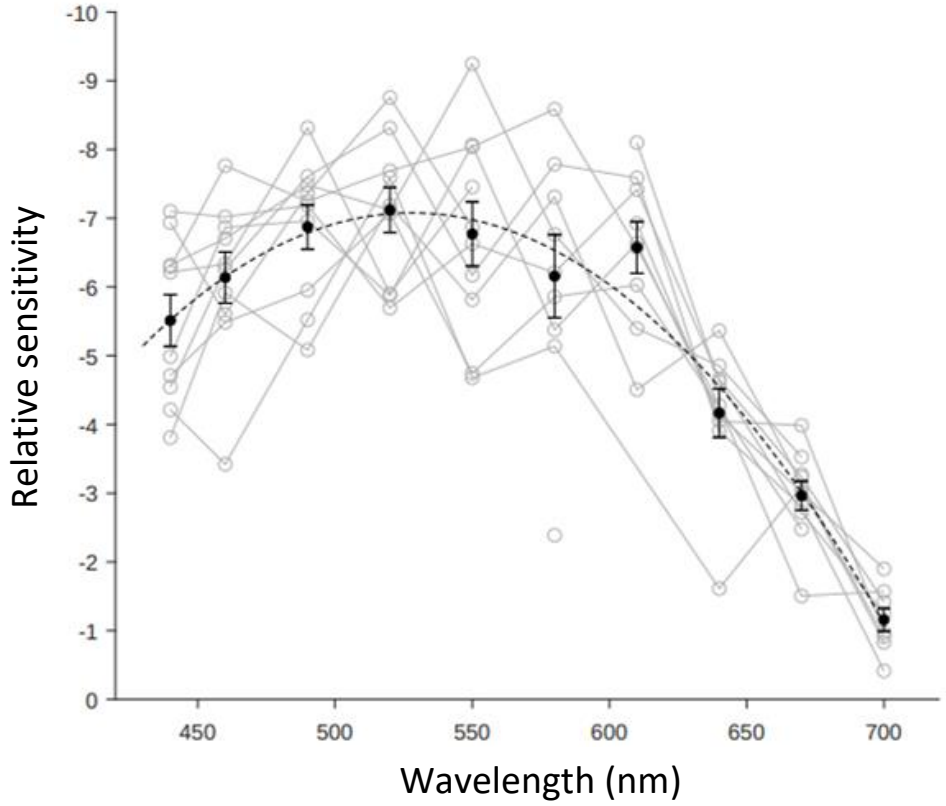

Fig. 22. The action spectrum of the presence of optokinetic responses in *G. chiragra* and *P. ciliata* individuals at several wavelength intervals across the visible spectrum. There is a single broad peak between 500 and 550 nm. Grey markers connected by interpolated lines indicate individual responses. Black markers with error bars indicate the mean sensitivity and standard error at each wavelength interval tested, with the black dashed line representing the rolling average. Taken from Gonzales, 2020.

After following the recommended improvements, this automated system may be capable of creating an accurate spectral sensitivity curve for *O. scyllarus,* which could then be

determined as originating from achromatic peripheral channels or chromatic midband channels. Further to this, minor alterations to the system could be made to investigate other visual modalities such as spectral discrimination, UV sensitivity, and polarization sensitivity (linear or circular). Adaptation of the automated system to species beyond stomatopods would be fairly simple, including both aquatic and terrestrial animals, and training animals that do not readily roam outside their burrow, as mantis shrimps do, may indeed be less challenging. Increasing automation of operant conditioning and other behavioural experiments is strongly advocated for, because of its high adaptability, increased productivity, and reduced researcher labour and bias.

4b.2. Hypotheses on spectral sensitivity and chromaticity

Due to the lack of accurate sigmoid curves and the apparent influence of the different wavelength intensities on the X50 values, these will be effectively ignored. If future research were to successfully produce an accurate spectral sensitivity graph, it is hypothesised to present a broad peak in the region 450-550 nm with the pinnacle just above 500 nm, decreasing toward either end of the visible spectrum especially beyond 600 nm. This is based on data concerning the normalised sensitivity functions of *O. scyllarus* photoreceptors (Fig. 5, 7c) (Cronin *et al.*, 2014; Marshall *et al.*, 2007) which have been calculated from MSP recordings of their intrarhabdomal filters and visual pigments (Fig. 7a-b) (Cronin *et al.*, 1994b). The hemispheres (and rows 5 and 6) possess flat-topped sensitivity functions that peak from 450-550 nm and contain photopigments with peak absorbance just above 500 nm. As the peripheral ommatidia cover the majority of the eye (Marshall *et al.*, 1991a), the high number of photoreceptors perhaps confers greatest sensitivity in this blue-green region (especially at the pigment absorption peak in the green), due to increased chance of photon capture (de Busserolles *et al.*, 2014; Locket, 1977). Any midband photoreceptors sensitive to the blue-green part of the spectrum could augment total sensitivity here as well. Sensitivity may reduce toward the violet-blue end as only rows 1 and 4 peak at these shorter wavelengths, which together only cover two narrow strips of the midband and may have reduced sensitivity due to serial filtering (Cronin *et al.*, 2014; Marshall *et al.*, 1991b, 2007). Sensitivity would likely reduce more dramatically toward the red end of the spectrum for the same reasons, compounded by the presence of all four intrarhabdomal filters in rows 2 and 3 (Fig. 7a) (Cronin *et al.*, 1994a, 1994c, 2014; Marshall *et al.*, 1991b, 2007), pushing underlying sensitivity functions to peak almost outside the absorbance spectra of their visual pigments (Fig. 7b). If this hypothesis were accurate, the stomatopods would be utilising both the midband and hemispheres to detect the wavelength stimuli, rather than just one of them. It has recently been discovered that the neural organisation of the stomatopod central

nervous system could potentially allow the integration of chromatic midband and achromatic peripheral information (Thoen *et al.*, 2018). From this, Gonzales (2020) intriguingly suggested that the middle-spectrum peak in their optokinetic action spectrum could have resulted from the combined sensitivities of the hemispheres and midband (Fig. 22), as suggested here.

Although much can be assumed from the MSP data on *O. scyllarus* visual pigments and intrarhabdomal filters, there is no information on threshold sensitivities of the photoreceptor classes which could vary widely. These could be tuned to ecologically important signals, most likely conspecific body colouration which is already proven to be of great importance in communication amongst six-row gonodactyloids (Caldwell & Dingle, 1975; Cheroske & Cronin, 2005; Chiou *et al.*, 2011; Dingle, 1964; Franklin *et al.*, 2016). Such a phenomenon has been documented in three firefly species that are each maximally sensitive to conspecific bioluminescent mating signals (Cronin *et al.*, 2000). Although there is some variation, *O. scyllarus* individuals generally have green bodies with leopard-like spots on the anterior carapace, orange/red antennal scales, legs and raptorial appendages, and uropods with blue rims and red setae (Fig. 1a, 23). Enhanced sensitivity to short-wavelength blue or long-wavelength orange/red signals could result in a very different spectral sensitivity curve to the one proposed. The apparent increased preference for yellow and reduced preference for red in *O. scyllarus* (Daly *et al.*, 2017) does not necessarily reveal anything about spectral sensitivity, but may complicate the task of retrieving accurate detection thresholds. Although a fairly shallow-living species, *O. scyllarus* does generally inhabit slightly deeper waters (2-30 m) than other gonodactyloids such as *N. oerstedii* (0-10 m). In keeping with ecological trends, the computed sensitivity functions of long-wavelength sensitive rows 2 and 3 are shifted to slightly shorter wavelengths in *O. scyllarus* than *N. oerstedii* (Marshall *et al.*, 2007). This supports a reduced sensitivity to longer wavelengths, especially those at the extreme end (e.g. 700 nm), but only further behavioural research or experimental definition of *O. scyllarus* photoreceptor class sensitivities through MSP or electrophysiological recordings (as has been done for *N. oerstedii* - Thoen *et al.*, 2017a) would substantiate this.

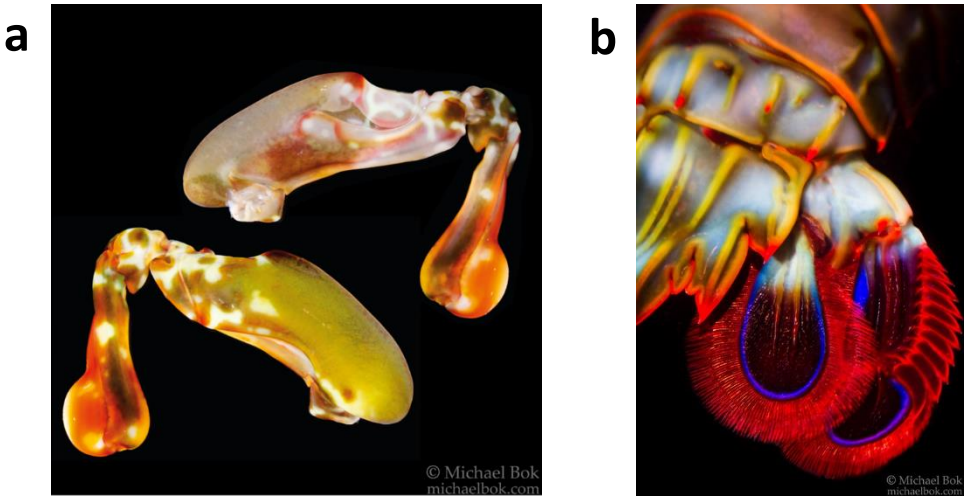

Fig. 23. (a) Raptorial appendages of the smasher *O. scyllarus*, displaying the orange-red colouration and leopard spots. (b) Telson and uropods of O. scyllarus, displaying the blue rim of the uropods and the red setae. Photographs: Michael Bok.

References

Abbott, B.C., Manning, R.B. and Schiff, H., 1984. 'An attempt to correlate pseudopupil sizes in stomatopod crustaceans with ambient light conditions and behavior patterns'. *Comparative Biochemistry and Physiology*, **78**, 419-426.

Adams, E.S. and Caldwell, R.L., 1990. 'Deceptive communication in asymmetric fights of the stomatopod crustacean *Gonodactylus bredini*'. *Animal Behaviour*, **39**, 706-716.

Ahyong, S.T. and Jarman, S.N., 2009. 'Stomatopod interrelationships: preliminary results based on analysis of three molecular loci'. *Arthropod Systematics & Phylogeny*, **67**, 91-98.

Barber, C.L., Prescott, N.B., Jarvis, J.R., Sueur, C.L., Perry, G.C. and Wathes, C.M., 2006. 'Comparative study of the photopic spectral sensitivity of domestic ducks (*Anas platyrhynchos domesticus*), turkeys (*Meleagris gallopavo gallopavo*) and humans'. *British Poultry Science*, **47**, 365-374.

Barlow, H.B., 1982. 'What causes trichromacy? A theoretical analysis using comb-filtered spectra'. *Vision Research*, **22**, 635-643.

Bok, M.J., n.d., *Mantis Shrimp*, Michael Bok's Homepage, accessed 25th November 2021, <https://www.michaelbok.com/MantisShrimp/>.

Bok, M.J., Porter, M.L., Place, A.R. and Cronin, T.W., 2014. 'Biological sunscreens tune polychromatic ultraviolet vision in mantis shrimp'. *Current Biology*, **24**, 1636-1642.

Bok, M.J., Roberts, N.W. and Cronin, T.W., 2018. ‘Behavioural evidence for polychromatic ultraviolet sensitivity in mantis shrimp’. *Proceedings of the Royal Society B: Biological Sciences*, **285**, 20181384.

Bowmaker, J.K., 1983. ‘Trichromatic colour vision: why only three receptor channels?’. *Trends in Neurosciences*, **6**, 41-43.

Caldwell, R.L., 1979. ‘Cavity occupation and defensive behaviour in the stomatopod *Gonodactylus festai*: evidence for chemically mediated individual recognition’. *Animal Behaviour*, **27**, 194-201.

Caldwell, R.L., 1985. ‘A test of individual recognition in the stomatopod *Gonodactylus festate*’. *Animal Behaviour*, **33**, 101-106.

Caldwell, R.L. and Dingle, H., 1975. ‘Ecology and evolution of agonistic behavior in stomatopods’. *Naturwissenschaften*, **62**, 214-222.

Cheroske, A.G., Barber, P.H. and Cronin, T.W., 2006. ‘Evolutionary variation in the expression of phenotypically plastic color vision in Caribbean mantis shrimps, genus *Neogonodactylus*’. *Marine Biology*, **150**, 213-220.

Cheroske, A.G. and Cronin, T.W., 2005. ‘Variation in stomatopod (*Gonodactylus smithii*) color signal design associated with organismal condition and depth’. *Brain, Behavior and Evolution*, **66**, 99-113.

Chiou, T.H., Kleinlogel, S., Cronin, T., Caldwell, R., Loeffler, B., Siddiqi, A., Goldizen, A. and Marshall, J., 2008. ‘Circular polarization vision in a stomatopod crustacean’. *Current Biology*, **18**, 429-434.

Chiou, T.H., Marshall, N.J., Caldwell, R.L. and Cronin, T.W., 2011. ‘Changes in light-reflecting properties of signalling appendages alter mate choice behaviour in a stomatopod crustacean *Haptosquilla trispinosa*’. *Marine and Freshwater Behaviour and Physiology*, **44**, 1-11.

Cronin, T.W., 1985. ‘The visual pigment of a stomatopod crustacean, *Squilla empusa*’. *Journal of Comparative Physiology A*, **156**, 679-687.

Cronin, T.W., Bok, M.J., Marshall, N.J. and Caldwell, R.L., 2014. ‘Filtering and polychromatic vision in mantis shrimps: themes in visible and ultraviolet vision’. *Philosophical Transactions of the Royal Society B: Biological Sciences*, **369**, 20130032.

Cronin, T.W. and Caldwell, R.L., 2002. ‘Tuning of photoreceptor function in three mantis shrimp species that inhabit a range of depths. II. Filter pigments’. *Journal of Comparative Physiology A*, **188**, 187-197.

Cronin, T.W., Caldwell, R.L. and Erdmann, M.V., 2002. ‘Tuning of photoreceptor function in three mantis shrimp species that inhabit a range of depths. I. Visual pigments’. *Journal of Comparative Physiology A*, **188**, 179-186.

Cronin, T.W., Caldwell, R.L. and Marshall, J., 2006. ‘Learning in stomatopod crustaceans’. *International Journal of Comparative Psychology*, **19**, 297-317.

Cronin, T.W., Caldwell, R.L. and Marshall, J., 2001. ‘Tunable colour vision in a mantis shrimp’. *Nature*, **411**, 547-548.

Cronin, T.W., Järvilehto, M., Weckström, M. and Lall, A.B., 2000. ‘Tuning of photoreceptor spectral sensitivity in fireflies (Coleoptera: Lampyridae)’. *Journal of Comparative Physiology A*, **186**, 1-12.

Cronin, T.W. and Marshall, N.J., 1989a. ‘A retina with at least ten spectral types of photoreceptors in a mantis shrimp’. *Nature*, **339**, 137-140.

Cronin, T.W. and Marshall, N.J., 1989b. ‘Multiple spectral classes of photoreceptors in the retinas of gonodactyloid stomatopod crustaceans’. *Journal of Comparative Physiology A*, **166**, 261-275.

Cronin, T.W., Marshall, N.J. and Caldwell, R.L., 1993. ‘Photoreceptor spectral diversity in the retinas of squilloid and lysiosquilloid stomatopod crustaceans’. *Journal of Comparative Physiology A*, **172**, 339-350.

Cronin, T.W., Marshall, N.J. and Caldwell, R.L., 1994a. ‘The intrarhabdomal filters in the retinas of mantis shrimps’. *Vision Research*, **34**, 279-291.

Cronin, T.W., Marshall, N.J. and Caldwell, R.L., 1994b. ‘The retinas of mantis shrimps from low-light environments (Crustacea; Stomatopoda; Gonodactylidae)’. *Journal of Comparative Physiology A*, **174**, 607-619.

Cronin, T.W., Marshall, N.J. and Caldwell, R.L., 2017. ‘Stomatopod vision’. *Oxford Research Encyclopedia of Neuroscience*.

Cronin, T.W., Marshall, N.J., Caldwell, R.L. and Shashar, N., 1994c. ‘Specialization of retinal function in the compound eyes of mantis shrimps’. *Vision Research*, **34**, 2639-2656.

Cronin, T.W., Marshall, N.J., Quinn, C.A. and King, C.A., 1994d. ‘Ultraviolet photoreception in mantis shrimp’. *Vision Research*, **34**, 1443-1452.

Cronin, T.W. and Porter, M.L., 2008. ‘Exceptional variation on a common theme: the evolution of crustacean compound eyes’. *Evolution: Education and Outreach*, **1**, 463-475.

Cronin, T.W., Porter, M.L., Bok, M.J., Wolf, J.B. and Robinson, P.R., 2010. ‘The molecular genetics and evolution of colour and polarization vision in stomatopod crustaceans’. *Ophthalmic and Physiological Optics*, **30**, 460-469.

Cronin, T.W., Yan, H.Y. and Bidle, K.D., 1992. ‘Regional specialization for control of ocular movements in the compound eyes of a stomatopod crustacean’. *Journal of Experimental Biology*, ***171***, 373-393.

Daly, I.M., How, M.J., Partridge, J.C., Temple, S.E., Marshall, N.J., Cronin, T.W. and Roberts, N.W., 2016. ‘Dynamic polarization vision in mantis shrimps’. *Nature Communications*, **7**, 1-9.

Daly, I.M., Tetley, A.E., Jared, S.L., How, M.J. and Roberts, N.W., 2017. ‘Colour preference in *Odontodactylus scyllarus* (Linnaeus, 1758)(Stomatopoda)’. *The Journal of Crustacean Biology*, **37**, 374-379.

Davis, J.F., Krause, E.G., Melhorn, S.J., Sakai, R.R. and Benoit, S.C., 2009. 'Dominant rats are natural risk takers and display increased motivation for food reward'. *Neuroscience*, **162**, 23-30.

De Busserolles, F., Fitzpatrick, J.L., Marshall, N.J. and Collin, S.P., 2014. 'The influence of photoreceptor size and distribution on optical sensitivity in the eyes of lanternfishes (Myctophidae)'. *PLoS One*, **9**, 99957.

DeVries, M.S., Murphy, E.A.K. and Patek, S.N., 2012. 'Strike mechanics of an ambush predator: the spearing mantis shrimp'. *Journal of Experimental Biology*, **215**, 4374-4384.

Dingle, H., 1964. 'A colour polymorphism in *Gonodactylus oerstedi* Hansen, 1895 (Stomatopoda)'. *Crustaceana*, **7**, 236-240.

Fleishman, L.J. and Persons, M., 2001. 'The influence of stimulus and background colour on signal visibility in the lizard *Anolis cristatellus*'. *Journal of Experimental Biology*, **204**, 1559-1575.

Franklin, A.M., Marshall, N.J. and Lewis, S.M., 2016. 'Multimodal signals: ultraviolet reflectance and chemical cues in stomatopod agonistic encounters'. *Royal Society Open Science*, **3**, 160329.

Gagnon, Y.L., Templin, R.M., How, M.J. and Marshall, N.J., 2015. 'Circularly polarized light as a communication signal in mantis shrimps'. *Current Biology*, **25**, 3074-3078.

Gonzales, D., 2020. 'Colour and luminance vision in stomatopod crustaceans.' MSci dissertation, University of Bristol, Bristol.

Harling, C., 2000. 'Reexamination of eye design in the classification of stomatopod crustaceans'. *Journal of Crustacean Biology*, **20**, 172-185.

Hemmi, J.M., 1999. 'Dichromatic colour vision in an Australian marsupial, the tammar wallaby'. *Journal of Comparative Physiology A*, **185**, 509-515.

Kelber, A., Vorobyev, M. and Osorio, D., 2003. 'Animal colour vision–behavioural tests and physiological concepts'. *Biological Reviews*, **78**, 81-118.

Keller, J., Strasburger, H., Cerutti, D.T. and Sabel, B.A., 2000. 'Assessing spatial vision—automated measurement of the contrast-sensitivity function in the hooded rat'. *Journal of Neuroscience Methods*, **97**, 103-110.

Kleinlogel, S. and Marshall, N.J., 2006. 'Electrophysiological evidence for linear polarization sensitivity in the compound eyes of the stomatopod crustacean *Gonodactylus chiragra*'. *Journal of Experimental Biology*, **209**, 4262-4272.

Koshitaka, H., Kinoshita, M., Vorobyev, M. and Arikawa, K., 2008. 'Tetrachromacy in a butterfly that has eight varieties of spectral receptors'. *Proceedings of the Royal Society B: Biological Sciences*, **275**, 947-954.

Land, M.F., Marshall, J.N., Brownless, D. and Cronin, T.W., 1990. 'The eye-movements of the mantis shrimp *Odontodactylus scyllarus* (Crustacea: Stomatopoda)'. *Journal of Comparative Physiology A*, **167**, 155-166.

Lind, O., 2016. 'Colour vision and background adaptation in a passerine bird, the zebra finch (*Taeniopygia guttata*)'. *Royal Society Open Science*, **3**, 160383.

Locket, N.A., 1977. 'Adaptations to the deep-sea environment', in Crescitelli, F. (ed.), *The Visual System in Vertebrates*. Springer, Berlin, 67-192.

Lozano-Montes, L., Astori, S., Abad, S., Guillot de Suduiraut, I., Sandi, C. and Zalachoras, I., 2019. 'Latency to reward predicts social dominance in rats: A causal role for the dopaminergic mesolimbic system'. *Frontiers in Behavioral Neuroscience*, **13**, 69.

Lunau, K., 2014. 'Visual ecology of flies with particular reference to colour vision and colour preferences'. *Journal of Comparative Physiology A*, **200**, 497-512.

Manning, R.B., Schiff, H. and Abbott, B.C., 1984. 'Eye structure and the classification of stomatopod Crustacea'. *Zoologica Scripta*, **13**, 41-44.

Marshall, N.J., 1988. 'A unique colour and polarization vision system in mantis shrimps'. *Nature*, **333**, 557-560.

Marshall, J. and Arikawa, K., 2014. 'Unconventional colour vision'. *Current Biology*, **24**, 1150-1154.

Marshall, J., Cronin, T.W. and Kleinlogel, S., 2007. 'Stomatopod eye structure and function: a review'. *Arthropod Structure & Development*, **36**, 420-448.

Marshall, N.J., Jones, J.P. and Cronin, T.W., 1996. 'Behavioural evidence for colour vision in stomatopod crustaceans'. *Journal of Comparative Physiology A*, **179**, 473-481.

Marshall, N.J., Land, M.F., King, C.A. and Cronin, T.W., 1991a. The compound eyes of mantis shrimps (Crustacea, Hoplocarida, Stomatopoda). I. Compound eye structure: the detection of polarized light. *Philosophical Transactions of the Royal Society B: Biological Sciences*, **334**, 33-56.

Marshall, N.J., Land, M.F., King, C.A. and Cronin, T.W., 1991b. 'The compound eyes of mantis shrimps (Crustacea, Hoplocarida, Stomatopoda). II. Colour pigments in the eyes of stomatopod crustaceans: polychromatic vision by serial and lateral filtering. *Philosophical Transactions of the Royal Society B: Biological Sciences*, **334**, 57-84.

Marshall, J. and Oberwinkler, J., 1999. 'The colourful world of the mantis shrimp'. *Nature*, **401**, 873-874.

Mead, K. and Caldwell, R., 2010. 'Mantis shrimp: olfactory apparatus and chemosensory behavior', in Breithaupt, T. and Thiel, M. (eds.), *Chemical Communication in Crustaceans*. Springer, New York, 219-238.

Nilsson, D.E., 1983. 'Evolutionary links between apposition and superposition optics in crustacean eyes'. *Nature*, **302**, 818-821.

Ninomiya, S., Mitsumasu, T., Aoyama, M. and Kusunose, R., 2007. ‘A note on the effect of a palatable food reward on operant conditioning in horses’. *Applied Animal Behaviour Science*, **108**, 342-347.

Olsson, P., Johnsson, R.D., Foster, J.J., Kirwan, J.D., Lind, O. and Kelber, A., 2020. ‘Chicken colour discrimination depends on background colour’. *Journal of Experimental Biology*, **223**, 209429.

Patek, S.N., Korff, W.L. and Caldwell, R.L., 2004. ‘Deadly strike mechanism of a mantis shrimp’. *Nature*, **428**, 819-820.

Piper, R., 2007. ‘Mantis shrimps’, in Piper, R., *Extraordinary Animals: An Encyclopedia of Curious and Unusual Animals*. Greenwood Publishing Group, London, 94-96.

Pongrácz, P., Bánhegyi, P. and Miklósi, Á., 2012. ‘When rank counts—dominant dogs learn better from a human demonstrator in a two-action test’. *Behaviour*, **149**, 111-132.

Porter, M.L., Awata, H., Bok, M.J. and Cronin, T.W., 2020. ‘Exceptional diversity of opsin expression patterns in *Neogonodactylus oerstedii* (Stomatopoda) retinas’. *Proceedings of the National Academy of Sciences*, **117**, 8948-8957.

Porter, M.L., Bok, M.J., Robinson, P.R. and Cronin, T.W., 2009. ‘Molecular diversity of visual pigments in Stomatopoda (Crustacea)’. *Visual Neuroscience*, **26**, 255-265.

Porter, M.L., Speiser, D.I., Zaharoff, A.K., Caldwell, R.L., Cronin, T.W. and Oakley, T.H., 2013. ‘The evolution of complexity in the visual systems of stomatopods: insights from transcriptomics’. *Integrative and Comparative Biology*, **53**, 39-49.

Porter, M.L., Zhang, Y., Desai, S., Caldwell, R.L. and Cronin, T.W., 2010. ‘Evolution of anatomical and physiological specialization in the compound eyes of stomatopod crustaceans’. *Journal of Experimental Biology*, **213**, 3473-3486.

Reaka, M.L., 1975. ‘Molting in stomatopod crustaceans. I. Stages of the molt cycle, setagenesis, and morphology’. *Journal of Morphology*, **146**, 55-80.

Romano, S., Fucci, D., Scanniello, G., Baldassarre, M.T., Turhan, B. and Juristo, N., 2021. ‘On researcher bias in Software Engineering experiments’. *Journal of Systems and Software*, **182**, 111068.

Rosenthal, R. and Lawson, R., 1964. ‘A longitudinal study of the effects of experimenter bias on the operant learning of laboratory rats’. *Journal of Psychiatric Research*, **2**, 61-72.

Salinas, J.A., Packard, M.G. and McGaugh, J.L., 1993. ‘Amygdala modulates memory for changes in reward magnitude: reversible post-training inactivation with lidocaine attenuates the response to a reduction in reward’. *Behavioural Brain Research*, **59**, 153-159.

Schönenberger, N., 1977. ‘The fine structure of the compound eye of *Squilla mantis* (Crustacea, Stomatopoda)’. *Cell and Tissue Research*, **176**, 205-233.

Schram, F.R., Ahyong, S.T., Patek, S.N., Green, P.A., Rosario, M.V., Bok, M.J., Cronin, T.W., Vetter, K.S.M., Caldwell, R.L., Scholtz, G. and Feller, K.D., 2013. ‘Subclass Hoplocarida Calman, 1904: Order Stomatopoda Latreille, 18171’, in von Vaupel Klein, C., Charmantier-Daures, M. and Schram, F. (eds.), *Treatise on Zoology - Anatomy, Taxonomy, Biology. The Crustacea, Volume 4 Part A*. Brill, Boston, 179-355.

Siegenthaler, A., Mastin, A., Dufaut, C., Mondal, D. and Benvenuto, C., 2018. ‘Background matching in the brown shrimp *Crangon crangon*: adaptive camouflage and behavioural-plasticity’. *Scientific Reports*, **8**, 1-12.

Smith, W.K. and McClean, T.M., 1989. ‘Adaptive relationship between leaf water repellency, stomatal distribution, and gas exchange’. *American Journal of Botany*, **76**, 465-469.

Telles, F.J., Lind, O., Henze, M.J., Rodríguez-Gironés, M.A., Goyret, J. and Kelber, A., 2014. ‘Out of the blue: the spectral sensitivity of hummingbird hawkmoths’. *Journal of Comparative Physiology A*, **200**, 537-546.

Thoen, H.H., Chiou, T.H. and Marshall, N.J., 2017a. ‘Intracellular recordings of spectral sensitivities in stomatopods: A comparison across species’. *Integrative and Comparative Biology*, **57**, 1117-1129.

Thoen, H.H., How, M.J., Chiou, T.H. and Marshall, J., 2014. ‘A different form of color vision in mantis shrimp’. *Science*, **343**, 411-413.

Thoen, H.H., Sayre, M.E., Marshall, J. and Strausfeld, N.J., 2018. ‘Representation of the stomatopod's retinal midband in the optic lobes: Putative neural substrates for integrating chromatic, achromatic and polarization information’. *Journal of Comparative Neurology*, **526**, 1148-1165.

Thoen, H.H., Strausfeld, N.J. and Marshall, J., 2017b. ‘Neural organization of afferent pathways from the stomatopod compound eye’. *Journal of Comparative Neurology*, **525**, 3010-3030.

Vagell, R., Vagell, V.J., Jacobs, R.L., Gordon, J. and Baden, A.L., 2019. ‘SMARTA: Automated testing apparatus for visual discrimination tasks’. *Behavior Research Methods*, **51**, 2597-2608.

Van Der Wal, C., Ahyong, S.T., Ho, S.Y. and Lo, N., 2017. ‘The evolutionary history of Stomatopoda (Crustacea: Malacostraca) inferred from molecular data’. *PeerJ*, **5**, 3844.

Von Frisch, K., 1914. ‘Der farbensinn und formensinn der biene’. *Zoologische Jahrbücher. Abteilung für allgemeine Zoologie und Physiologie der Tiere*, **35**, 1–188.

Wise, R.A., Spindler, J. and Legault, L., 1978. ‘Major attenuation of food reward with performance-sparing doses of pimozide in the rat’. *Canadian Journal of Psychology/Revue Canadienne de Psychologie*, **32**, 77.

Supplementary

Fig. S1. Photograph of three podtrainer units placed onto the tanks and each running trials on an individual stomatopod in parallel.

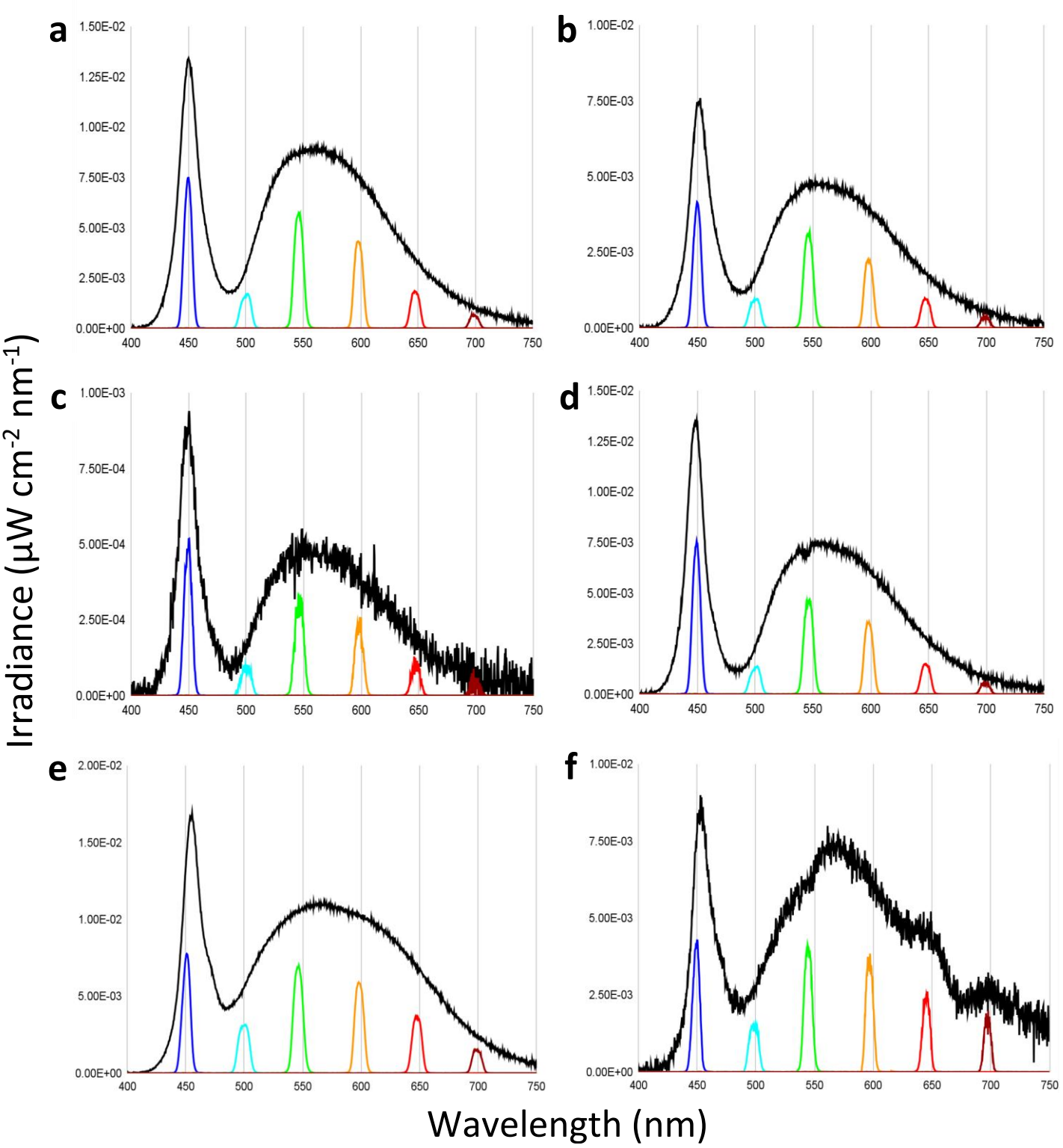

Fig. S2. Podtrainer LED spectral irradiance curves. The black line depicts the bare white LED irradiance values, whereas the coloured lines depict the six spectrally filtered irradiance curves: blue - 450 nm, cyan - 500 nm, green - 550 nm, orange - 600 nm, red - 650 nm, dark red - 700 nm. The colour of the spectrally filtered irradiance curves approximately matches the spectral appearance of that wavelength. The graphs for the remaining six podtrainers are recorded in the supplementary section. (a) Podtrainer 2. (b) Podtrainer 3. (c) Podtrainer 4. (d) Podtrainer 5. (e) Podtrainer 6. (f) Podtrainer 7.

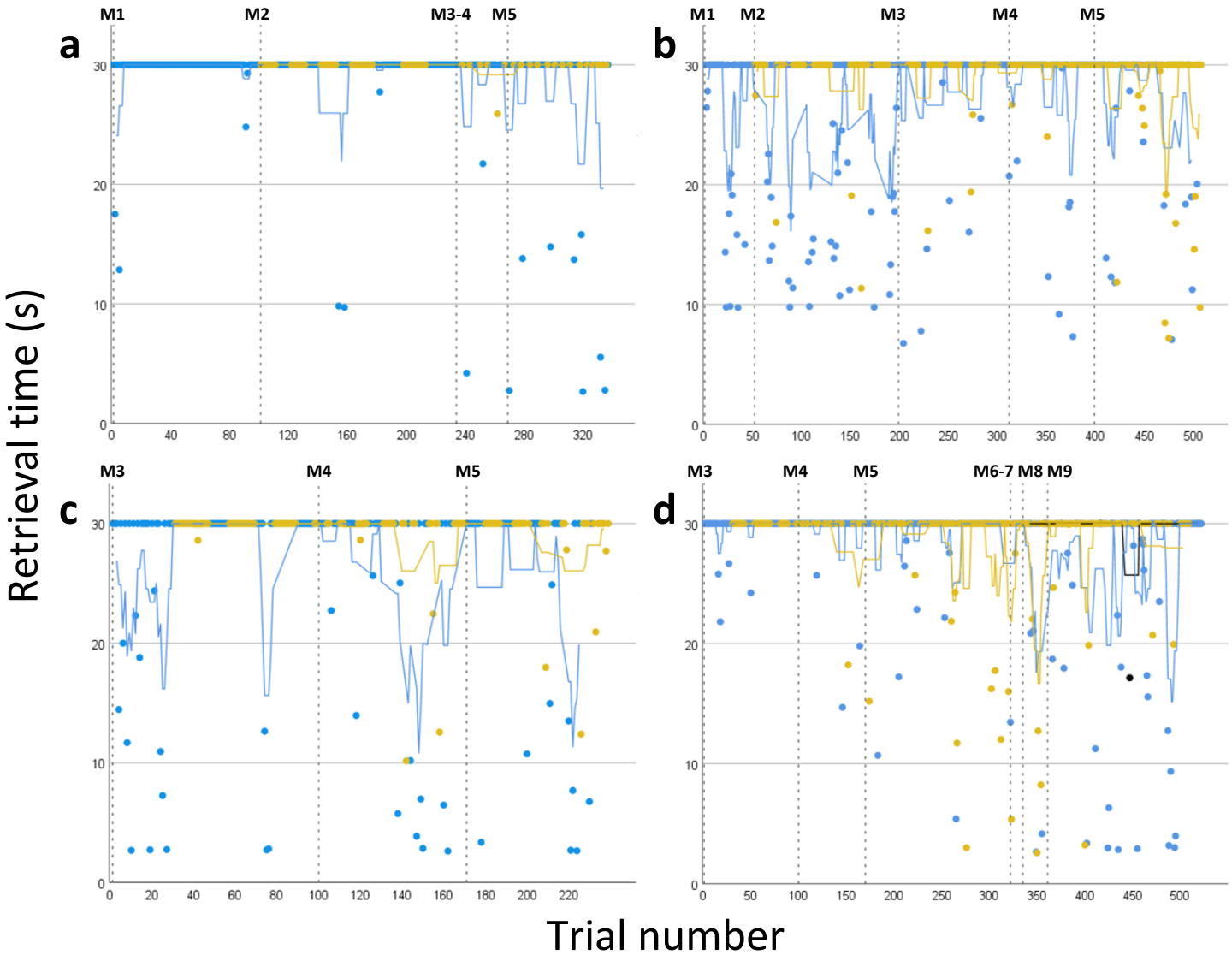

Fig. S3. Results of the white light trials for four separate individuals. Blue markers indicate priming trial results, orange markers testing trial results, and black markers control trial results. A rolling average line is shown for each trial type, with the colour matching that of the markers. vertical dashed lines topped with labels corresponding to Table 2 indicate a particular method change at that point in time. (a) Pod 21a. (b) Pod 3a. (c) Pod 2a. (d) Pod 4a.

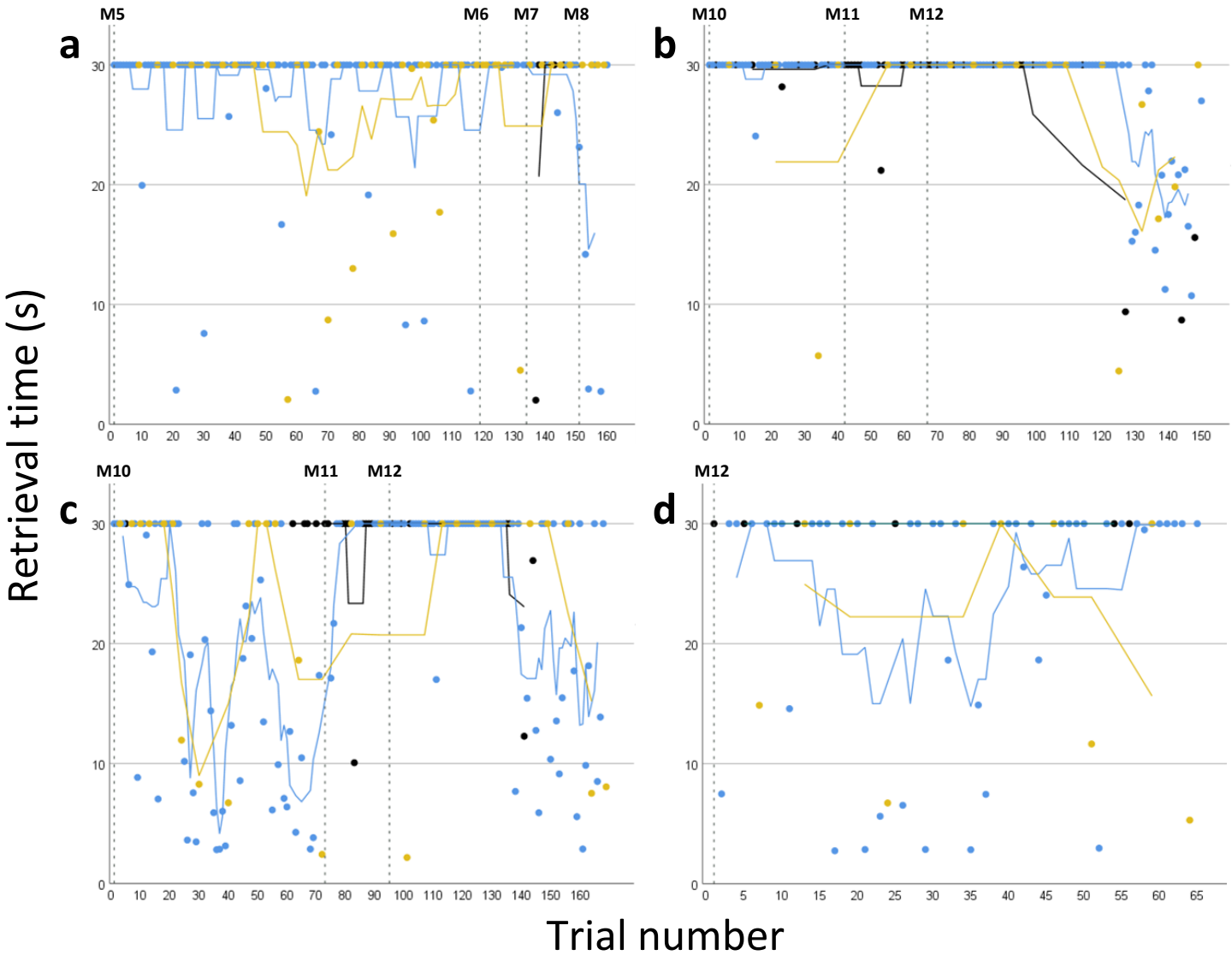

Fig. S4. Results of the white light trials for four separate individuals. Blue markers indicate priming trial results, orange markers testing trial results, and black markers control trial results. A rolling average line is shown for each trial type, with the colour matching that of the markers. vertical dashed lines topped with labels corresponding to Table 2 indicate a particular method change at that point in time. (a) Pod 1b. (b) Pod 6a. (c) Pod 3b. (d) Pod 7b.

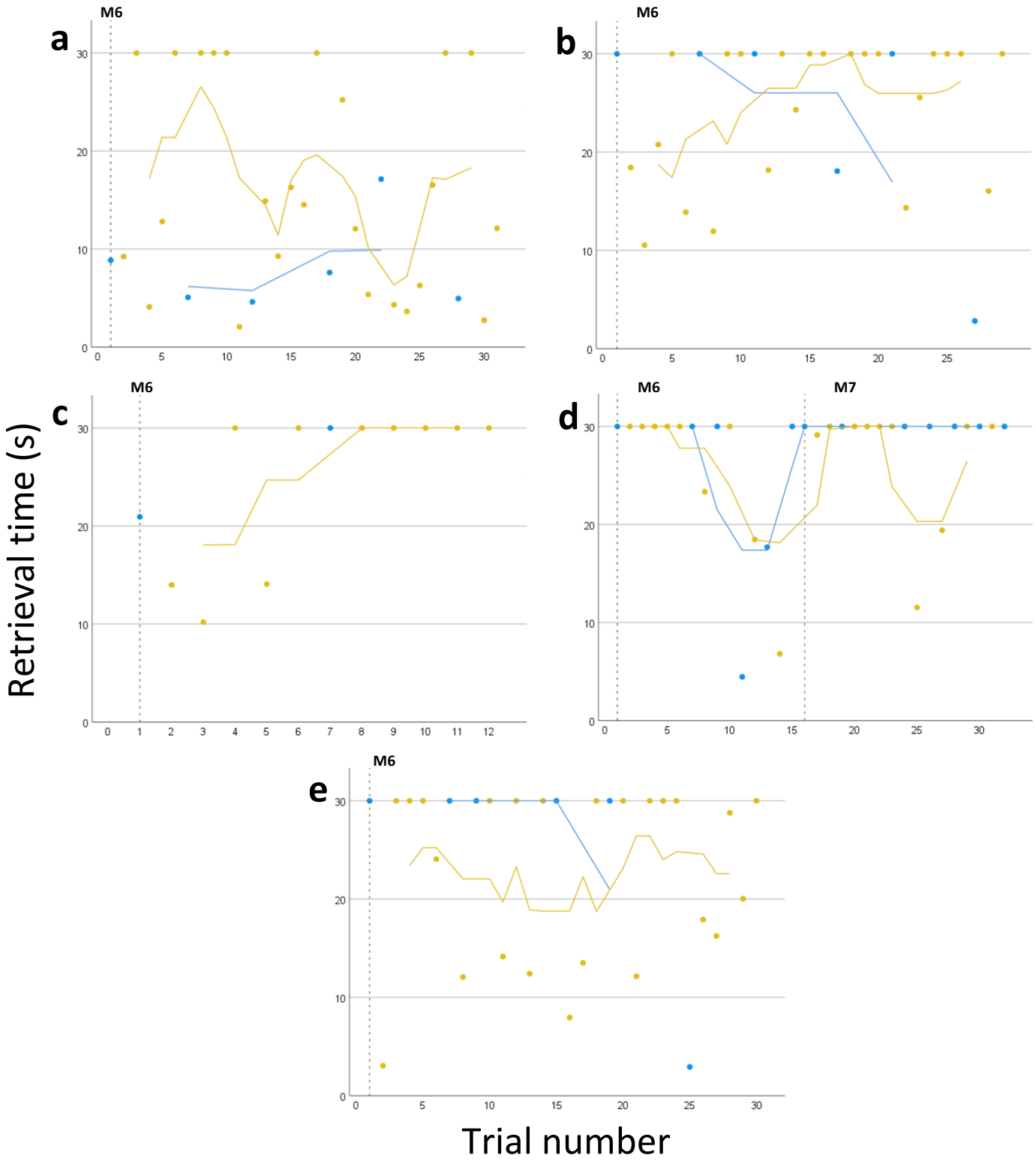

Fig. S5. Results of the spectral light trials for Pod 3a and Pod 4a. Blue markers indicate priming trial results, orange markers testing trial results, and black markers control trial results. A rolling average line is shown for each trial type, with the colour matching that of the markers. vertical dashed lines topped with labels corresponding to Table 2 indicate a particular method change at that point in time. Each graph represents trials under a different spectral filter. (a) Pod 3a at 500 nm. (b) Pod 3a at 600 nm. (c) Pod 3a at 700 nm. (d) Pod 4a at 500 nm. (e) Pod 4a at 600 nm.

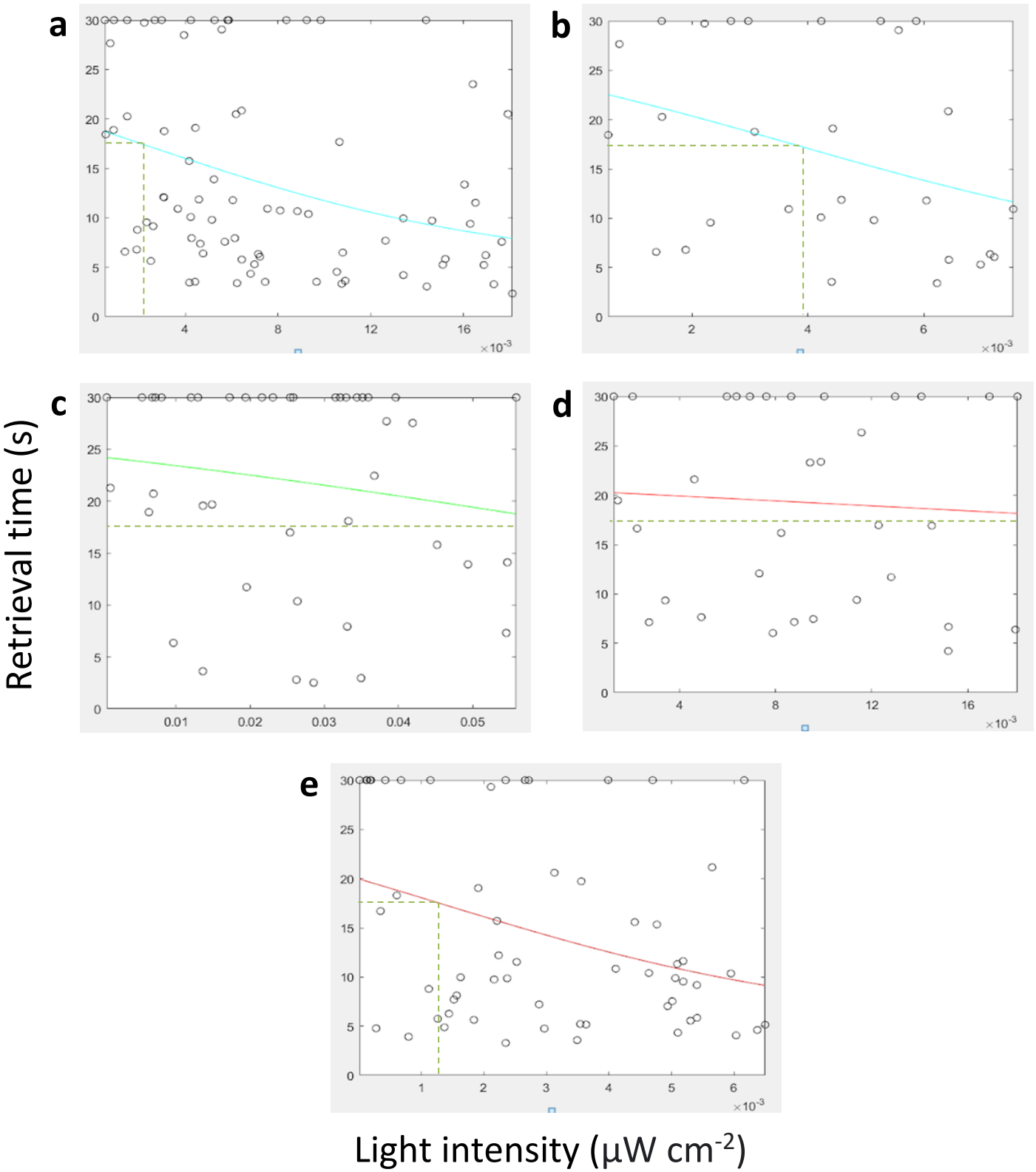

Fig. S6. Detection threshold graphs created from the data recorded from Pod 2a at certain wavelengths. Markers indicate individual testing trial results and the solid coloured line represents the successful or unsuccessful attempt to fit a sigmoid curve to the data. The colour of the line approximately matches the spectral appearance of the wavelength. Some graphs consist of data

recorded solely before the addition of ND filter to the LED stimulus (Table 2 (M11)) - labelled pre-ND data; others consist of data recorded solely afterwards - labelled post-ND data; and others consist of combined data from before and after - labelled combined data. The dashed lines represent the point at 17.5 s where the X50 light intensity value was calculated, to 3 decimal places. Note the x-axis scale varies between panels. (a) 500 nm, combined data, X50 = 0.002 µW cm^{-2}. (b) 500 nm, post-ND data, X50 = 0.004 µW cm^{-2}. (c) 550 nm, pre-ND data, X50 = 0.067 µW cm^{-2}. (d) 650 nm, pre-ND data, X50 = 0.023 µW cm^{-2}. (e) 700 nm, combined data, X50 = 0.001 µW cm^{-2}.

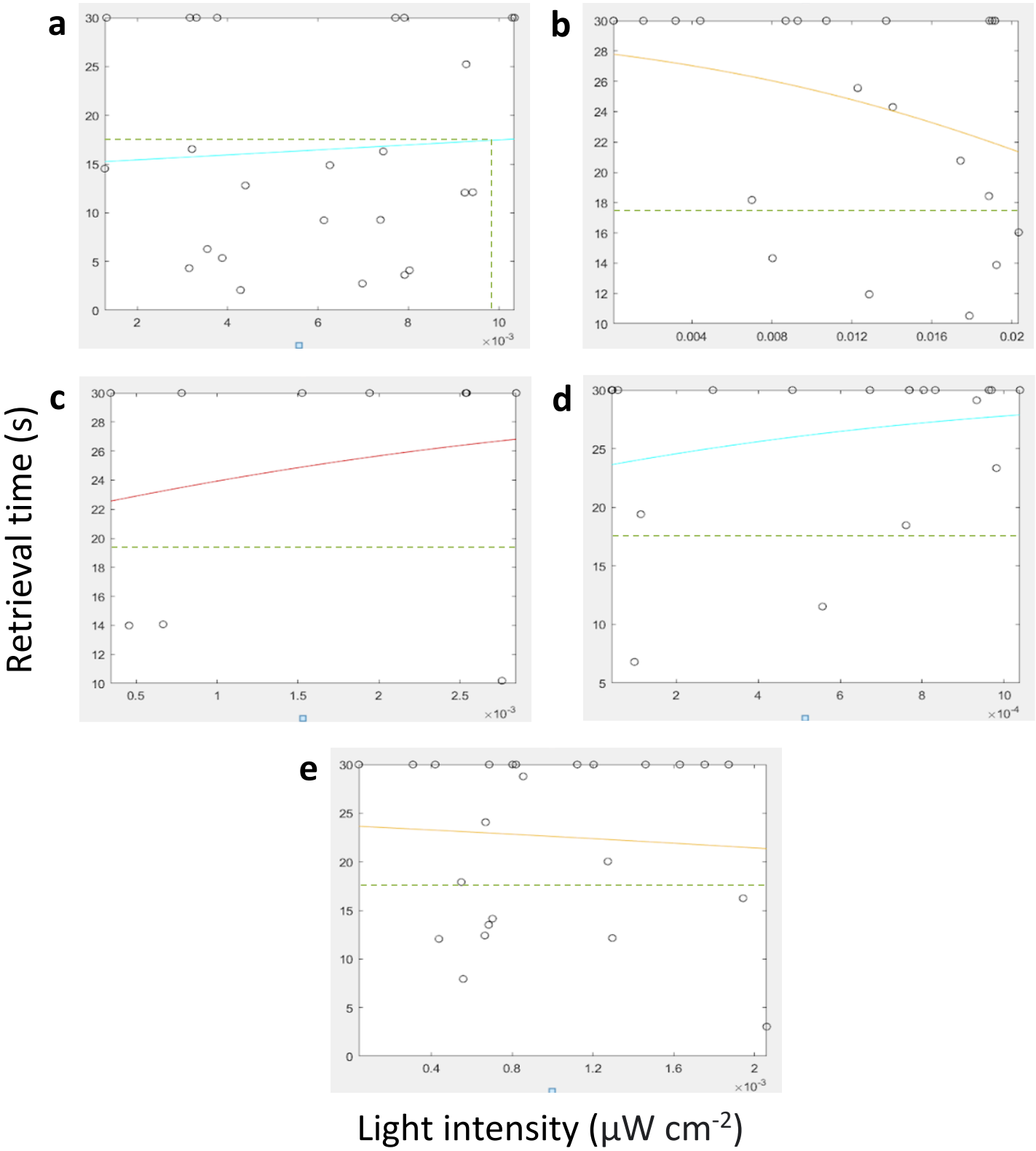

Fig. S7. Detection threshold graphs created from the data recorded from certain individuals at certain wavelengths. Markers indicate individual testing trial results and the solid coloured line represents the successful or unsuccessful attempt to fit a sigmoid curve to the data. The colour of the line

approximately matches the spectral appearance of the wavelength. Some graphs consist of data recorded solely before the addition of ND filter to the LED stimulus (Table 2 (M11)) - labelled pre-ND data; others consist of data recorded solely afterwards - labelled post-ND data; and others consist of combined data from before and after - labelled combined data. The dashed lines represent the point at 17.5 s where the X50 light intensity value was calculated, to 3 decimal places. Note the x-axis scale varies between panels. (a) Pod 3a at 500 nm, pre-ND data, X50 = 0.010 µW cm^{-2}. (b) Pod 3a at 600 nm, pre-ND data, X50 = 0.028 µW cm^{-2}. (c) Pod 3a at 700 nm, pre-ND data, X50 = -0.002 µW cm^{-2}. (d) Pod 4a at 500 nm, pre-ND data, X50 = -0.001 µW cm^{-2}. (e) Pod 4a at 600 nm, pre-ND data, X50 = 0.005 µW cm^{-2}.

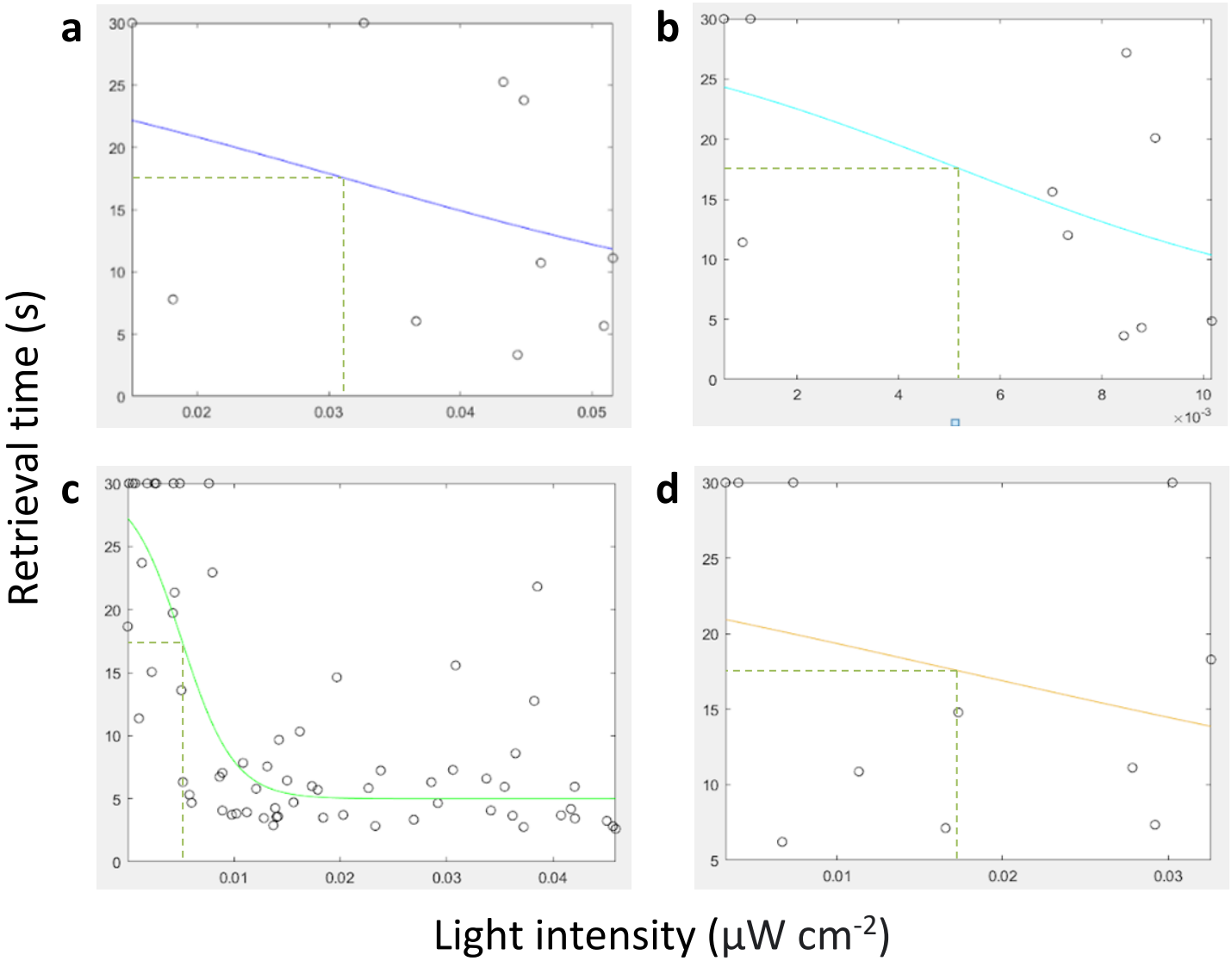

Fig. S8. Detection threshold graphs created from the data recorded from Pod 5a at certain wavelengths. Markers indicate individual testing trial results and the solid coloured line represents the successful or unsuccessful attempt to fit a sigmoid curve to the data. The colour of the line approximately matches the spectral appearance of the wavelength. Some graphs consist of data recorded solely before the addition of ND filter to the LED stimulus (Table 2 (M11)) - labelled pre-ND

data; others consist of data recorded solely afterwards - labelled post-ND data; and others consist of combined data from before and after - labelled combined data. The dashed lines represent the point at 17.5 s where the X50 light intensity value was calculated, to 3 decimal places. Note the x-axis scale varies between panels. (a) 450 nm, pre-ND data, X50 = 0.031 µW cm^{-2}. (b) 500 nm, pre-ND data, X50 = 0.005 µW cm^{-2}. (c) 550 nm, combined data, X50 = 0.005 µW cm^{-2}. (d) 600 nm, pre-ND data, X50 = 0.017 µW cm^{-2}.

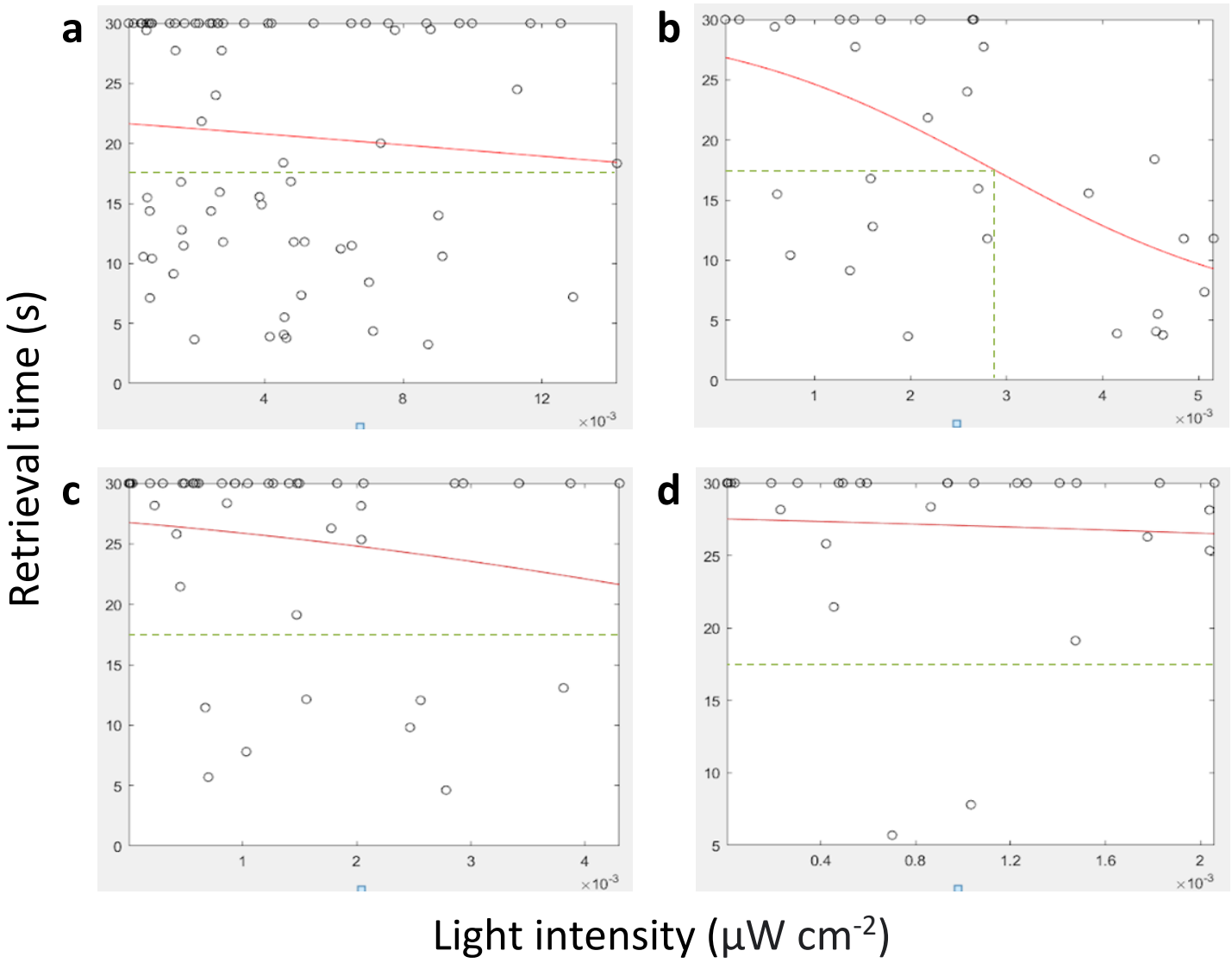

Fig. S9. Detection threshold graphs created from the data recorded from Pod 5a at certain wavelengths. Markers indicate individual testing trial results and the solid coloured line represents the successful or unsuccessful attempt to fit a sigmoid curve to the data. The colour of the line approximately matches the spectral appearance of the wavelength. Some graphs consist of data recorded solely before the addition of ND filter to the LED stimulus (Table 2 (M11)) - labelled pre-ND data; others consist of data recorded solely afterwards - labelled post-ND data; and others consist of combined data from before and after - labelled combined data. The dashed lines represent the point

at 17.5 s where the X50 light intensity value was calculated, to 3 decimal places. Note the x-axis scale varies between panels. (a) 650 nm, combined data, X50 = 0.018 µW cm^{-2}. (b) 650 nm, post-ND data, X50 = 0.003 µW cm^{-2}. (c) 700 nm, combined data, X50 = 0.007 µW cm^{-2}. (d) 700 nm, post-ND data, X50 = 0.012 µW cm^{-2}.